Cindy Nunes Soares

Licenciatura em Bioquímica

Isolation and Characterization of Novel Iron-Sulphur Proteins from DvH Involved in Cell Division

Dissertação para obtenção do Grau de Mestre em

Bioquímica

Orientadora: Doutora Sofia Rocha Pauleta, Investigadora Principal,

Faculdade de Ciências e Tecnologia da UNL

Júri:

Presidente:	Doutor José Ricardo Ramos Franco Tavares, FCT/UNL
Arguente:	Doutora Maria Cristina Oliveira Costa, FCT/UNL
Vogal:	Doutora Sofia Rocha Pauleta, FCT/UNL

FACULDADE DE CIÊNCIAS E TECNOLOGIA
UNIVERSIDADE NOVA DE LISBOA

Outubro, 2016

LOMBADA

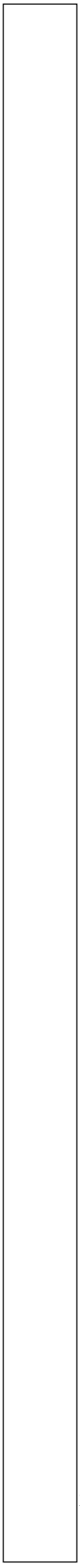

Cindy Nunes Soares

Licenciatura em Bioquímica

Isolation and Characterization of Novel Iron-Sulphur Proteins from DvH Involved in Cell Division

Dissertação de Mestre em Bioquímica

Orientadora: Doutora Sofia Rocha Pauleta, Investigadora Principal, Faculdade de Ciências e Tecnologia da UNL

Júri:

Presidente: Doutor José Ricardo Ramos Franco Tavares, FCT/UNL

Arguente: Doutora Maria Cristina Oliveira Costa, FCT/UNL

Vogal: Doutora Sofia Rocha Pauleta, FCT/UNL

Outubro 2016

Isolation and Characterization of Novel Iron-Sulphur Proteins from DvH Involved in Cell Division?

Acknowledgments

O trabalho desenvolvido nesta dissertação de mestrado não teria sido possível sem a participação, direta ou indireta, de várias pessoas a quem gostaria de expressar os meus agradecimentos.

Em primeiro lugar gostaria de agradecer à Doutora Sofia Rocha Pauleta, a minha orientadora, por todo o tempo que me dispensou, pelas orientações, pela disponibilidade que manifestou e pela transmissão de conhecimentos que contribuíram para aumentar o meu gosto por esta área cientifica.

Gostaria também de agradecer à Prof. Isabel Moura e ao Prof. José G. Moura por me terem acolhido nos seus laboratórios e grupos de investigação e por me proporcionarem todas as condições necessárias para a realização deste trabalho.

Queria agradecer a todos os membros do grupo Bioin e Bioprot pela boa disposição sempre presente, pelos momentos de descontração e conversas diárias, pelo companheirismo e pelo bom ambiente vivido no local de trabalho que me proporcionaram. Um agradecimento muito muito especial à Cíntia Carreira por toda a ajuda que me deu no laboratório, por todos os conselhos, por todas as ajudas (que ainda foram imensas) em situações complicadas, pelo exemplo de dedicação à investigação científica, pela preocupação, pelos telefonemas a meio da noite para saber se não tinha incendiado o laboratório, pela boa e má disposição que mostrou que calhava sempre bem a qualquer momento do dia e até por me fazer chorar e de cada vez me tornar mais segura de mim mesma. Também queria agradecer à Rute Nunes por toda a ajuda que me deu, pela alegria que transmitiu a cada momento, pelo companheirismo, pelas conversas divertidas e por ser a melhor companheira de gabinete que podia ter. Quero agradecer à Cláudia Nóbrega por toda a motivação, pelas conversas que me animavam, pela ajuda em coisas simples, mas importantes, pela boa disposição e estado de espirito *zen* demonstrados todos os dias que me acalmavam quando estava nervosa. Não poderia esquecer de agradecer ao Rui Almeida pelos almoços divertidos que ele me proporcionou com as suas conversas nem sempre próprias e pela boa disposição que sempre demonstrava. Acima de tudo quero agradecer a todos pela paciência em me aturarem e por me divertirem em momentos de maior tristeza, mesmo com o *bullying* que sofri vocês sabem que vos adoro. Esta tese nunca teria sido possível sem vocês, um obrigado gigantesco do fundo do coração.

Não poderia deixar de agradecer também às pessoas que estiveram comigo durante 5 anos e que me acompanharam durante este percurso que foi Bioquímica, sem vocês não teria

conseguido. Obrigada Cindy, Carina, Marisa, Inês e Filipa pelos almoços divertidos, pelas conversas que me descontraíram, pelo *bullying* sempre positivo, pelas piadas, pela compreensão, pelas conversas em momentos difíceis, pela ajuda a resolver situações boas e más, pela amizade acima de tudo. Nunca conseguirei expressar de forma 100 % verdadeira tudo o que vocês significam para mim, mas eu sei que vocês sabem. Rita não podias ficar de fora, tenho de te agradecer todo o apoio, todas as conversas, tudo o que fizeste por mim todos os dias quando chegava a casa exausta e mesmo assim conseguias animar-me, és e serás sempre a melhor colega de casa que poderei ter na vida e uma amiga que guardarei para sempre no coração, adoro-te imenso.

Tenho de agradecer também aos meus pais sem os quais a minha vinda para a faculdade não seria possível e que sempre me apoiaram nesta minha jornada. Muito obrigada mãe por toda a paciência que demonstraste comigo sempre e principalmente nas horas que mais precisei, pelas palavras de carinho que sempre me disseste, por ouvires as minhas explicações e reclamações apesar de nem sempre saberes muito bem do que eu estava a falar, mas concordavas na mesma. Pai muito obrigada pelo apoio, pelas saudades e por todos os momentos em que falar contigo me animava. A ti Julie que sempre ouviste os meus desabafos (maioritariamente maus), me deste na cabeça quando precisava, me fizeste rir e apoiaste de força incondicional em todas as fases que tive ao longo destes últimos anos, sem uma irmã como tu não me teria tornado a pessoa que sou hoje.

Muitas outras pessoas foram importantes para mim durante esta tese e estes anos e queria agradecer a todos do fundo do coração. Não nomeie os nomes todos senão nunca entregaria esta dissertação dentro do prazo, mas vocês sabem que são importantes para mim e não se preocupem que quando precisar vou chorar para ao pé de vocês. Muito obrigada!

Abstract

Firstly, isolated from *Desulfovibrio gigas*, the Orange Protein presents a unique type of mixed metal sulphur cluster composed by two different metals, molybdenum and copper. This protein forms a complex with other proteins, that has recently been proposed to be involved in anaerobic cell division of *D. vulgaris* Hildenborough.

In this Master thesis, DVU2103 ATPase from *D. vulgaris* Hildenborough was purified and biochemically characterized. Since the metal cluster present in this protein has been proven to be oxygen sensitive, the purification was performed under anoxic environment. The protein was co-purified with other proteins of the *orp* operon, DVU2108 and possibly DVU2104, as a protein complex (heterotrimer) confirming that this complex has physiological meaning. The protein complex was purified with an average yield of 58 ± 28 µg, and presents 5.3 ± 0.3 Fe atoms/Total protein. DVU2103 complex presents a broad absorption band at 400 nm in its visible spectrum characteristic of [4Fe-4S] clusters and ICP-AES analysis confirm the presence of either one or two [4Fe4S] clusters. As-isolated protein is mainly EPR active presenting a rhombic signal, with g values of 2.06, 1.89 and 1.85, that switches to an axial signal when reduced with dithionite. Dithionite, unlike ascorbate, is responsible for the full reduction of the metallic centre. Studies to determine the apparent molecular mass of the complex revealed that ATP affects its conformational structure, making it more compact, and oxic conditions lead to the destruction of the [Fe-S] cluster, with concomitant formation of a larger oligomer. ATPase activity of "DVU2103" complex was tested under anoxic and oxic conditions, showing that the protein has a higher activity under the former. Considering that the exposure to oxygen leads to the destruction of the [Fe-S] cluster, it can be concluded that it is essential for higher activity.

In this thesis the homologous expression and purification of DVU2108 in *D. vulgaris* Hildenborough was also performed. No Mo/Cu heterometallic cluster was detected in this protein after purification under anoxic conditions, nevertheless Fe/protein ratio of 1 was estimated for this sample.

KeyWords

Desulfovibrio vulgaris Hildenborough – ORP complex - ATPase – [4Fe-4S] cluster - Orange Protein - DVU2108 - DVU2103

Resumo

Isolado pela primeira vez de *Desulfovibrio gigas*, esta proteína laranja possui um centro metálico único composto por dois metais diferentes, molibdénio e cobre, misturado com enxofre. Esta proteína forma um complexo com outras proteínas recentemente proposto como estando envolvido na divisão celular anaeróbia de bactérias sulfato-redutoras *D. vulgaris* Hildenborough.

Neste trabalho, a proteína ATPase DVU2103 de *D. vulgaris* Hildenborough foi purificada e caracterizada bioquimicamente. Uma vez que o centro metálico presente nesta proteína se revelou ser sensível ao oxigénio toda a purificação foi realizada em ambiente anóxico. A proteína foi co-purificada junto com outras proteínas do operão *orp*, DVU2108 e possivelmente a DVU2104 num complexo proteico (heterotrimero), o que indica a formação de um complexo com significado fisiológico entre estas proteínas. O complexo proteico foi purificado com um rendimento médio de 58 ± 28 µg, e apresenta 5,3 ± 0,3 átomos de ferro/total de proteína. O complexo "DVU2103" apresenta uma banda alargada de absorção a 400 nm no seu espectro de visível característica de centros [4Fe-4S] e a análise de ICP-AES confirma a presença de um ou dois centros [4Fe-4S]. A proteína nativa apresenta um sinal rômbico de EPR com valores de g a 2,06, 1,89 e 1,85, que muda para um sinal axial quando reduzida com ditionito. O ditionito, ao contrário do ascorbato, é responsável pela complexa redução do centro metálico. Estudos para determinar a massa molecular aparente do complexo revelaram que a presença de ATP afeta a sua estrutura conformacional, tornando-a mais compacta, e condições oxidantes levam à destruição do centro [Fe-S], com consequente formação de um oligómero de maiores dimensões. A atividade ATPase do complexo "DVU2103" foi testada em condições anóxicas e oxidantes, mostrando que a proteína tem uma maior atividade em condições anóxicas. Considerando que a exposição ao oxigénio leva à destruição do centro de [Fe-S], pode concluir-se que este é essencial para atividades mais elevadas.

Neste trabalho realizou-se também a expressão homóloga e purificação da DVU2108 em *D. vulgaris* Hildenborough. Nenhum centro heterometálico Mo/Cu foi detetado nesta proteína após purificação em condições anóxicas, no entanto um rácio de 1 Fe/proteína foi estimado para esta amostra.

Termos Chave

Desulfovibrio vulgaris Hildenborough – ORP Complex - ATPase – Centro [4Fe-4S] - ORange Protein – DVU2108 – DVU2103

Contents

Figure Index

Table Index

Abbreviations

Ɛ	Molar Extinction Coefficient
λ	Wavelength
Abs	Absorbance
ATP	Adenosine Triphosphate
AU	Arbitrary Unit
BLAST	Basic Local Alignments Search Tool
COG	Cluster of groups of orthologous proteins
D.	*Desulfovibrio*
EBP	Enhancer binding activator protein
EPR	Electron Paramagnetic Resonance
EXAFS	Extended X-ray absorption fine structure
Fds	Ferredoxines
[Fe-S]	Iron-Sulphur cluster
G	Gauss
HiPIP	High Potential Iron-Sulphur Protein
ICP	Induced Coupled Plasma
LMW	Low Molecular Weight
MALDI-TOF-MS	Matrix Assisted Laser Desorption Ionization – Time of Flight – Mass Spectrometry
Min	Minute
MM	Molecular Mass
NCBI	National Center for Biotechnology Information
OD_{600}	Optical Density at 600nm

ORP	Orange Protein
PAGE	Polyacrylamide Gel Electrophoresis
RNA	Ribonucleic Acid
SDS	Sodium Dodecyl Sulphate
SDS-PAGE	Polyacrylamide Gel Electrophoresis in denaturant conditions
SRB	Sulphate Reducing Bacteria
TM	Thiomolybdate
Tris	Tris(hydroxylmethyl)aminomethane
UV	Ultraviolet

1

Introduction

1.1 Sulphate-Reducing Bacteria

The biogeochemical sulphur cycle (Figure 1.1) is known due to the chemical and biological complexity of its main intervenient, sulphur [1]. Sulphur is one of the most abundant elements on Earth, being present mainly in rocks and sediments [1]. In the sulphur cycle, sulphur goes through a huge range of oxidation states, from - 2 (completely reduced) to + 6 (completely oxidized) [1]. Microorganisms have an important role in this cycle, being responsible for sulphur transformations [1].

Oxidation and reduction reactions of this element are very important in some microorganisms for the generation of metabolic energy [1]. One of the most studied classes of these organisms are the sulphate-reducing bacteria (SRB) [1]. SRB are anaerobic microorganisms that use sulphate as a terminal electron acceptor for the degradation of organic compound (commonly acetate or lactate), producing hydrogen sulphide (H_2S) and carbon dioxide (CO_2) as final products [1].

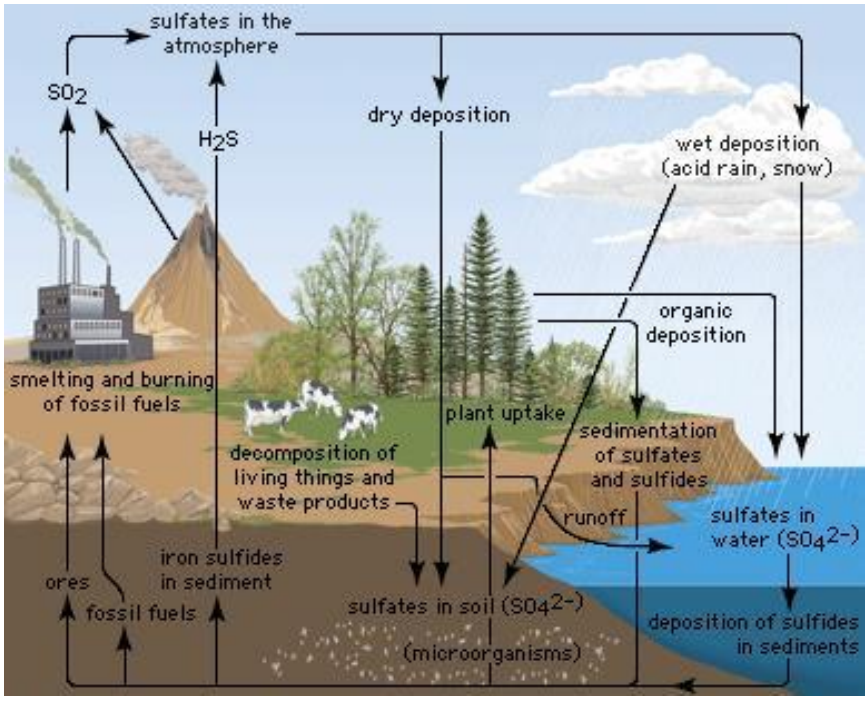

Figure 1.1 - The sulphur cycle. The arrows represent sulphur transformation through oxidation and reduction reactions. Image from [2]

SRB were identified in more than 60 genera, making a total of about 220 species widely distributed around Earth, from terrestrial to marine ecosystems [3], [4]. It is believed that these microorganisms have inhabited our planet for 3.5 billion years, being considered ancestral microorganisms [4]. Regarding its cellular classification, SRB can be classified as gram-negative eubacteria, gram-positive eubacteria or archaea [3]. In terms of acquiring organic compounds to growth, SRB can be heterotrophic, autotrophic, lithoautotrophic or respiration-type, always under anaerobiosis [4]. For many years, scientists thought that lactate and pyruvate were the only two compounds used by SRB to support growth, a theory that was dropped after confirming that these microorganisms can use a variety of compounds [4]. Nowadays, SRB can also be divided in two main groups according to how they degrade organic compounds: incomplete or complete degradation. Incomplete oxidizers refer to a group of microorganisms that carry out an incomplete lactate oxidation leading to the formation of a mixture of acetate and CO_2 [5]. Considered a group of oxidizers less effective than the group of SBR that possesses complete degradation, this group rarely oxidize fatty acids being more common the use of low-molecular-weight alcohols [5]. Various SRB are included in this category, such as *Desulfomonas, Desulfobubus, Desulfolobus* and *Desulfovibrio* genera [6]. In the latter group, sulphate reducers degrade organic compounds to carbon dioxide, using acetate as a carbon source [1]. Organisms present in this

group are usually metabolically more diverse and have slower growth rates. They can oxidize a variety of compounds, including fatty acids and aromatic compounds, to CO_2 [6].

The capacity to couple anaerobic electron transport to ATP synthesis makes SRB a unique physiological group of prokaryotes, being mainly present in Bacteria and Archaea [1], [3]. Found in marine sediments, polluted environments, cyanobacterial microbial mats, rice fields and even responsible for human diseases, these bacteria have a functional importance in many ecosystems [4]. Able to grow in extreme environments, SRB can reach from high acidic (pH 4) to basic habitats (pH 9.5), without affecting its way of living [3]. Cultures of SRB obtained at extreme temperatures have already been documented, confirming that these microorganisms can adapt their metabolism from psychrophilic to hyperthermophilic conditions [7]. The same happens when SRB are exposed to variable ranges of salt concentrations [7].

Relative to the terminal electron acceptor, sulphate is not the only compound used by SRB, as these bacteria are able to use various other organic and inorganic compounds [4]. SRB are now considered the microorganisms that reduce the greatest number of different terminal electron acceptors [4].

More than 125 compounds are known to be used by pure cultures of SRB, most of them are fermentation products and intermediate break-down products, such as glycerol, amino acids and fatty acids [7]. Sulphate-reducing bacteria's metabolism focuses on the oxidation of hydrogen or an organic compound with the reduction of sulphate to sulphide [8]. The chemistry involved in that process was discovered in 1984 by Postgate and is represented in the following chemical equation (Equation 1) [6]:

$$4\,AH_2 + SO_4^{2-} + H^+ \rightarrow 4\,A + HS^- + 4\,H_20 \qquad (1)$$

Referred as a dissimilatory process, SRB oxidize an electron donor (AH_2) with subsequent reduction of sulphate in a bioenergetic reaction [6]. Electrons are transferred from the interior of the cell to the exterior, with the help of proteins associated with the membrane [6]. This reaction is catalysed in a single step by a single enzyme, bisulphite reductase [6].

Metabolism of a particular substrate can involve modification or removal of a special group from the substrate, an incomplete oxidation to an important intermediate (such as acetate) or its complete oxidation to CO_2 [7]. Several experiments have been conducted to understand

more about the biochemistry and physiology of SRB mainly on the genus *Desulfovibrio (D.)*, specifically in *D. vulgaris* Hildenborough and *D. alaskensis* G20 [9].

Beyond their function in the sulphur cycle, SRBs also play important roles in other biogeochemical cycles, as for example in the carbon cycle [9]. In anaerobiosis, SRB are part of the conglomerates that mineralize organic carbon (mainly polymers like cellulose) along with other microbes, producing organic acid and reduced gas (CO and H_2) as a result of fermentation or oxidative pathways [9].

The fact that these microorganisms possess the ability to inhabit deeply extreme environments reflects its metabolic and phylogenetic versatility [4]. Thus, SRB display significant roles in Nature by virtue of their potential for numerous interaction, not only in sulphur cycle [1]. In biogeochemistry, SRB contribute to the complete oxidation of organic matter, through sulphide production and/or metal reduction, which would be very difficult without this kind of organisms [4]. Many biotechnological processes are affected by the presence of SRB, both in a positive and in a negative way.

Many industrial processes are prejudiced due to the presence of SRB, since the use of sulphuric acid results in the production of sulphate in waste waters because of the presence of these microorganisms [1]. The reduction of sulphate then occurs and when this happens in anaerobic environments, like anaerobic treatment of agro-industrial waste waters, a lower amount of methane is produced [1]. The formation of hydrogen sulphide as product of this reaction is therefore undesirable due to its toxic, odorous and corrosive properties [1]. Biocorrosion of ferrous metals in anaerobic environments is another severe problem with which the industries have to deal [9]. Because SRB are abundant in oil fields, many negative consequences come for the petroleum industry [9]. The issues associated to corrosion of machinery, acidification of oil and sulphide precipitation due to their metabolism are some [9]. Due to increasing concern about the environment, scientists were forced to innovate these processes, finding new ways to resolve these issues without minimizing profits [4].

On the other hand, the advances made in the past few years in the field of biotechnologies are making SRB more economically interesting [4]. The unique electron transport components found in SRB give them the possibility to be used in important environmental activities [4]. Areas like bioremediation, fuel production and wastewater treatment implicate nowadays the use of SRB, in a more economical way than that used a few years ago [4]. The implementation of SRB in systems for the removal of sulphate and heavy metals from waste waters is becoming increasingly utilized, such as the removal of sulphur dioxide from flue gas [7]. Bioremediation of BTEX compounds (Benzene, Toluene,

Ethylbenzene and Xylene) in contaminated soils are today made resorting to SRB because of its capability of utilizing hydrocarbons [4]. The SRB also contribute to bioremediation of toxic metal ions from anaerobic sediments [9]. The increase of pH in the surrounding environment due to their metabolism cause the precipitation of toxic metal, such as copper, cadmium and nickel as metal sulphides in acidic aquatic environments [9]. Nowadays, microbiologists consider that SRB are one of the cleaner ways to minimize pollution caused by toxic compounds used in industrial activities [4]. For that reason the use of SRB in bioremediation and biocontrol fields has become very appealing, both economically and ecologically [4].

1.2 *Desulfovibrio vulgaris* genera

The extreme versatility presented by SRB has always intrigued researchers that have tried to understand the processes behind how some microorganisms are able to support conditions such as high pressure or temperature [1]. *Desulfovibrio* (*D.*) genus has been the most extensively studied of the SRB members, both at the biochemical and physiological level, due to its extreme versatility [10].

The first species of *Desulfovibrio* genera was identified in 1895 by W. M. Beyerink in contaminated sewage and since then various species and strains of *Desulfovibrio* have been described, between then *D. vulgaris* Hildenborough (in 1946) [11]. Belonging to the sulphate-reducing class of bacteria that are ubiquitous in Nature, *D. vulgaris* Hildenborough presents the major metabolic versatility and is actually an organism of great interest by researchers [12]. Present in places with high toxicity levels due to heavy metal contamination (as uranium and chromate) or high concentration of nitrates, *Desulfovibrio* genus is able to colonize almost all kind of environments [4].

D. vulgaris Hildenborough was initially envisage as a strict anaerobic organism, however, studies suggested that it is in fact an aero-tolerant microorganism [10]. *D. vulgaris* Hildenborough was the first SRB to have its genome completely sequenced, which allowed functional genomic studies in order to expand the understanding of its electron transport and energy transduction mechanisms, as well as other metabolic studies [12]. Several genomic studies have shown that *D. vulgaris* Hildenborough is involved in the activation of different response pathways that are specific in a wide range of stresses [13]. A high number of response regulators have been reported to be involved in signal transduction, since *D. vulgaris* Hildenborough genome encode 64 histidine kinase sensors and 74 response regulators involved in the detection and integration of environmental stimulus [13], [14]. This diversity is believed

to be related to the various stresses that SRB face in its growth environments [4]. The fact that this microorganism is easily and rapidly grown renders it a perfect genetic, biochemical and genomic tool to investigate and perform physiological studies, using it as a model for SRB [4], [11].

In terms of metabolic features, *D. vulgaris* Hildenborough belongs to a group of incompletely-oxidizing sulphate reducers, in which acetate is formed by enzymatic oxidation of organic acids and alcohols, subsequently operating as electron donor for sulphate reduction [12]. Fumarate, ethanol, malate, lactate or pyruvate can also act as electron donors to sulphide reduction [12]. This species generate energy by reducing sulphate, playing an important role in sulphur cycle and complete mineralization of organic matter [4]. Capable of chemolithotrophic growth, this microorganism can also use H_2 as electron donor to sulphate reduction, using acetate and CO_2 as carbon source [4].

Although its pejorative impacts as biocorrosion agent (in oils and gas pipelines in oceans), this organism also acts as a bioremediator agent, making it economically viable [1].

1.3 Iron-sulphur Proteins

Iron-sulphur clusters ([Fe-S] clusters) are considered the most ancient and versatile inorganic cofactors being widely distributed in all kingdoms life [18]. Chemical versatility of these clusters allied with the abundance of iron and sulphur in prebiotic Earth, facilitated their use in a large number of different proteins (referred to Fe-S proteins), such as simply structural cofactors, redox sensors or catalysts [12]. Composed of iron and inorganic sulphide, these [Fe-S] clusters are formed from attachment to the polypeptide chain primarily via cysteinate iron ligation [19]. Other metals apart from iron can be part of these clusters, such as nickel and molybdenum, however these are less common [20].

[Fe-S] clusters can participate in a wide range of biological and biochemical processes, such as biosynthesis of [Fe-S] clusters, substrate binding and catalysis, DNA repair and gene regulation, central metabolism or even respiration [15], [16]. Biological electron transfer is the main functional role of [Fe-S] clusters, since they are able to delocalize electron density over both Fe and S atoms [16]. Propensity of iron to formally switch between oxidative states + 2 and + 3, makes [Fe-S] clusters excellent donors and acceptors of electrons in many biological reactions [15]. [Fe-S] clusters are also used in enzyme catalysis because they are able to reach very low reduction potentials, being able to reduce redox resistant substrates [15], [17]. These

clusters also play an important role in sensing environmental or intracellular conditions for regulation of gene expression due to their reversible interconversion between clusters [15], [17].

[Fe-S] clusters may be distinguished by the number of iron and inorganic sulphur atoms present in their structure as [1Fe], [2Fe-2S], [3Fe-4S] and [4Fe-4S] [20]. In general, [Fe-S] clusters feature two main conformations, rhombic [2Fe-2S] and cubic [4Fe-4S] types [18]. Both clusters contain iron atoms however its oxidation state can differ depending on the type of cluster, number of ferrous (Fe^{2+}) or ferric (Fe^{3+}) iron, and sulphide (S^{2-}) that present always the same oxidation state [21]. [Fe-S] clusters are usually integrated into proteins via coordination of the iron ions by cysteine or histidine residues, but in more complex clusters alternative ligands have also been observed (Asp, Ser, CO or CN-) [18], [22].

1.3.1 Types of [Fe-S] Clusters

As previously mentioned, [Fe-S] cluster can be classified based on the number of iron and sulphur atoms in the cluster [16]. In addition to the number of atoms, protein can also be classified due to certain structural motifs and spectroscopic and electrochemical properties [18]. Four main groups of Fe-S proteins can be identified based on the type of cluster that they possess ([1Fe], [2Fe-2S], [3Fe-4S] or [4Fe-4S] cluster) (Figure 1.2) [18].

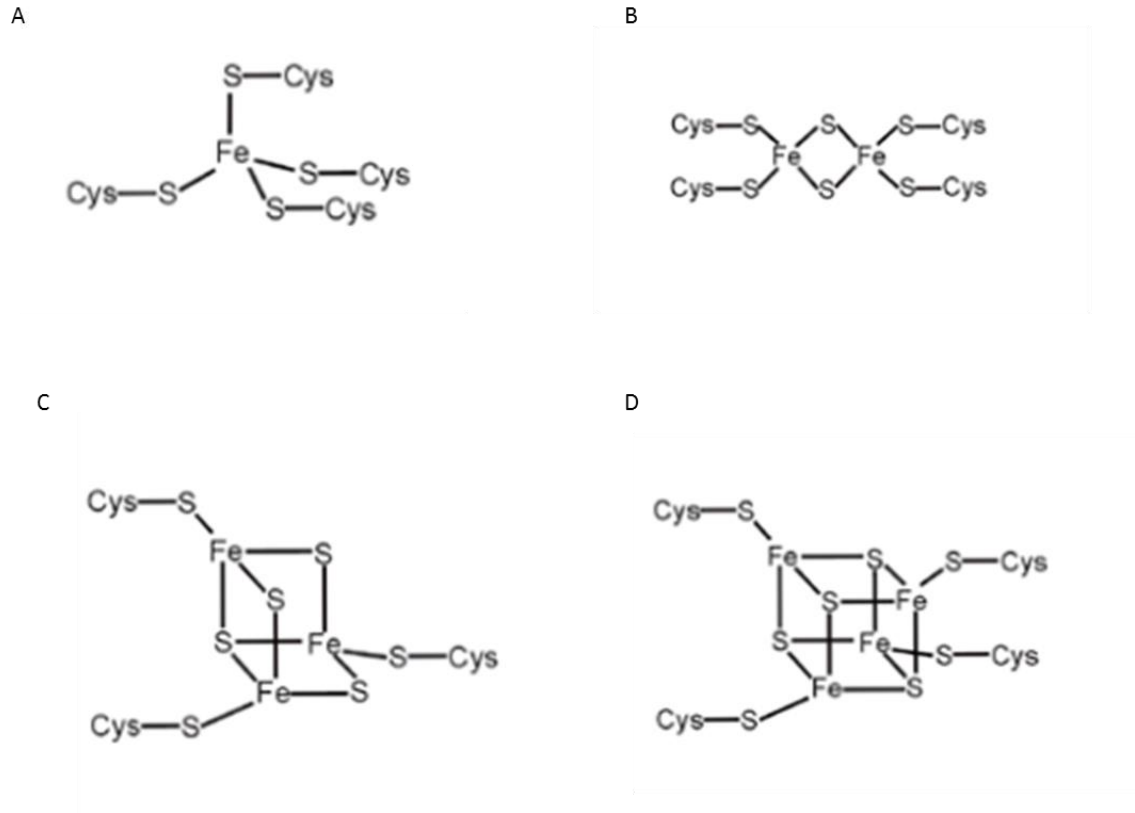

Figure 1.2 - Schematic representation of different types of [Fe-S] clusters. A – [1Fe] cluster. B – [2Fe-2S] cluster. C – [3Fe-4S] cluster. D – [4Fe-4S] cluster. Image from [19]

Rubredoxins (Rd) are the simplest group of Fe-S proteins mainly found in Bacteria, Archaea and anaerobes [20]. With approximately 55 residues, these proteins have a unique [1Fe] cluster and does not have inorganic sulphur [20]. The single iron atom is coordinated by four thiolate ligands provided by cysteine segments located around the cluster [17]. As other Fe-S proteins, rubredoxins are electron carriers in several redox chains, such as oxygenation reactions or protection against reactive oxygen species (ROS) [16]. Able to switch between two redox states, $[1Fe]^{3+}$ and $[1Fe]^{2+}$, rubredoxins can reach reduction potentials ranging from - 100 to + 200 mV [18]. The iron in this metal centre can also be replaced by other metals, such as cobalt, nickel and zinc, *in vitro*, which makes them an interesting group of proteins [18].

Several proteins, such as plant type ferredoxins (involved in electron transport between photosystem I and several enzymes), biothin synthase (involved in the conversion of desthiobiotin into biotin by sulphur donation) or MitoNEET (involved in redox-sensitive signalling in [Fe-S] cluster transfer) coordinate a [2Fe-2S] cluster [20]. This cluster can exist in two redox states, $[2Fe\text{-}2S]^{2+}$ and $[2Fe\text{-}2S]^{1+}$, possessing a high reducing power since their

reduction potentials can range from - 250 to - 420 mV [16]. EPR active, iron sites of [2Fe-2S] clusters in the reduced form present an S = 1/2 group state resulting in localized valences (S = 5/2 /(Fe^{3+}) and S = 2 (Fe^{2+})) antiferromagnetially coupled [16]. A subclass of the [2Fe-2S] protein is composed by the Rieske proteins, where [Fe-S] cluster is coordinated by a nitrogen atom of a histidine residue instead of the usual cysteine sulphur [20]. These proteins were first discovered as subunits of respiratory and photosynthetic electron-transfer complexes, and later identified in small electron-transfer proteins, such as ferredoxins, bacterial and eukaryotic oxygenases [18]. With the same redox transition as other 2Fe-2S proteins, the Rieske protein have the highest reduction potential of these type of centres due to the presence of the histidine ligation, reaching positive redox potential from + 400 to + 100 mV [17], [18].

[3Fe-4S] clusters were firstly recognized in anaerobic nitrogen-fixing bacterium *Azotobacter vinelandii*, that beside a [3Fe-4S] cluster also holds a [4Fe-4S] cluster [16]. This cluster was later identified in two other proteins (*D. gigas* ferredoxin II and aconitase), as well as in other ferredoxins and several enzymes, such as succinate dehydrogenase, nitrate reductase and [NiFe] hydrogenases [18]. Coordinating four cysteine residues this type of cluster, like other Fe-S proteins, presents magnetic and electronic properties [18]. Two stabilized oxidation states were observed in these clusters, + 1 and 0. In the oxidized state + 1, the cluster exhibits an isotropic EPR signal resulting in spin coupled form (S = 1/2) of three high-spin ferric ions, the signal is lost when the cluster is reduced to the $[3Fe\text{-}4S]^0$ state [20]. The redox potential of this redox pair varies between - 70 and - 460 mV, depending on the protein [20]. The interconversion of [3Fe-4S] into [4Fe-4S] clusters can occur (particularly in proteins where the fourth iron atom is not coordinated by a cysteinyl ligand**)** and have been extensively studied in order to better understand the presence of iron-sulphur in enzymes like aconitase [18]. This type of clusters is rare when compared with other [Fe-S] clusters, like [2Fe-2S] and [4Fe-4S], that are more ubiquitously distributed [17].

Several proteins present in bacteria, mammalian tissues and some plants are constituted by [4Fe-4S] clusters [21]. These are one of the most common [Fe-S] clusters found in Nature and function mainly as ubiquitous electron transfer members in anaerobic bacteria [20], [22]. In some organisms, such as *Clostridium*, these proteins also play a role as immediate electron donor to nitrogenase and hydrogenase [20].

First detected in *Desulfovibrio gigas*, this type of cluster acts as electron paramagnetic resonance signatures in mitochondrial membrane proteins and are also involved in electron transfer in small proteins, such as ferredoxins (Fds) [16]. Ferredoxins are one of the major classes of electron transfer proteins in Nature [18]. These are important in a series of processes

essentials to life as oxidative phosphorylation, nitrogen fixation and photosynthesis [18]. Ferredoxins are usually distinct based on their reduction potential in two major classes: low-potential Fe-S proteins (- 150 to - 700 mV) and high-potential Fe-S proteins (+ 100 to + 450 mV), HiPIPs [16]. Although the distinction made between these proteins, these are all classified as ferredoxins and have in common the presence of a [4Fe-4S] cluster [16].

Metalloproteins usually coordinate metals using amino acid residue as ligands to increase stability [20]. Concerning [Fe-S] clusters, the most commonly observed ligand is cysteine [22]. In most ferredoxins, the [4Fe-4S] cluster is bound to the polypeptide recurring to cysteines residues, that link to Fe provide four thiolate donors to the 1Fe, 2Fe or 4Fe cluster [16], [20]. However, there are also others amino acids residues that have been observed as histidine, glutamine, aspartate or serine (Table 1.1) [22].

Table 1.1 - Structural motifs of different [4Fe-4S].

Protein	Iron-Sulphur Ligation Mode	Reference
4Fe Ferredoxin	Cys8 Cys11 Cys14 Cys50	[23]
4Fe Ferredoxin (*Pyrococcus furiosus*)	Cys12 **Asp15(Nδ)** Cys18 Cys57	[24]
8Fe Ferredoxin	Cys8 Cys11 Cys14 Cys47	[25]
8Fe Ferredoxin (2x [4Fe-4S])	Cys18 Cys37 Cys40 Cys43	[25]
HiPIP	Cys41 Cys46 Cys61 Cys75	[26]
Hybrid cluster protein	Cys3 Cys6 Cys15 Cys21	[27]
[NiFe] hydrogenase	**His185(N)** Cys188 Cys213 Cys219	[28]
[FeFe] hydrogenase	**His94(N)** Cys98 Cys101 Cys107	[29]

Due to its disposition in the cluster, iron and sulphur atoms are positioned alternatively in the apexes causing the cluster to take the form of a distorted cube [18]. The cysteine ligands are arranged in a Cys-X_2-Cys-X_2-Cys, the so-called [4Fe-4S] motif [16]. In this particular motif, three iron atoms are bound to almost adjacent cysteines, while the last one is bound to a more distant cysteine residue in the polypeptide chain [16]. The fact that the cluster is bound by cysteine residues from different parts of the polypeptide chain confers an extra stabilization of the tertiary structure of the protein [16].

The [4Fe-4S] clusters can exist in three stable oxidation states in proteins, which allows the change between two oxidation states through a simple electron transfer [20]. For this structure, the three accessible states are $[4Fe\text{-}4S]^{3+}$, $[4Fe\text{-}4S]^{2+}$ and $[4Fe\text{-}4S]^{1+}$ corresponding to

[$3Fe^{3+}$- Fe^{2+}], [$2Fe^{3+}$- $2Fe^{2+}$] and [Fe^{3+}- $3Fe^{2+}$] valence-state combinations, respectively [20], [22].

Usually proteins can present one or more [Fe-S] clusters [18]. In the case of a protein with more than one cluster, it will usually present a brown colour and a broad absorption band in the 380-400 nm region [18]. Characteristic of proteins containing $[4Fe\text{-}4S]^{2+}$ clusters, this absorption band arises from [Fe-S] charge transfer bands resulting from the interaction of [Fe-S] clusters [21]. Studies indicate that the absorption band observed is attributed to *d-d* transitions of Fe^{2+} atoms from the lowest layer *d* orbital into t_{2g} sets [18]. The overlapping of bands from S $\rightarrow$ Fe^{3+} charge transfer results in a spectrum with a broad absorption band [18].

EPR spectroscopy is also used to characterize this type of metal clusters [21]. Weak spin-spin interactions between paramagnetic clusters are responsible for the appearance of the EPR signal [21]. [4Fe-4S] clusters exhibit EPR resonances, detectable at low temperatures (below 35 K), only when the cluster is in the Fe^{3+} - $3Fe^{2+}$ (S = 1/2) state, being EPR silent when it goes to a $2Fe^{3+}$ - $2Fe^{2+}$ state (S = 0) [18]. Depending on the polypeptide environment and number of [4Fe-4S] clusters present in the protein, the EPR spectrum can exhibit different forms [18]. In the case of a single $[4Fe\text{-}4S]^{1+}$ cluster, the spectrum can present either an axial or rhombic signal, while a more complex EPR spectrum is observed in the presence of two $[4Fe\text{-}4S]^{1+}$ clusters [21]. $[4Fe\text{-}4S]^{3+}$ cluster spectrum is also more sensitive to peptide environment comparing to that of a $[4Fe\text{-}4S]^{1+}$ cluster [18].

1.3.2 Biosynthesis of Iron-Sulphur Clusters

In the 1990s, scientists improved chemical assemble of [Fe-S] clusters into apoproteins, determining that this process *in vitro* was different from what occurring *in vivo* [15]. Fe-S assembly require sources of inorganic iron and sulphur, although *in vitro* this can be achieved by spontaneous processes, with FeCl and Na_2S through metallic reconstitution, in living cells this process is more complex and needs to be catalysed [12]. Thus, organisms need to resort to multicomponent systems, so-called Fe-S biogenesis systems, to perform the production of Fe-S proteins [17]. Cellular surroundings are also protected by these systems, avoiding potentially harmful effects of free Fe^{2+} , Fe^{3+} and S^{2-} ions [17]. Depending on the organism, the number and the type of Fe-S biogenesis systems varies, also as the enzymes and compounds involved [12]. Three different systems for the biogenesis of bacterial Fe-S proteins have been identified based on biochemical evidence and organization of genes in bacterial operons: NIF, ISC and SUF systems [15], [30].

NIF system (Figure 1.3) is specific for the maturation of nitrogenase in azotrophic bacteria, being involved in nitrogen fixation, ISC and SUF systems are more common in prokaryotes [12], [16]. ISC system have as main objective to promote the formation of [Fe-S] clusters, while SUF system clusters in mobilization of sulphur [16]. Conserved in eubacteria and eukaryotes (mitochondria), ISC system has a broad specificity targeting general Fe-S proteins [12]. SUF system represent an alternative pathway to the ICS system and operates under iron starvation and can be found in eubacteria, archaea and eukaryotes (plastids) [15]. However, both act in maturation of all Fe-S proteins in the cell and are important for their organization under normal and oxidative-stress conditions, respectively [12].

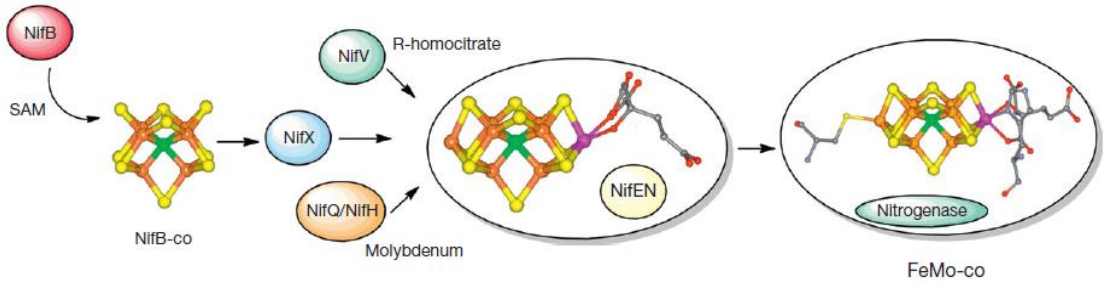

Figure 1.3 – Biochemical model of the NIF system specifically FeMo-co biosynthesis in nitrogenase maturation. Image from [31].

Fe-S biogenesis is a molecular process divided in two major steps: assembly and traffic [17]. The ISC system (Figure 1.4) consists in a set of genes that encodes several proteins necessary to its operation, such as a regulator (IscR), a cysteine desulphurase (IscS), a scaffold (IscU in bacteria and Isc1 in mitochondria), an A-type protein (IscA), a DnaJ-like co-chaperone (HscB), a DnaK-like chaperone (HscA) and a ferredoxin (Fdx) [17]. In the first step, sulphur is acquired from amino acid L-cysteine produced by the cysteine desulphurase (IscS) [17]. This reaction involves the conversion of L-cysteine into L-alanine through IscS and the release of a sulphur atom, in the form of a hydrogen disulphide [17]. Scaffold proteins contain three conserved cysteine residues (Cys37, Cys63 and Cys106) that helps in coordination of the [Fe-S] cluster [16]. Iron is provided to the system through CyaY protein, which is an iron donor [17]. A close interaction between it and the components of *isc* operon is necessary to provide iron atoms to the system, preventing any leakage of harmful free ions [17].

Since sulphur present in cysteine residues is in a S^0 form, it is necessary that a reduction to sulphide (S^{2-}) occurs in order for it to be used in the [Fe-S] cluster [15]. An electron transfer

mechanism generally provided by ferredoxin reductase and ferredoxin of the Isc assembly machineries is required for that step [15]. Then the [Fe-S] cluster is initially assembled in the scaffold proteins (IscU) [15]. IscU is necessary because it interacts with IscS and the iron source, allowing sulphur and iron to meet, receiving sulphur directly from IscS [12]. The IscU-IscS interaction is provided by the chemical and structural environment prepared, which facilitates the formation of the [Fe-S] cluster [12], [17]. The second step refers to the release of the [Fe-S] cluster from IscS-IscU, through interaction with an ATP-hydrolysing component [12], [15]. HscA and HscB, two members of DnaK/DnaJ chaperones/co-chaperones family, increase the cluster transfer rate [12]. HscA interacts with IscU while HscB regulates their interaction with the scaffold protein [12]. Then transfer to apo-protein targets occurs by coordination with specific amino acid residues and finally its assembly into the apo-protein [15]. The contribution of these components to [Fe-S] cluster biogenesis is crucial, as indicated by the gene knockout experiments performed [17].

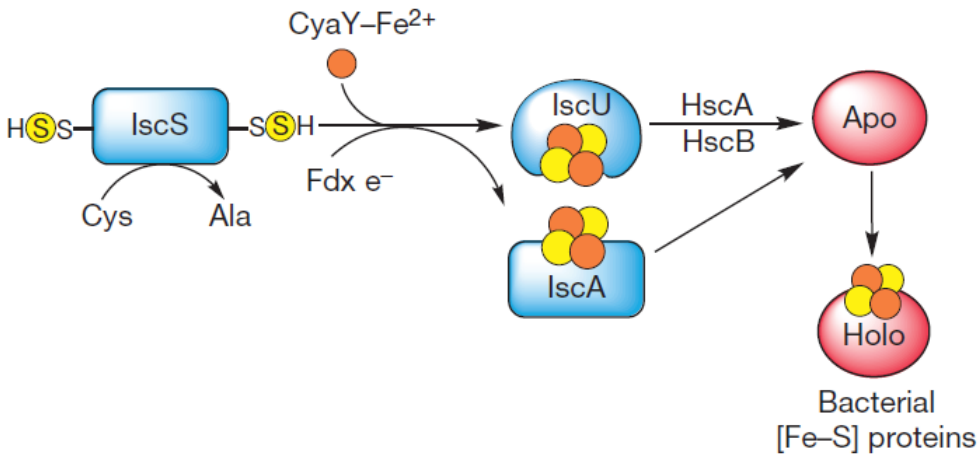

Figure 1.4 – Schematic model for the bacterial iron-sulphur protein biosynthesis by the ISC machinery. Image from [31].

In vitro experiments demonstrated that when $FeCl_3$, L-cysteine and IscS are incubated with IscU, this last protein binds and forms a [Fe-S] cluster in a sequential way [17]. Starting with a dimeric form containing one [2Fe-2S] cluster, IscU then converts it to two [2Fe-S2] clusters and finally to one [4Fe-4S] cluster [17]. Exposure to oxic conditions reverses this process, converting a [4Fe-4S] cluster back into a [2Fe-2S] cluster [17]. Despite that this is not a reversible electrochemical process, spectroscopic studies support that theory [17].

SUF and ISC systems play the same role in [Fe-S] cluster biogenesis, however are triggered under different environmental conditions [30]. When organisms are under oxidative-stress or iron limitation conditions, SUF system is activated [30]. The *suf* operon encodes an A-type protein (SufA), a heterodimeric cysteine desulphurase (composed of SufS and SufE) and a pseudo-ABC (ATP-binding cassette)-transporter (composed of SufB, SufC and SufD) that might act as a scaffold, as binding and transfer of [4Fe-4S] clusters to apo-protein is mediated by SufBCD complex [12], [30]. Interaction of SufB and SufD is involved in iron entry into the complex, SufB acts as a scaffold promoting the formation of the cluster [18]. Role of SufC is not clear yet [12]. The heterodimeric complex SufSE acts as the sulphur donor for [Fe-S] cluster assembly. SufS is a homologue of IscS, a cysteine desulphurase, which mobilizes sulphur from L-cysteine, while SufE enhances SufS activity [12]. SufE exhibits a structure similar to that of IscU, but is unable to bind a cluster or interact with HscA/B [12]. Sulphur is then transferred from SufS to SufE and finally to SufB [12]. The assembly of [2Fe- 2S] to [4Fe-4S] occurs thanks to SufA, that acts as a scaffold protein [12].

[Fe-S] biogenesis regulation is important to maintain, rebuild and when necessary repair groups of [Fe-S] cluster-containing proteins in environments with variable conditions [12]. Regulation of ISC and SUF systems is made by [Fe-S] proteins present in each operon, namely IscR and SufR, respectively [15]. These proteins act as transcriptional repressors of their respective operons [15]. In case of iron deficiency or oxidative stress, regulator IscR in the apo form activates SUF operon [30]. The accumulation of apo IscR that occurs, leads to induction of the expression of both operons and consequently accumulation of both systems in the cell [12]. Efficiency of Fe-S proteins maturation depends in this way on the expression of the two operons [15]. IscR also acts as a sensor for Fe-S homeostasis [12]. Due to capacity to detect poorest Fe-S substrates in ISC machinery, IscR is able to instruct the cell about the equilibrium between [Fe-S] cluster demand and its capacity to respond to it [12].

1.4 Motives commonly found in ATPases

Some structural elements (or motifs) can be conserved among different proteins representing a specific pattern of required or permitted amino acids and it may be associated with certain functions [32]. The study of sequences through database similarity search (performed by bioinformatics programs as FASTA or BLAST) allows the identification of common patterns along proteins or family of proteins [32]. The results associated with these

experiments enables the association of certain motifs to a particular function, making it easier to study related or analogous proteins [32].

In the past few years, computer-assisted comparative analysis of amino acid sequences has had significant impact on the identification and functional characterization of the nucleic acid-dependent ATPases [33]. These proteins can present a group of several conserved motifs that are normally found in the nucleotide binding domain (NBD): the Walker motif, Q-loop, signature, D-loop and H-loop [33], [34]. Three main conserved motifs can be found in ATPases of the ATP-binding cassette family: P-loop, the Walker A and the Walker B motifs [32], [35].

Regions of highest sequence homology in ATPases (the putative ATP-binding domains) are generally maintained in this type of proteins and appears in the form of the so-called Walker-type purine NTP binding pattern [33], [36]. Represented as the sequence GXXXXGKT (X, any residue) this motif has a common nucleotide binding fold in several ATP-requiring enzymes and was first recognized by Walker and colleagues in 1982 [37]. Found in many proteins that bind nucleotides, crystal structure data of this proteins indicated that this motif is present in a loop around nucleotides and uses its highly conserved residues of lysine and threonine to bind to the phosphate oxygen atoms [37]. Due to this structural characteristic, the consensus sequence of GXXXXGKT (S) (with serine substituting threonine in some cases) is also commonly known as Walker loop or P-loop (phosphate binding loop) [37]. P-loop NTPases represent a large protein family that are involved in a variety of cellular functions as signal transduction, protein transport, translation, membrane transport, among others [35].

The Walker ATPase domain consists of two separate motifs, the conserved Walker A and Walker B motifs, crucial components of the nucleotide binding site [36].

The Walker A ATP-binding motif (also called the P-loop or phosphate-binding loop) is a common feature of P-loop NTPase fold that bind nucleotide [33]. Known as one of the most common and highly conserved motifs found in genomes, this pattern is considered to be a fundamental and ancient functional motif in biological systems [38]. Several studies proved that the Walker sequence is widely distributed and that the P-loop structure is not restricted to nucleotide binding proteins [37]. Proteins that use and bind nucleotide phosphates also share this common loop structure being present, for example, in kinases, phosphatases, ATPases and heat shock proteins [37]. More recent studies have proved the existence of this type of motifs in ATPase protein and this pattern is believed to be essential for proteins' ATPase activity [39].

Experiments have shown that the lysine residue in the GKT/S box of the Walker A motif is essential for the ATP/GTP-binding and contact the phosphate of the nucleotide [36].

This motif has been proven to have as main function to stabilize the hydrolysis transition state by counteracting the build-up negative charge that occurs in the protein [34]. Studies have indicated that Walker A also play a role in catalysis due to high closeness value of some invariant residues (G, K and S/T) [35].

Another motif present in proteins that is associated with phosphate binding is the Walker B motif [38]. This consensus pattern is present in most P-loop proteins situated well downstream of the Walker A motif [38]. This motif is normally represented by the consensus sequence R/K-X-X-X-G-X-X-X-L-h-h-h-h-D (X, any residue and h, hydrophobic residue) [38], [40]. Two main residues present in Walker B sequence are important for its function: the aspartate and the glutamate residues [40]. Aspartate is virtually always involved in binding of the Mg^{2+} cation and the glutamate that follows the aspartate is believed to be the catalytic base that abstracts a proton from the attacking water molecule [34].

Containing a highly conserved aspartate/glutamate residue, the Walker B motif is involved in the formation of hydrogen bonds with the threonine/serine of the GKT/S box of Walker A, facilitating nucleotide hydrolysis upon the bound of a water molecule [36]. Mutations in either Walker A lysine or Walker B glutamate leads to defects in this procedure leading to the belief that the conjugation of these two motifs is indispensable for ATPase activity [41].

1.5 The Orange Protein – Novel Mo-Cu Cluster

Isolated for the first time from the sulphate reducing organism *D. gigas*, the orange protein (ORP) presents a unique type of mixed metal sulphur cluster [42]. A genomic search showed that the gene encoding ORP is present in many organisms that are syntrophic with methanogenic archaea, such as others species of *Desulfovibrio*, examples being *D. vulgaris* Hildenborough and *D. desulfuricans* G20 [43]. This novel and unique metal core was identified by EXAFS (*Extended X-Ray Absorption Fine Structure)* analysis as containing two different metals, molybdenum and copper, in a coordination of the type $[S_2MoS_2CuS_2MoS_2]^{3-}$, being the cofactor stoichiometry 2Mo:1Cu:8S (Figure 1.5) [43]. With approximately 12 kDa and 117 residues, this protein is not attached to the polypeptide chain [43]. This is the only known biological heterometal sulphide cluster that does not contain an iron atom [42].

Molybdenum is generally found in soils in the form of molybdate (ion MoO_4^{2-}), but sulphide producing bacteria in rumen induces its transformation into thiomolybdates (TMs)

[44]. Also, copper has an important functional and structural role, being present in many proteins and enzymes [44], [45]. Due to their ability to sequester copper, TMs play an antagonist role with this element, which results in it deficiency in organisms [45], [46]. Due to this problem and because of the known reactivity between copper and TM, the detection of a protein containing a Mo-Cu cluster in its native state was a surprise for scientists [43].

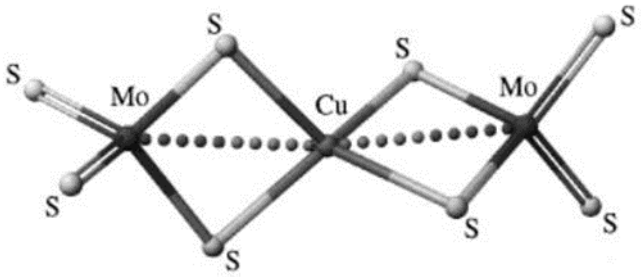

Figure 1.5 – Structure of heterometalic cluster of ORP [$S_2MoS_2CuS_2MoS_2$] proposed by EXAFS analysis. Image from [42].

EXAFS analysis allowed to determine the relative distance between the atoms present in the heterometalic cluster [43]. Studies indicates that for molybdenum atom four Mo-S links are present distanced by 2.21 Å, in an interaction Mo···Cu at 2.75 Å, while in the case of copper it was set the presence of four links Cu-S at 2.31 Å, with two interactions Cu···Mo at 2.74 Å [47] [42]. Spectra obtained from this analysis indicated a thio-coordination between Mo and Cu atoms, in which Mo is at + 6 and Cu + 1 oxidation state, with approximately tetrahedral geometry [47], [48]. Recent studies have shown that electrostatic and hydrophobic interactions are responsible for Mo-Cu cluster binding, but unlike other clusters, this connexion does not involve cysteine, histidine or methionine side chains as metal binding residues [43] [42]. Reconstitution experiments performed by Carepo and co-workers through different strategies in apo-ORP have allowed to deepened the knowledge about this topic [43]. NMR and visible analysis of presynthesized inorganic cluster added to apo-ORP indicates that minor and no spectroscopic changes, respectively, are observed when the cluster binds to the protein [47]. Contrary to the expected of a bulky metal cluster, studies suggest that Mo-Cu cluster binds on the surface of the protein [47], [48]. NMR data suggested that positive residues and bulky hydrophobic side chains are involved in the binding in a way to stabilize the metal clusters that

is negatively charged [43]. The presence of EPR active species was not detected in the native protein [43].

Information about secondary structure of ORP was provided by far-UV CD analysis indicating that the protein contains α-helical motifs (31 %) as main secondary structure followed by β-turns (30 %), β-strands (10 %) and other unordered forms (29%) [48].

Spectroscopic studies features two absorption maxima at 340 and 480 nm in the UV-visible spectrum of ORP corresponding to ligand to-metal charge-transfer band involving molybdenum (Figure 1.6) [43].

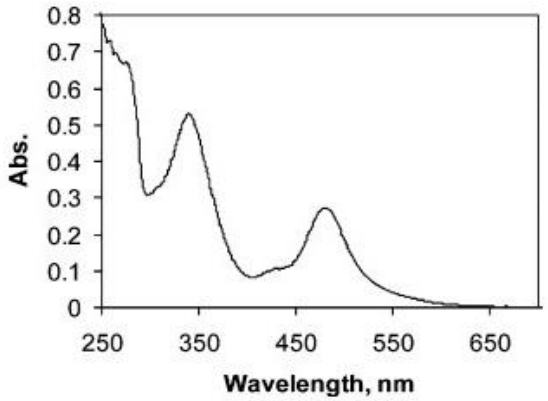

Figure 1.6 – UV-visible spectrum of native ORP from *D.* gigas in 50 mM Tris-HCl pH 7.6 and 60 mM NaCl buffer. Adapted from [43].

The exact function of ORP is not yet known, but one hypothesis that has been raised is that this protein is involved in the activation of a metabolic pathways when growth conditions change from syntrophic to sulphate reducing [47]. Resorting to databases, it was possible to compare ORP with other hypothetical proteins, some of them conserved, from hyperthermophilic archaea and eubacteria, revealing some similarities between them [43]. It has been proposed also that the Mo-Cu-S cluster observed in ORP is involved in anaerobic cell division of SRB of *D. vulgaris* Hildenborough (see below) [42]. Due to the chemical properties of its cofactor, ORP might also play a role as a Cu-scavenger, metal storage protein or even have a function in electron reduction [43].

Studies of bacterial genomes revealed that their genome encoded more than 30 % hypothetical and conserved hypothetical proteins whose function remains unknown [49]. In anaerobic organisms, many of these proteins play important roles in anaerobic processes

essential to maintain their way of life [43]. In order to know more about these proteins, COG database (cluster of group of orthologous proteins database), a bioinformatics tool was used to compare genomes from anaerobic and aerobic microorganisms [50]. This allowed the identification of 33 COGs that are now considered specific to the anaerobic way of life of several organisms [51]. COG1433 contain uncharacterized conserved proteins and is one of the five COGs that were assumed to play a crucial role in anaerobiosis [51]. In *D. vulgaris* Hildenborough species, three protein locus tags belong to COG1433, which are DVU2107, DVU2108 and DVU2109 [49]. While DVU2107 and DVU2108 are two putative proteins completely comprised in COG1433 domain, DVU2109 is composed of two domains: one belonging to COG1433 (the N-terminal domain) and another that belongs to COG0489 (the C-terminal domain) [49], [50]. Homologues of *DVU2108* genes are present in most archaeal and several bacterial genomes and phylogenetic analysis shows that these tend to be systematically clustered with other two proteins, DVU2103 and DVU2104 [50]. Belonging to COG1149, DVU2103 and DVU2104, which are 41 % similar to one another [50].

In the case of *D. vulgaris* Hildenborough, the structural organization of these proteins shows that *DVU2108* is located in a divergent cluster from genes *DVU2103* and *DVU2104* [9]. *DVU2107*, *DVU2108* and *DVU2109* genes form a gene cluster with a transcriptional direction opposite to that of the gene cluster constituted by *DVU210*3, *DVU2104* and *DVU2105* [9]. Between these divergent gene clusters is located *DVU2106*, that encodes a σ^{54}-dependent transcription factor [9]. All these genes together constitute a large cluster named *orp* gene cluster [9]. PCR analysis allowed the interpretation of *orp* gene cluster organization, indicating that this is constituted by three different transcriptional units, two separated operons, *DVU2103-DVU2104-DVU2105* genes (*orp2*) and *DVU2107-DVU2108-DVU2109* genes (*orp1*) separated by the monocistronic transcriptional unit, *DVU2106* (Figure 1.7) [49].

Physiological ORP complex is constituted by several proteins encoded in both *orp1* and *orp2* operons [49].

Figure 1.7 - Schematic representation of genes belonging to the *orp* gene cluster in *D. vulgaris* Hildenborough. Adapted from [49].

Fiévet and co-workers demonstrated that the expression of *orp1* and *orp2* was dependent on the σ^{54}-RNA polymerase [49]. Two consensus sequences in DNA at 35 bp and 43 bp upstream of the translational starting sites of the *orp1* and *orp2* operons were identified as locals where σ^{54} factor binds [49]. This discovery suggests that the transcription of both operons depends on σ^{54}-RNA polymerase [49]. Besides RNA polymerase associated with σ^{54}, another specialized transcription factor is also necessary to initiate transcription at σ^{54} promoters, which are the EBP (*Enhancer Binding activators Proteins*) [49]. EBPs are required to initiate transcription since they are responsible for the opening of the σ^{54} – RNA polymerase promoter complex, through a catalysed ATP hydrolysis reaction [52]. Three common domain structures are shared by most σ^{54} – associated EBPs: the C-terminal DNA-binding domain, the central module carrying the ATPase activity and responsible for interaction with the σ^{54} – RNA polymerase, and the N-terminal regulatory domain [53]. Environmental stimuli control σ^{54} – dependent transcription activation through the most variable part of EBP structure, the regulatory module [49]. *DVU2106* gene possess a PAS domain (Per-ARNT-Sim) attached to the N-terminal regulatory domain, that acts as a sensor detecting a still unknown chemical and physical stimuli (such as oxygen, light or redox potential) that is responsible for the regulatory processes [49]. Studies have proved the association of the PAS domain of *DVU2106* with the expression of the *orp* gene cluster when lifestyle is switched from syntrophic to sulphate reduction in *Desulfovibrio* [49].

Experimental data obtained by Fiévet and co-workers have proven that *DVU2106* regulator binds specifically to the intergenic region of the *orp1* and *orp2* operons [49]. The influence of σ^{54} – RNA polymerase and the role of *DVU2106* on the expression of the two operons and of *DVU2106* itself was evaluated recurring to gene fusion experiments [49]. *E. coli* strain was used to express heterologously a constructed *lacZ* vector in order to measure β-galactosidase activities in two conditions: σ^{54} – proficient (wild-type (WT) strain) and σ^{54} –

deficient (Δ*rpoN* strain) [49]. A very low activity was detected for *orp1* and *orp2* promoter fusions, however no difference was observed between the strains [49]. For *DVU2106* expression, the activity of the fusions increased in the wild-type in the presence of DVU2106, while in the case of Δ*rpoN* strain the production of DVU2106 do not caused any change [49]. The data obtained revealed that the transcription of *orp1* and *orp2* is dependent on the simultaneous presence of σ^{54} – RNA polymerase and DVU2106, while in contrast *DVU2106* expression is independent of σ^{54} [49]. *DVU2106-lacZ* fusion experiments also revealed that DVU2106 negatively retro-controls its own expression, as its over-expression led to a significant decrease of *DVU2106-lacZ* fusion activity [49].

Monocistronic transcriptional unit *DVU2106*, encodes a homologue EBP that binds to the promoter regions of the *orp1* and *orp2* operons, allowing the positive control of the expression of these genes, such as its own regulation, by factor σ^{70} of RNA polymerase [49]. Under anaerobic lactate/sulphate conditions, experimental data shows similar transcription levels of *orp1* and *orp2* operons in *D. vulgaris* Hildenborough, while expression of *DVU2106* is about 300 times lower [49]. Expression of *orp2* occurs mainly due to the presence of a functional σ^{54} promoter, however *DVU2106* is not controlled by this component [49]. This explains the differences between the transcription levels registered [49]. Transcriptional regulator *DVU2106* is responsible for the activation of the transcription of the two divergent operons *orp1* and *orp2*, but also controls negatively its own expression [49]. Data collected by Fiévet and collaborators shows that, since the *orp1* and *orp2* operons are co-regulated, the corresponding gene products are expected to collaborate in the same metabolic pathway [49]. Endogenous pull-down experiments provided evidence that some of the protein present in this operon interact with each other, due to synchronized expression of DVU2103, DVU2104 and DVU2108 [49]. This was the first evidence that DVU2103, DVU2104, DVU2105, DVU2108 and DVU2109 physically interact *in vivo* and form a physiological multiprotein complex (Figure 1.8) [49].

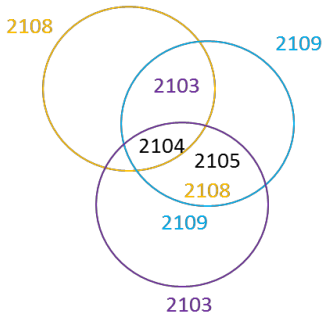

Figure 1.8 - Schematic representation of ORP interaction network. Adapted from [49].

Experimental studies about *orp* operon show that when *DVU2106* is inactivated, morphological defects in the cells are observed [49]. This suggest that the absence of a functional *DVU2106* regulator, linked to the absence of the ORP complex, leads to defects in cell division or in cell growth control processes [49]. Mutant experiments performed in *D. vulgaris* Hildenborough showed that when a truncate form of *DVU2106* is produced, a drastic down regulation of both the *orp1* and *orp2* operons occurs [49]. The interaction between the intergenic regions of both operons and DVU2106 does not occur when this fragment is mutated, leading to inactivation of *orp1* and *orp2* expression [49]. The cell morphological modifications observed in these conditions, is attributed to the absence of the genes, whose transcription is dependent on *DVU2106*, and this effect is consequently attributed to the absence of the ORP complex that is thus responsible directly or indirectly for the morphological phenotype of the mutant strain [49].

1.5.1 Homologous Proteins of the *orp* operon

Further studies of proteins encoded by the *orp* operon have been performed in order to better understand the biochemical mechanisms behind this complex, as well as characterize the Fe-S proteins that constitute it.

A putative Fe-S protein from *orp* operon of *D. desulfuricans* G20 (Dde 3197) was recently studied recurring to spectroscopic and biochemical techniques [54]. *D. desulfuricans* G20 is a sulphate reducing bacterium that also present the gene that encodes ORP (*Dde*_3198) [54]. Contrary to what was observed in *D. vulgaris* Hildenborough, in *D. desulfuricans* G20 is a polycistronic unit that is under regulation of a transcriptional regulator similar to *DVU2106* (Dde_3196*)* [55]. This unit codes for several proteins: two [Fe-S] cluster ATPases (*Dde_3200* and *Dde_3201*), a MinD-like protein (*Dde_3202*) and a small putative protein (*Dde_3197*) [55]. A small protein localized in COG1433 (same as ORP) is encoded by *Dde_3197* ORF (*Open Reading Frame*) containing several cysteine residues in its primary sequence is found in *D. desulfuricans* G20 [55]. UV-visible studies demonstrated that refolded and reconstituted Dde_3197 possess a [2Fe-2S] cluster in its structure and EPR spectroscopy revealed that this protein is EPR active when reduced with a dithionite solution [54]. Complementary data suggests that one or two [2Fe-2S] clusters oxygen stable can be present in Dde_3197, being one of them more stable than the other [54]. The second labile cluster was shown to be formed from iron and sulphide stored inside the protein only under reducing conditions and upon partial destruction of the cluster [54]. One hypothesis is that this protein could assists the biosynthesis

of the ORP heteronuclear Mo-Cu clusters, which requires sulphide, which can be one of the reasons why this partial destruction occurs [54], [55]. Primary sequence analysis has indicated that cysteine residues present in Dde_3197 are not conserved in Orange Protein nor are arranged in the usual motifs found in Fe-S proteins [54].

Although binding motifs for [Fe-S] cluster have not been identified, primary sequence analysis revealed that Dde_3197 contain 8 cysteine residues (C^{21}, C^{31}, C^{61}, C^{65}, C^{67}, C^{84}, C^{107} and C^{115}) that can potentially act as binding sites in two cysteine-rich motifs: C^{62}-GGI-C^{65}-G-C^{67}-X_{16}-C^{84} and C^{21}-X_9-C^{31}-X_{76}-C^{107}-X_7-C^{115} [54]. Biochemical and spectroscopic data demonstrate that these flexible motifs only bind a single [2Fe-2S] in Dde_3197 [54]. The presence of a region with a high content of glycine residues, - C<u>GG</u>ICGC-X_{18}-CGG -, being two of them conserved, confers flexibility to the backbone of the protein, which allows it to switch between alternative conformations or be involved in protein-protein interaction associated with dynamic roles [54]. This flexibility confers to Dde_3197 the ability to alternate between conformations during the sulphur transfer process and thereby be involved in ORP complex formation [54].

As previously described, *D. vulgaris* Hidenborough operon encode six proteins organized in two distinct transcriptional units (*orp 1* and *orp2*), under the control of the same regulator [49]. Domains present in proteins of *orp* operon were analysed recurring to MicrobesOnline database, SMART and *Expasy* bioinformatics programs [56]–[58]. The identification of conserved domains through analysis of COGs of NCBI for proteins DVU2103 and DVU2104 revealed the presence, in both proteins, of a MinD superfamily P-loop ATPase domain, identifying them as ATPases. DVU2105 protein is identified as a hypothetical protein with no known domains. The regulator DVU2106, was identified as containing a AAA-type ATPase and DNA-bind domains. The presence of a domain involved in the biosynthesis of the iron-molybdenum cofactor (FeMo-co) found in the dinitrogenase enzyme of nitrogenase complex in nitrogen-fixing bacteria is found in both DVU2107 and DVU2108 proteins. Contrary to this hypothetical protein DVU2107, DVU2108 possess a MTH1175 domain in COG1433, that is conserved in the Orange protein of *D. gigas*. In the protein DVU2109, an ATPases involved in chromosome partitioning domain is present in COG489, as well as an ATPase-like, ParA/MinD and MTH1175 domain. Physical properties of these proteins are showed in Table 1.2.

Table 1.2 - Molecular Mass and pI of proteins encoded by *orp* operon of *D. vulgaris* Hildenborough. Data obtained by [56]–[58]

Protein Name	Nr. residues	MM (kDa)	pI	Domain
DVU2103	287	30.5	5.8	[Fe-S] cluster binding Min D superfamily P-loop ATPase
DVU2104	301	31.4	5.6	[Fe-S] cluster binding Min D superfamily P-loop ATPase
DVU2105	170	16.8	11.1	Hypothetical protein
DVU2106	458	50.6	6.4	σ^{54} dependent transcriptional regulator
DVU2107	136	32.5	7.2	Hypothetical protein Dinitrogenase iron-molybdenum cofactor biosynthesis
DVU2108	119	12.5	5.7	MTH1175-like domain family protein Dinitrogenase iron-molybdenum cofactor biosynthesis
DVU2109	487	50.0	5.4	MTH1175-like domain family protein ATPase involved in chromosome partitioning ATPase-like, ParA/MinD

1.6 Aims

Many questions remain unanswered about the biological role of the protein DVU2103 encoded by the *orp* gene cluster. This operon is highly conserved in anaerobic bacteria and studies showed that it is essential to maintain this type of lifestyle. The function/structure of several proteins/enzymes of this operon is still unknown, just knowing that they might play a role in cellular division (either directly or indirectly). The specific role of ATPase DVU2103 has not yet been discussed. The identification and characterization of metalloproteins encoded in this operon is crucial to define precisely its function in this bacteria and its importance for anaerobic organisms.

This work has as main objective the isolation and characterization of DVU2103 from *D. vulgaris* Hildenborough, its involvement in the formation of the ORP complex, as well as the homologous isolation of DVU2108, and its biochemical characterization.

To accomplish these aims, a work plan was elaborated involving the following steps:

- Homologous expression and purification of DVU2103 in *Desulfovibrio vulgaris* Hildenborough
- Biochemical characterization and enzymatic properties of ATPase DVU2103
- Spectroscopic characterization of DVU2103 protein (EPR). Identification of the [Fe-S] cluster
- Homologous expression and purification of DVU2108 in *Desulfovibrio vulgaris* Hildenborough
- Purification and biochemical characterization of StrepDVU2108/DvH

2

Materials and Methods

2.1 Homologous production of DVU2103 in *Desulfovibrio vulgaris* Hildenborough

DVU2103 is encoded by *orp2* operon, which was cloned in a plasmid under the promoter of cytochrome c_3 and introduced into *Desulfovibrio vulgaris* Hildenborough (DvH) for homologous production of this protein. This part of the work was performed in collaboration with the research group of Dr. Corinne Aubert at CNRS (*Centre Nacional de la Recherche Scientifique)* in Marseille. The pBCM6 vector was used to express the genes of *orp2* transcriptional unit, namely *DVU103*, *DVU2104* and *DVU2105* genes. This technique produces proteins in a soluble form to allow easier expression and purification. A histidine tag (6 x His residues) was also added to DVU2103 in order to facilitate the purification procedure.

DvH-*orp2* strain was grown in Medium C [59] (pH 7.4) (Table 6.2, Appendix 2) supplemented with thiamphenicol in anaerobic flasks. In order to obtain a large volume of culture it was necessary to perform a series of pre-inoculums. The growth started in an anaerobic flask of 5 mL that contained 4.5 mL of medium, 0.5 mL of inoculum (10 %) and 0.02 mg/mL thiamphenicol and were incubated at 32º C without agitation for 24 h (in a Sanyo Incubator, Model MR-162). The culture was progressively transferred to other anaerobic flasks of higher volume (5 mL, 10 mL, 100 mL, 1 L or 2 L), until a total of 20 L was obtained (10 x 2 L). The inoculum's optical density ($OD_{600\ nm}$) was measured in regular timeframes (each 24 h) until it reached 0.7 (Table 6.1, Appendix 1) and only after reaching that value it was used to inoculate the next flask of higher volume (as a 10 % inoculum).

Afterwards, the cells were centrifuged at 7500 rpm, for 20 min at 6º C, in a Beckman Coulter centrifuge, model Avanti J-26XPI (JA-10 rotor). The supernatant was discarded and the

collected cells were resuspended in 20 mM Tris-HCl, pH 7.6 (approximately at 1 mL buffer/1 g wet cells). Cells were stored at - 80º C until further use.

2.1.1 Purification of HisDVU2103

Before lysing the cells, DNase I (2000 U/mg, Roche) and protease inhibitor EDTA-free (prepared in 100 mM phosphate buffer, pH 7, Roche) were added to the cell suspension. Cells were lysed through mechanic lysis using a *French press* (Thermo, Electron Corporation). After being disrupted four times with the *French press*, the cells were resuspended in 20 mM Tris-HCl, pH 7.6 (volume of buffer equal to half of the volume of soluble fraction). This suspension was centrifuged at 7500 rpm, over 30 min at 6º C, in a Beckman Coulter centrifuge, model Avanti J-26XPI (JA 25-50 rotor) to remove cell debris. The supernatant was collected, resuspended and centrifuged again at 20000 rpm, over 1 h at 6º C, in a Beckman Coulter centrifuge, model Avanti J-26XPI (JA 25-50 rotor), in order to separate the membranes from the protein soluble fraction. Between all the steps the protein extract was deaerated with argon gas in order to minimize the contact with oxygen.

From then on, all the steps were performed inside an anaerobic chamber under 2 % H_2 in argon atmosphere to maintain anoxic conditions (Coy Labs). The sample was load into an affinity column, His-Trap HP (GE Healthcare, 1.6 cm Ø × 2.5 cm, 5 mL), previously equilibrated with the binding buffer 20 mM Tris-HCl pH 7.6, 300 mM NaCl and 1 mM DTT. Proteins were eluted from the column with a stepwise gradient of imidazole: 20 mM, 50 mM, 100 mM and 500 mM in the same buffer. The protein of interest was eluted in 20 mM Tris-HCl pH 7.6, 300 mM NaCl, 1 mM DTT and 100 mM imidazole. These fractions were concentrated in a Vivacell 70, 30 kDa membrane (Sartorius) and loaded into a PD-10 column (GE Healthcare) equilibrated with 20 mM Tris-HCl pH 7.6 and 1 mM DTT, for buffer exchange and to remove imidazole. An ion exchange column, Hi-Trap Q FF (GE Healthcare, 1.6 cm Ø × 2.5 cm, 5mL), previously equilibrated with 20 mM Tris-HCl pH 7.6 and 1 mM DTT buffer was used in the second purification step. The protein of interest was eluted with a gradient of NaCl in the equilibration buffer, also in a stepwise gradient: 0 mM, 50 mM, 200 mM, 300 mM and 500 mM. The protein of interest was eluted in 20 mM Tris-HCl pH 7.6, 1 mM DTT and 500 mM NaCl. After elution, DVU2103 containing fractions were concentrated in a Vivacell 70, 30 kDa membrane (Sartorius) and loaded into a PD-10 column (GE Healthcare) equilibrated with 20 mM Tris-HCl pH 7.6 and 3 mM DTT. At the end, the protein was concentrated in a Amicon Ultra-4, 3 kDa (Merck)/Vivaspin 500, 3 kDa (Sartorius) inside the anaerobic chamber, and

stored in small aliquots in liquid nitrogen until further use. The scheme of the DVU2103 purification is represented in Figure 2.1.

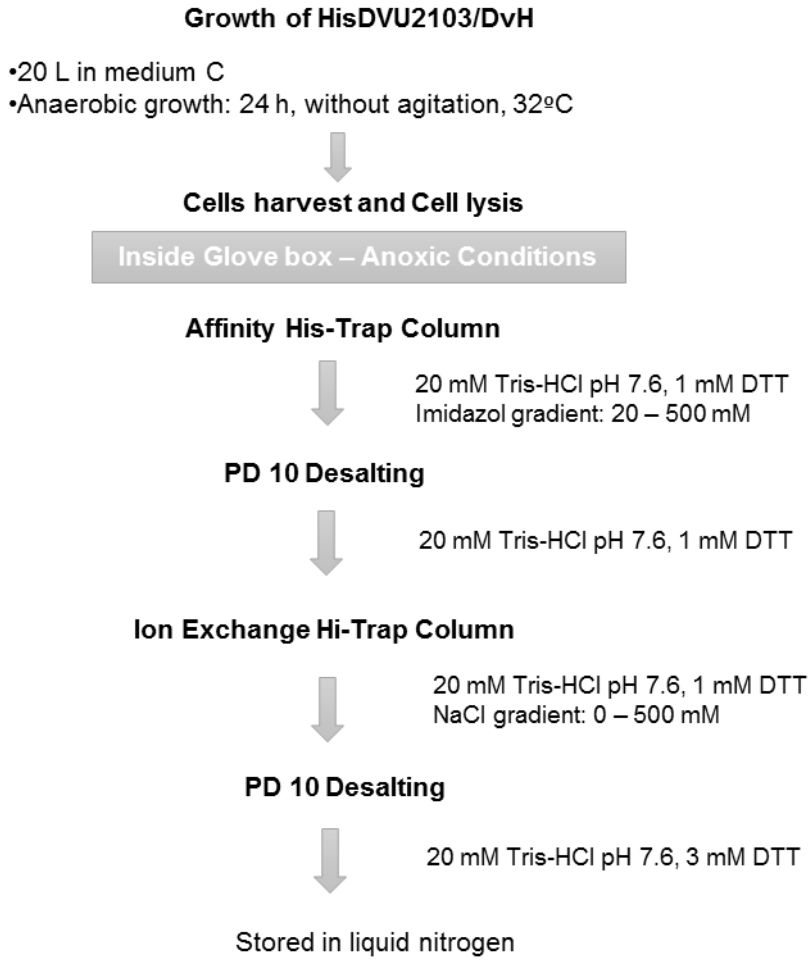

Figure 2.1 - Scheme of the purification process of HisDVU2103 from DvH

A size-exclusion chromatography was performed as a polishing step at least in some cases. A Superdex 75 10/300 GL (GE Healthcare, 24 mL) column was used equilibrated in the running buffer composed by 20 mM Tris-HCl pH 7.6, 150 mM NaCl and 1 mM DTT. The chromatography was also performed inside a glove box under anoxic environment. A volume of approximately 250 µL of final fraction was injected into the column and the chromatography was performed at a flow rate of 0.5 mL/min. All fractions were collected in eppendorfs (fractions of 1 ml). A chromatogram of this purification step was drawn reading the absorbance of each fraction at 280 nm and 400 nm in a Nanodrop 200c Spectrophotometer (Thermo

Scientific). In order to verify the existence of [Fe-S] cluster in any of the fractions, UV-visible spectra were collected in a UV-spectrophotometer Shimadzu UV-1800.

The protein's purity was accessed after each purification step in a 12.5 % Tris-Tricine SDS-PAGE and the final fraction was also analysed under native conditions (10 % Tris-Tricine PAGE). Gel composition in presented in Table 6.3 (Appendix 3).

2.2 Homologous production of StrepDVU2108 from Desulfovibrio vulgaris Hildenborough

DVU2108 is encoded by *orp1* operon. DVU2108 was cloned with a STREPII tag (Trp-Ser-His-Pro-Gln-Phe-Glu-Lys) in the plasmid pBCM6 under the promoter of cytochrome c_3 and introduced into *Desulfovibrio vulgaris* Hildenborough (DvH) for homologous expression and production [49]. This part of the work was performed in collaboration with the research group of Dr. Corinne Aubert at CNRS (*Centre Nacional de la Recherche Scientifique)* in Marseille.

2.2.1 StrepDVU2108: Normal Bacterial Growth

StrepDVU2108DvH strain was grown in the same conditions as previously described for DVU2103 protein, Medium C [59] (pH 7.4) (Table 6.2, Appendix 2) supplemented with thiamphenicol in anaerobic flasks. In order to obtain a large volume of culture it was necessary to perform a series of pre-inoculums. Growth was started in an anaerobic flask of 5 mL that contained 4.5 mL of medium, 0.5 mL of inoculum (10 %) and 0.02 mg/mL thiamphenicol. Inoculums were incubated at 32^{o} C without agitation for 24 h (in a Sanyo Incubator, Model MR-162). The culture was successively transferred to other anaerobic flasks of higher volume (5 mL to, 10 mL, then to 100 mL, and finally to 1 L or 2 L), until a total of 20 L could be obtained. The inoculum's optical density ($OD_{600\ nm}$) was measured in regular timeframes (each 24 h) until it reached 0.7 (Table 6.1, Appendix 1) and only after reaching that value, was it used to inoculate the next flask of higher volume (as a 10 % inoculum).

2.2.1.1 Purification of StrepDVU2108

The cell lysis was performed similarly to what was described for DVU2103, in Section 2.1.1. Similarly, to the purification of DVU2103, the purification of DVU2108 was also performed under anoxic conditions inside an anaerobic chamber.

The protein soluble fraction was loaded into an affinity column Strep-Trap HP (GE Healthcare, 1.6 cm Ø × 2.5 cm, 5 mL), previously equilibrated with a binding buffer composed of 100 mM Tris-HCl pH 7.6, 500 mM NaCl and 3 mM DTT. A washing step was performed in order to remove all the proteins that were not bound to the matrix, at least three washes with binding buffer were made. The protein was eluted from the column using an elution buffer composed of 100 mM Tris-HCl pH 7.6, 500 mM NaCl, 3 mM DTT and 2.5 mM desthiobiotin. The eluted fraction containing the protein of interest was concentrated in a Vivacell 70, above a 5 kDa (Sartorius) membrane under argon atmosphere.

2.2.1.2 Polishing step

An extra polishing step was performed in order to have a more pure fraction of DVU2108. For that a size-exclusion chromatography was performed using a Superdex75 10/300 GL (GE Healthcare, 24 mL) column. The column was equilibrated with 50 mM Tris-HCl pH 8.1, 150 mM NaCl and 1 mM DTT and the flow rate was set at 0.6 mL/min. All the fractions corresponding to peaks at the chromatogram were recovered and applied in a Tris-Tricine SDS-PAGE to evaluate the purity. The scheme of the DVU2108 purification is represented in Figure 2.2.

The protein's purity was accessed after each purification step in a 12.5 % Tris-Tricine SDS-PAGE and the final sample was also analysed under native conditions (10 % Tris-Tricine PAGE). The purified DVU2108 was stored in liquid nitrogen until further use.

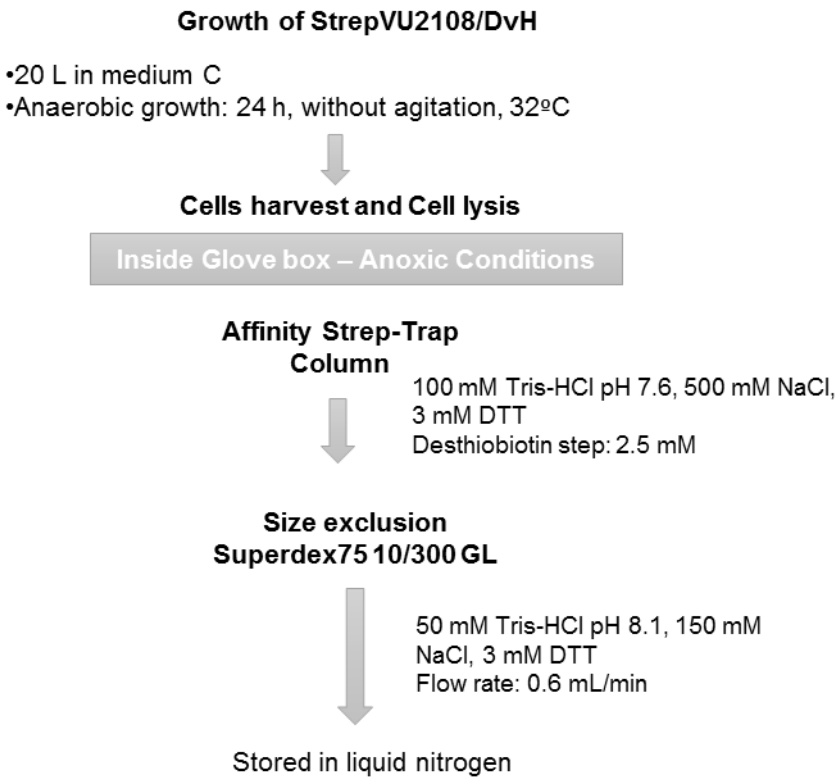

Figure 2.2 - Scheme of purification process of DVU2108 from DvH.

2.2.2 StrepDVU2108: Bacterial Growth Supplemented with Mo

StrepDVU2108DvH strain was also grown in Medium C [59] (pH 7.4) (Table 6.2, Appendix 2) supplemented with thiamphenicol and $Na_2MoO_4.2H_2O$ in anaerobic flasks. In order to obtain a large volume of culture it was necessary to perform a series of pre-inoculums. Growth was started in anaerobic flask of 5 mL that contained 4.5 mL of medium, 0.5 mL of inoculum (10 %), 0.02 mg/mL thiamphenicol and 2.81 µM and 5.625 µM of $Na_2MoO_4.2H_2O$. Inoculums were incubated at 32º C without agitation for 24 h (in a Sanyo Incubator, Model MR 162). The culture was successively transferred to other anaerobic flasks of the same volume with increasing concentration of $Na_2MoO_4.2H_2O$ (11.25 µM to 19.8 µM, then to 24.75 µM and finally to 29.7 µM). To reach higher concentrations of $Na_2MoO_4.2H_2O$, incubation time of the culture was increased to 24 h to at least 48 h (in some cases incubation time was of 72 h). Concentration of $Na_2MoO_4.2H_2O$ was increased from 29.7 µM to 33.75 µM, then to 40.5 µM and finally to 45 µM. After growing in 45 µM $Na_2MoO_4.2H_2O$ in 24 h, the culture was successively transferred to other anaerobic flasks of higher volume (5 mL to, 10 mL, then to

100 mL, and finally to 1 L or 2 L), until a total of 20 L could be obtained. The inoculum's optical density ($OD_{600\ nm}$) was measured in regular timeframes (each 24 h) until it reached 0.7 (Table 6.1, Appendix 1) and only after reaching that value, was it used to inoculate the next flask of higher volume (as a 10 % inoculum).

2.2.2.1 Purification of StrepDVU2108

The purification of DVU2108 was also performed under anoxic conditions inside an anaerobic chamber as previously described in Section 2.2.1.1.

2.3 Spectroscopic Characterization

2.3.1 UV-visible spectroscopy

At the end of the purification, UV-visible spectrum of HisDVU2103 and StrepDVU2108 final fraction was acquired, between 250 nm and 900 nm, in a UV-visible spectrophotometer Shimadzu UV-1800. The sample was diluted in a 20 mM Tris-HCl pH 7.6 and 3 mM DTT buffer. All the spectra were acquired at room temperature, under anoxic conditions, using 500 µL Quartz cuvettes. Concentration of DVU2103 was estimated using the absorbance at 400 nm and the extinction coefficient determined before, $\varepsilon_{400\ nm}$ (molar extinction coefficient) of 32600 $mM^{-1}cm^{-1}$ [60].

UV-visible reduction spectra of 1.6 µM DVU2103 in 20 mM Tris-HCl pH 7.6 and 3 mM DTT were acquired under oxic conditions, between 250 nm and 900 nm using 500 µL Quartz cuvettes in a UV- spectrophotometer Shimadzu UV-1800, at room temperature. The reduction was followed by UV-visible spectroscopy after addition of increasing amounts of two reducing agents (sodium dithionite, from 5 to 26 µM, and ascorbate, from 12 to 143 µM). Both solutions were freshly prepared under oxic atmosphere in 20 mM Tris-HCl pH 7.6 and 3 mM DTT, with initial concentration of reducing agents of 2 mM and 2.5 mM or 10 mM for sodium dithionite and ascorbate, respectively.

2.3.2 Electron paramagnetic resonance (EPR)

DVU2103 sample was analysed by EPR spectroscopy. EPR sample (150 µL) was prepared in 20 mM Tris-HCl buffer, pH 7.6 and 3 mM DTT. The EPR spectra of DVU2103 were recorded on a X-band Bruker EMX 8/2.7 spectrometer equipped with a rectangular cavity (model ER 4102T) and an Oxford Instruments continuous liquid helium flow cryostat. Three different conditions were tested in the same EPR tube: as-isolated, reduced with ascorbate solution and reduced with a dithionite solution. As-isolated condition was performed at 10 K and 20 K. Then, the sample was reduced by addition of a freshly prepared and oxygen free ascorbate solution to a final concentration of 1 mM and 2 mM. Solutions were incubated for 30 min and 1 h, respectively inside an anaerobic chamber (Braun). The second reducing condition was performed adding a freshly prepared and oxygen free sodium dithionite solution to a final concentration of 1 mM and 2 mM. Incubate time was 30 min and 1 h, respectively, inside an anaerobic chamber (Braun). The tube was sealed with a rubber septum after each addition and immediately frozen in liquid nitrogen until measurement. The EPR spectra were acquired at a microwave frequency 9.65 GHz, attenuation of 15 dB and modulation amplitude of 0.5 mT and receiver gain of 1.0×10^5. Spectra were analysed using WINEPR SimFonia software version 1.2 from Bruker.

2.3.3 Protein quantification-660 nm Pierce Protein Quantification Method

After purification, the protein of interest was quantified using 660 nm Pierce Protein Quantification method (Thermo Scientific). This colorimetric assay is based on a colour change from reddish brown to green when the dye-metal (polyhydroxy benzene sulfonephthalein-type dye and a transition metal) complex present in the main solution binds to mainly basic amino acid residues in proteins. A shift in the absorption maximum of the dye-metal complex happens when it binds to the protein moving the maximum from 450 to 660 nm. Many features have to be considered when choosing a protein assay once that each one has limitations depending on the application and the specific protein sample analysed. In this case the presence of a reducing agent (DTT) lead to the choice of this quantification method. The calibration curve was made using as standard protein Bovine Serum Albumin (BSA) (Protein Standard, 2 mg protein/Ml, Sigma-Aldrich) ranging between 0 to 0.30 mg/mL in Milli-Q water. Samples were also diluted in Milli-Q water before using. The assay was performed in eppendorf tubes.

The procedure consists of adding 150 µL of assay reagent solution (as received from Thermo Fisher Scientific) to 10 µL of diluted protein sample, mix and incubated at room temperature for 5 min. After this incubation time, the absorbance of all the samples and standards were measured at 660 nm against Milli-Q water in a Nanodrop 200c Spectrophotometer (Thermo Scientific). A standard curve was generated by plotting the average blank-corrected 660 nm measurement for each standard *versus* its concentration in milligrams per millilitre (mg/mL) (Figure 2.3).

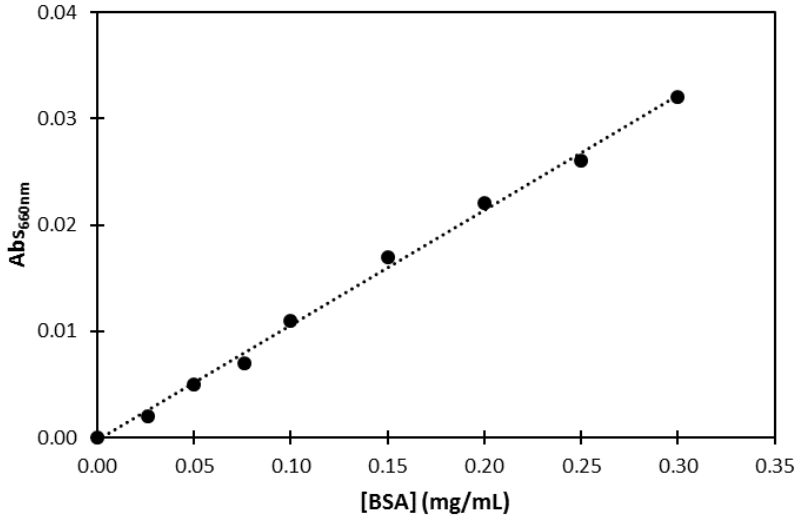

Figure 2.3 - A typical calibration curve for protein quantification using 660 nm Pierce protein Quantification method. Y = 0.1083x-0.0003, with a R = 0.9982

2.3.4 ICP Metal Quantification

Metal quantification (Fe, Cu and Mo) in DVU2103 and DVU2108 final fractions was performed by ICP-AES (Inductively Coupled Plasma-Atomic Emission Spectrometer) at Analyse Laboratory Service at FCT/UNL using a Horiba Jobin Yvon Ultima equipment. The standard metal solution used was Reagecom 23 ICP Multielement Standard, with the concentration was each metal ranging from 0 to 3 ppm. The samples were diluted in 20 mM Tris-HCl pH 7.6, 150 mM NaCl and 1 mM DTT so that the final concentration would be approximately 0.6 ppm. At least duplicated samples of different volumes were analysed to increase accuracy.

2.3.5 Determination of the apparent molecular mass of DVU2103

In order to determine the apparent molecular mass of the protein of interest a size-exclusion chromatography was performed. This chromatography allows the separation of molecules according to their molecular mass and shape, as they pass through a gel matrix. Unlike other types of chromatography, such as ion exchange or affinity, in size-exclusion chromatography molecules do not bind to the chromatographic medium so resolution of separation is not directly affected by buffer composition. The molecular mass of protein of interest was determined by size-exclusion chromatography using a Superdex 200 10/300 GL column (GE Healthcare, 24 mL) equilibrated with 50 mM Tris-HCl pH 7.6, 150 mM NaCl and 1 mM DTT. The flow rate of the elution was set as 0.5 mL/min. A calibration curve was made injecting 150 µL of a mix of standard proteins from the calibration kit (Gel filtration chromatography, GE Healthcare), composed of Ferritin (440 kDa), Aldolase (158 kDa), Conalbumin (75 kDa) and Ovalbumin (43 kDa). The proteins were prepared according to Table 6.6 (Appendix 4).

The molecular mass of DVU2103 was estimated through the calibration curve presented in Figure 2.4.

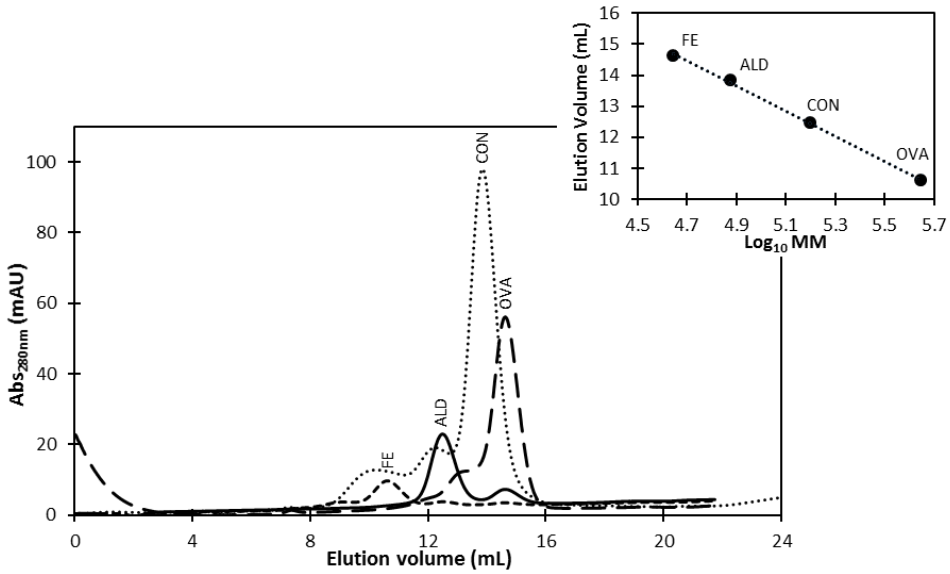

Figure 2.4 - Chromatogram obtained for the calibration curve of size-exclusion chromatography in a Superdex200 10/300 GL column. The figure represents the proteins of the calibration kit of size-exclusion chromatography (LMW GE Healthcare): FE – Ferritin, ALD – Aldolase, CON – Conalbumin and OVA – Ovalbumin. A typical Calibration Curve for Superdex 200 size-exclusion chromatography in 50 mM Tris-HCl buffer pH 7.6, 150 mM NaCl and 1 mM DTT. Y = - 4.0559x + 33.5363, with a R = 0.9990 (y correspond to elution volume and x to the Log_{10}MM).

In order to determine the molecular mass of DVU2103, 2 nmol of protein in 100 µL, was injected, after being centrifuged at 10000 rpm for 12 min (Benchtop Centrifuge, Model 1-15P, Sartorius) at RT. The samples were collected in fractions of 1 mL (from 1 to 7 mL and 22 to 26 mL) and of 500 µL (from 7 to 22 mL). The elution was monitored at 280 nm and 400 nm. The samples collected were analysed in a 12.5 % Tris-Tricine SDS-PAGE to identify the eluted proteins.

2.3.5.1 Effect of ATP in the formation of the DVU2103 complex

In order to determine whether ATP influences the DVU2103 complex, another size-exclusion chromatography was performed. A Superdex75 10/300 GL (GE Healthcare, 24mL) column was used and two elutions were made, one using a buffer containing ATP and one without ATP. In the first elution the column was equilibrated with 50 mM Tris-HCl pH 8.1, 150 mM NaCl, 1 mM DTT, 5 mM $MgCl_2$ and 0.5 mM ATP. The flow rate was set at 0.5 mL/min. The second elution was performed in the same column equilibrated with 50 mM Tris-HCl pH

8.1, 150 mM NaCl and 1 mM DTT. The flow rate was the same as before. A volume of 100 µL (with 4 nmol of total protein) was injected into the column, and the elution was monitored at 280 nm and 400 nm. The samples were collected in fractions of 1 mL (from 1 to 7 mL and 22 to 26 mL) and 500 µL (from 7 to 22 mL). The molecular mass was determined using the calibration curve. The samples collected were afterwards analysed in a 12.5% Tris-Tricine SDS-PAGE to identify the eluted proteins.

A calibration curve was made injecting 100 µL of a mix of standard proteins. The proteins constituents of the calibration kit to size-exclusion chromatography LMW (GE Healthcare) used were: Conalbumin (75 kDa), Ovalbumin (43 kDa), Carbonic Anhydrase (29 kDa), Ribonuclease A (13.7 kDa) and Aprotinin (6.5 kDa). The proteins were prepared according to Table 6.7 (Appendix 4).

The molecular mass of DVU2103 was calculated through the calibration curve presented in Figure 2.5.

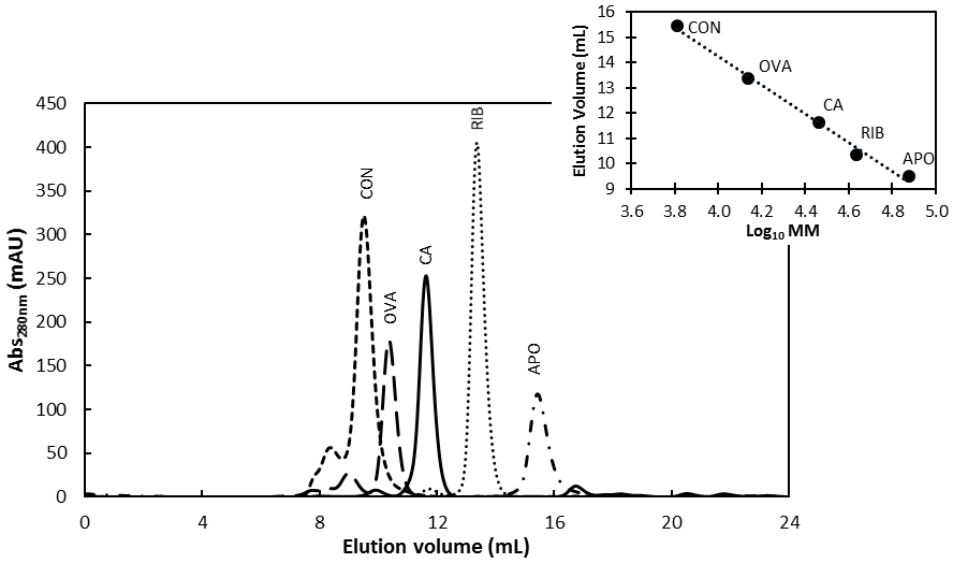

Figure 2.5 - Chromatogram obtained for the calibration curve of size-exclusion chromatography in a Superdex75 10/300 GL column. The figure represents the proteins of the calibration kit of size-exclusion chromatography (LMW GE Healthcare): CON – Conalbumin, OVA – Ovalbumin, CA – Carbonic Anhydrase, RIB – Ribonuclease, APO – Apoprotein. A typical calibration curve for Superdex 75 size-exclusion chromatography in 50 mM Tris-HCl buffer pH 7.6, 150 mM NaCl and 1 mM DTT. Y = -5.7026x + 37.0710, with a R = 0.9963 (y correspond to elution volume and x to the Log_{10}MM).

2.3.5.2 Effect of oxygen in the formation of DVU2103 complex

The effect of oxic environment in the molecular mass of "DVU2103" was determined using a Superdex75 10/300 GL (GE Healthcare, 24 mL) column equilibrated with 50 mM Tris-HCl pH 7.6, 150 mM NaCl and 1 mM DTT. The first sample consisted of fresh "DVU2103" (little exposure to oxic conditions) and the second sample consisted of "DVU2103" that had been exposed to oxic conditions for 96 h.

The samples were run separately both at a flow rate of 0.5 mL/min. The volume of the sample injected in the column was 80 µL (60 µL of protein + 20 µL of running buffer, corresponding to 4 nmol of total protein) previously centrifuged at 10000 rpm for 12min (Benchtop Centrifuge, Model 1-15P, Sartorius). The chromatographic profile of the samples was monitored at 280 nm and 400 nm. The samples were collected in fractions of 1 mL (from 1 to 7 mL and 22 to 26 mL) and 500 µL (from 7 to 22 mL). The samples collected were afterwards analysed in a 12.5% Tris-glycine SDS-PAGE to identify the eluted proteins.

2.3.6 ATPase activity of DVU2103 - Malachite Green Phosphate Assay

Assays were performed in order to determine the specific activity of the “DVU2103” as an ATPase enzyme. All solutions used were previously deaerated. The Malachite Green Phosphate Assay Kit from BioAssays Systems was used to performed the activity assays. This assay is based on the quantification of the green complex formed between Malachite Green, molybdate and free orthophosphate present in the reactional mixture (Figure 2.6). The assay was performed in two different conditions: under anoxic conditions (inside an anaerobic chamber) and under oxic condition.

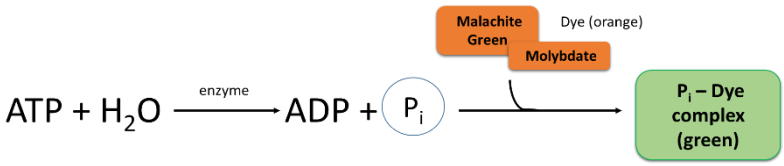

Figure 2.6 – Schematic model for the Malachite Green Phosphate Assay reaction. Malachite Green and molybdate react with free orthophosphate released from the ATP hydrolysis reaction to form a green complex.

2.3.6.1 Oxic conditions

The assay was performed using 10 µM of "DVU2103" in a buffer containing 50 mM Tris-HCl pH 8.1, 100 mM NaCl, 2 mM $MgCl_2$, 2 mM DTT and two concentrations of ATP (0.25 and 2.5 mM). The activity was measured at incubation times of 0, 15, 30 and 60 min after the addition of the ATP solution. The Malachite Green assay consists in the addition of 80 µL of test sample in an eppendorf and the measurement of its absorbance at 620 nm. A calibration curve of Abs620 nm *versus* Phosphate concentration was made using the Premix solution of the kit, ranging from 0 to 16 µM phosphate (Figure 2.7). All solutions were prepared in Milli-Q water.

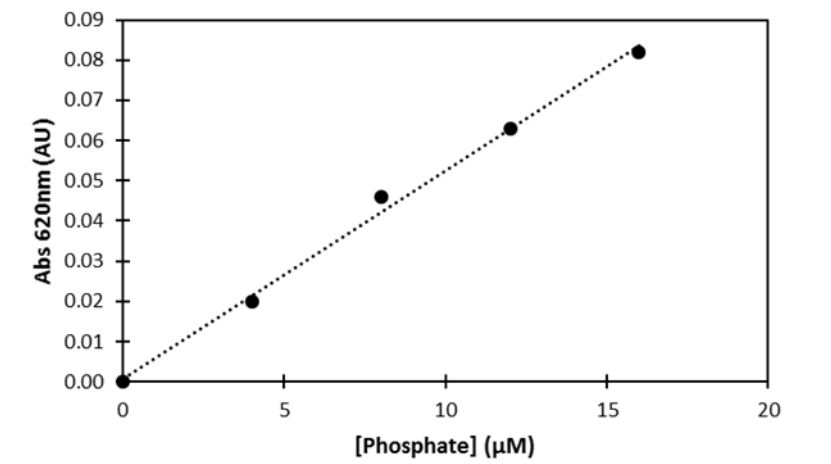

Figure 2.7 - Calibration curve for Malachite Green Phosphate Assay under oxic conditions. The equation of curve for the calibration curve obtained, Abs_{620nm} = 0.0052[Phosphate] (µM) + 0.0080, with a R = 0.9977, was used to determine the amount of phosphate produced in the reaction.

A stock solution was made containing the protein and the desired concentration of ATP. After each incubation time established, 80 µL of test solution was pipetted to an eppendorf and mixed with 20 µL of the working reagent. This last reagent acts as a stopping agent, allowing colour development. Dilutions were made whenever ATP's concentration was higher than 0.25 mM. The mixture was then allowed to stand for 30 min at room temperature to colour development. The absorbance of the samples was then measured at 620 nm against buffer in a Nanodrop 200c Spectrophotometer (Thermo Scientific).

2.3.6.2 Anoxic conditions

The same assay was repeated under anoxic conditions, for that all additions were performed inside of an anaerobic chamber (COY type). A concentration of 10 µM of "DVU2103" was used in the assays in a buffer containing 50 mM Tris-HCl pH 8.1, 100 mM NaCl, 2 mM $MgCl_2$, 2 mM DTT and two different concentrations of ATP (0.25 and 2.5 mM). Activity was measured at incubation times of 0, 15, 30 and 60 min after the addition of the ATP solution. A calibration curve of Abs620 nm *versus* Phosphate concentration was made exactly in the same conditions as described in the previous section (section 3.3.6.1). The calibration curve for this assay is presented below (Figure 2.8**)**.

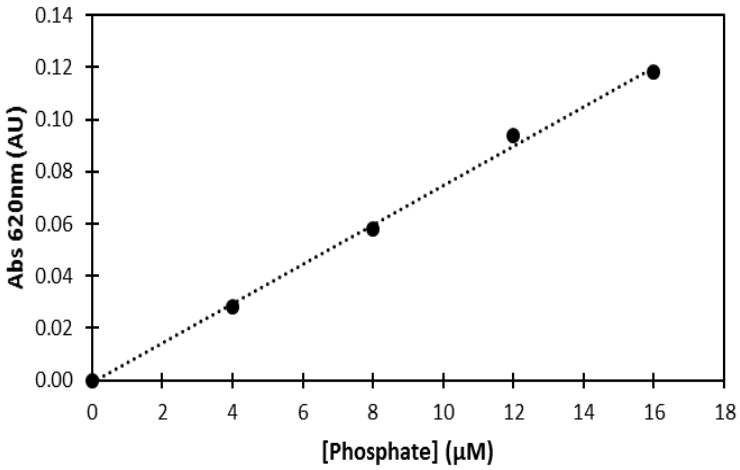

Figure 2.8 - Calibration curve for Malachite Green Phosphate Assay in anaerobiosis. The equation of the calibration curve obtained, Abs_{620nm} = 0.0076[Phosphate] (µM) - 0.0008, with a R = 0.9985, was used to determine the amount of phosphate produced in the reaction.

3

Results and Discussion

The *DVU2103* ORF is annotated as encoding a protein with ATPase features highly conserved in anaerobic bacteria, however its function remains unknown. In order to better understand this protein several biochemical and enzymatic studies were performed. Table 1.2 (in Section 1.5.1) shows physical properties of some of the proteins present in the *orp* gene cluster of *Desulfovibrio vulgaris* Hildenborough, and that form the ORP complex.

3.1 DVU2103 from Desulfovibrio vulgaris Hildenborough

The analysis of the primary sequence of DVU2103 from *Desulfovibrio vulgaris*, was performed using interface *Blastp* available in NCBI database. The search of similarities between the sequences in sequenced and partially sequenced genomes was made and revealed that DVU2103 from *D. vulgaris* Hildenborough (NCBI code: WP_010939380.1) is a conserved protein in the *Desulfovibrio* genera. This protein shows greater similarity with the conserved protein from *D. termitidis* (NCBI code: WP_035068143.1), *D. aminophilus* (NCBI code: WP_051202990.1) and *D. bastinii* (NCBI code: WP_027178178.1), with 65 %, 61 % and 55 %, percentage of identity, respectively. The sequence alignment allowed us to identify that DVU2103 from *D. vulgaris* Hildenborough presents 54 % of identity with the same protein from *D. alaskansis* (NCBI code: WP_011368948.1) and 48 % with the one from *D. gigas* (NCBI code: WP_051286230.1). The analysis performed also revealed that DVU2103 is not an exclusive protein of the *Desulfovibrio* genera and that similar proteins are found in different genera of anaerobic sulphate reducing bacteria, such as *Geobacter sulfurreducens* (NCBI

code: WP_045668345.1) (52 %), *Clostridiales bacterium* DRI-13 (NCBI code: WP_034421650.1) (50 %) and *Methanolobus tindarius* (NCBI code: WP_048135825.1) (47 %).

From the sequences found in the *Desulfovibrio* genera, six with the highest homology were selected to perform the alignment, using the bioinformatic tools CLUSTALX 2.1 [61] and Jalview2.9, for multiple sequence alignment, which is represented in Figure 3.1.

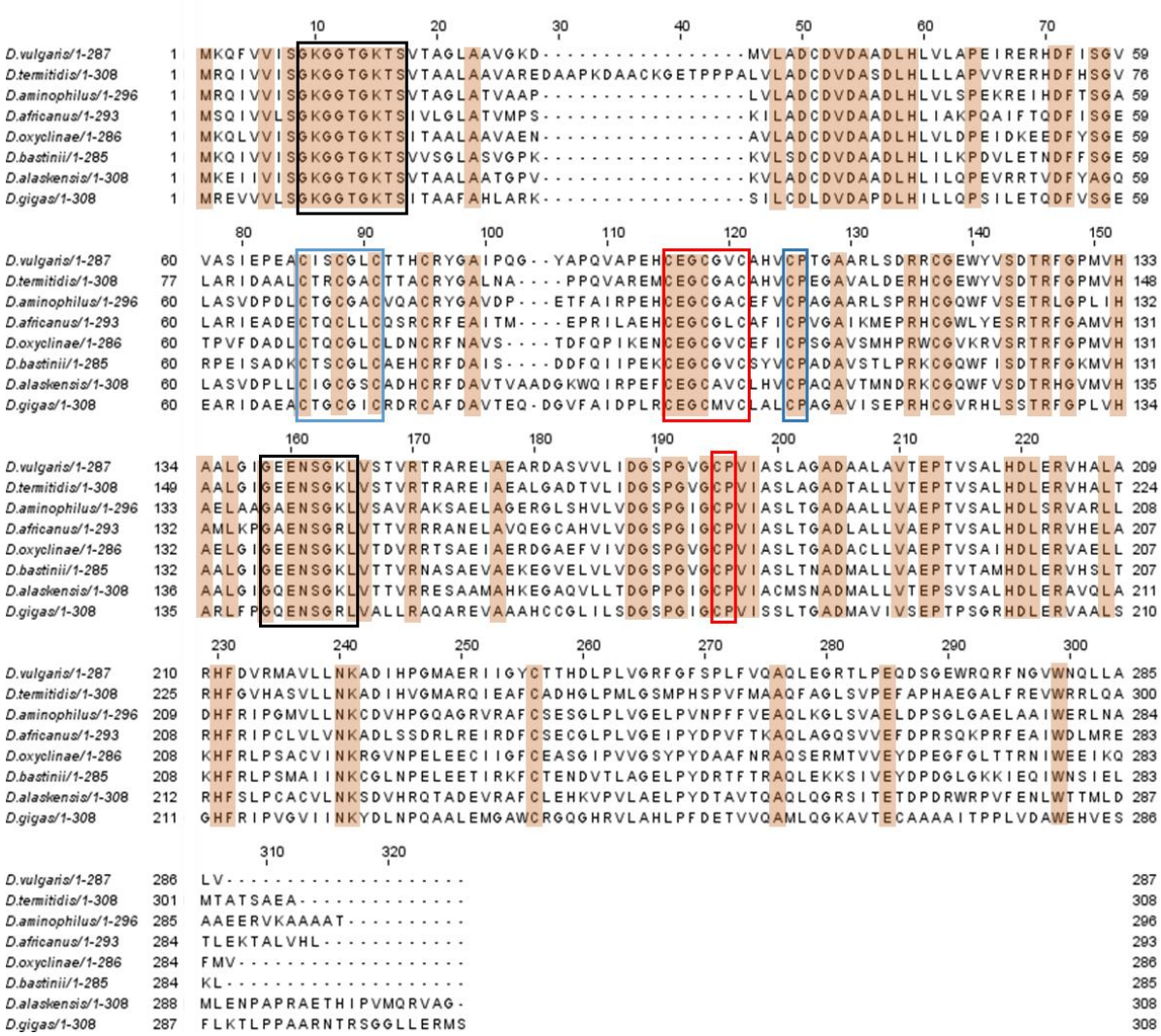

Figure 3.1 - Sequence alignment of DVU2103 from *D. vulgaris* Hildenborough (NCBI code: WP_010939380.1) with the similar proteins from *D. termitidis* (NCBI code: WP_035068143.1), *D. aminophilus (*NCBI code: WP_051202990.1), *D. africanus* (NCBI code: WP_027367473.1), *D. oxyclinae* (NCBI code: WP_018123934.1) *D. bastinii* (NCBI code: WP_027178178.1), *D. alaskensis* (NCBI code: WP_011368948.1) and *D. gigas* (NCBI code: WP_051286230.1). The sequences were obtained from the interface *Blastp*, and bioinformatics CLUSTALX [61] 2.1 and Jalview2.9 was used for multiple sequence alignment. Highlight the conserved amino acid residues. The Walker A motifs, Cys-X-X-Cys motifs and locals of [Fe-S] cluster binding are indicated in boxes black, red and blue, respectively.

Conserved regions that can be important for functional/structural roles can be identified from the sequence alignment. The analysis of the sequence revealed the presence of N-terminal sequences (between residues 8 and 16), containing the conserved Walker A motif (GKGGTGKTS). Mutational analyses have shown that Cys-X-X-Cys and Walker A motifs are directly involved in ATPase activity

of proteins, as the presence of a signature lysine is indispensable for ATPase activity [62], [63]. Experiments demonstrated that proteins with a conserved motif containing two close cysteine residues (Cys-X-Cys) might be involved in metal binding, and some of these signatures can indicate the presence of a [Fe-S] cluster [63], [64]. Genetic studies showed that these motifs were required for *in vivo* functionality and that significant changes can inhibit protein activity [63], [65]. Studies performed by Boyd and co-workers in ApbC protein, that contains both a Walker A and B nucleotide-binding domains, revealed that key residues are essential for function *in vivo* but not for [Fe-S] cluster binding [65], [66].

Cysteine residues organization in the amino acids sequence of the protein suggest the ligation of a [4Fe-4S] cluster. Eight cysteine residues are also identified as conserved between sequences, that may be involved in the bound of a [Fe-S] cluster to the polypeptide chain through sulphur atoms. As each three inorganic sulphurs and one thiol from a cysteine in the protein coordinate each iron from the cluster, the fact that the sequence presents eight residues is a data that suggests that one or more [4Fe-4S] clusters is present in the DVU2103 protein. Through its analysis it appears that cysteines Cys68-X_2-Cys70-X_2-Cys72-X_{31}-Cys106Pro are involved in the coordination of one [4Fe-4S] cluster, since this is a sequence of residues constitutes a sequence motif usually binding these type of metal cluster [18]. The repetition afterwards of this motif (Cys96-X_2-Cys99-X_2-Cys102–X_{75}–Cys176Pro) leads to the hypothesis that it may coordinate a second [4Fe-4S] cluster. Note that the last cysteine residue needed to coordinate the [4Fe-4S] cluster may be exchanged among the motifs marked, leading to the motifs Cys68-X_2-Cys70-X_2-Cys72-X_{31}-Cys176Pro and Cys96-X_2-Cys99-X_2-Cys102–X_{75}–Cys106Pro. Since no crystallographic structure of DVU2103 protein from *D. vulgaris* Hildenborough is available, it is impossible to know which cysteine residue belongs to each motif. The presence of cysteine residues allows to infer that the metallic cluster in DVU2103 from *D. vulgaris* Hildenborough is covalently bound to the protein, contrary to what happens in the case of ORP protein in *D. gigas*.

3.1.1 Homologue expression of protein DVU2103 in *D. vulgaris* Hildenborough

The cells used to purify DVU2103 were collected at the end of their exponential phase, approximately 24 h after inoculation (OD_{600nm} = 0.7) (Table 6.1, Appendix 1) in Medium C, without agitation under an anoxic environment. After harvesting the cells and cell lysis, the protein soluble extract was analysed in a 12.5 % Tris-Tricine SDS-PAGE. The profile of protein is presented in Figure 3.2.

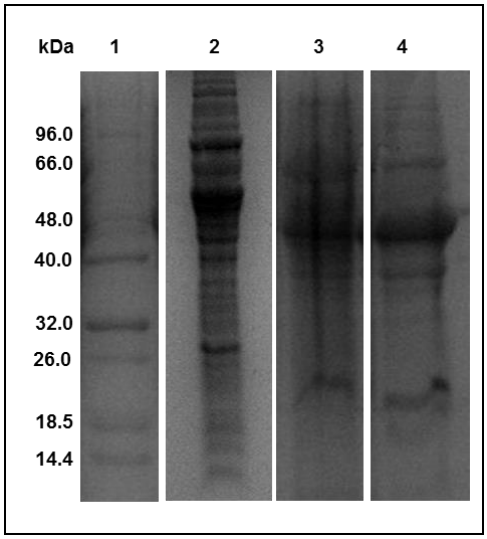

Figure 3.2 - Proteins expression profile in 12.5% Tris-Tricine SDS-PAGE. Lanes: 1. Low Molecular Mass Marker (LMW – NZYTech), 2. Soluble Fraction, 3. Cell Debris, 4. Membrane fraction.

3.1.2 Purification of DVU2103

Previously it was observed that during oxic purification, DVU2103 lost its brown colour. The brown colour was attributed to the presence of an [Fe-S] cluster, which was unstable under oxic conditions. Therefore, in order to preserve the [Fe-S] cluster present in DVU2103, the purification was performed under anoxic conditions, as described in Section 2.1.1 Materials and Methods, which consisted of two chromatographic steps.

The first chromatographic step consisted in an affinity chromatography using a His-Trap HP. This chromatography uses a high-performance matrix of Ni-Sepharose medium that allows a fast, simple and easy separation of contaminants by immobilized metal ion affinity chromatography (IMAC). The His-Trap column allows the separation of the major contaminants of the sample, being ideal to purify histidine-tagged recombinant proteins. In this step of purification, HisDVU2103, produced with a histidine tag, interacts specifically with the matrix allowing its purification. At the same time, other proteins that have a specific interaction with this protein can also be co-purified, and also proteins that have affinity (for example *E. coli* extract) to this matrix are also separated. A stepwise gradient of imidazole, ranging from 20 to 500 mM, was used to elute DVU2103. This strategy was adopted in order to minimize the presence of contaminants in the sample that can interact non-specifically with the column matrix. The fact that the imidazole present in the buffer compete with the Ni^{2+} of the matrix enables the separations of different proteins. DVU2103 was eluted between

140 and 220 mL with an imidazole concentration of 100 mM. The fraction obtained presented a brownish colour indicating the presence of [Fe-S] clusters, as expected.

Analysis of Figure 3.3 indicates that His-Trap affinity chromatography was very efficient in the purification process since it allowed the separation of most of the contaminants present in the initial soluble fraction.

The following step consisted on an anion exchange chromatography using a Hi-Trap Q FF. This chromatography is based on the binding of charged molecules to oppositely charged groups attached to an insoluble matrix. When substances carry a net charge opposite to that of the ion exchanger these bound to the matrix in an electrostatic and reversible way. The binding depends on the pH value at which a biomolecule carries no net charge, called the isoelectric point (pI). When at a pH above or below its pI, the biomolecule carries a negative or positive net charge, respectively. In the case of Hi-Trap Q FF column, which is an anion exchanger, biomolecules will bind to the matrix when they carry a negative net charge, which occurs when the buffer is above its pI. According to the bioinformatic program *Expasy/Protparam* DVU2103 isoelectric point is around 6 (Table 1.2). The charged groups on the side chains of amino acids aspartate and glutamate provide a negative charge to protein at a pH 7.6. This allows its interaction with the positively charged chromatographic matrix, leading to its separation from other proteins in the mixture. An ionic strength gradient using NaCl ranging from 0 to 500 mM was applied to the column in order to separate the protein of interest from other proteins. The fractions containing DVU2103 were eluted between 150 and 210 mL with a NaCl concentration of 500 mM (Figure 3.3). Initially, we believed that the protein left the column at 300 mM NaCl, however after some purifications we conclude that the protein is eluted effectively at 500 mM NaCl. Since the protein was eluted from the column with the maximum ionic strength used, the gradient of NaCl could have been increased until 1 M, in order to improve the resolution of the purification. Thus, the protein would have abandoned the column in the middle of the gradient, as recommended.

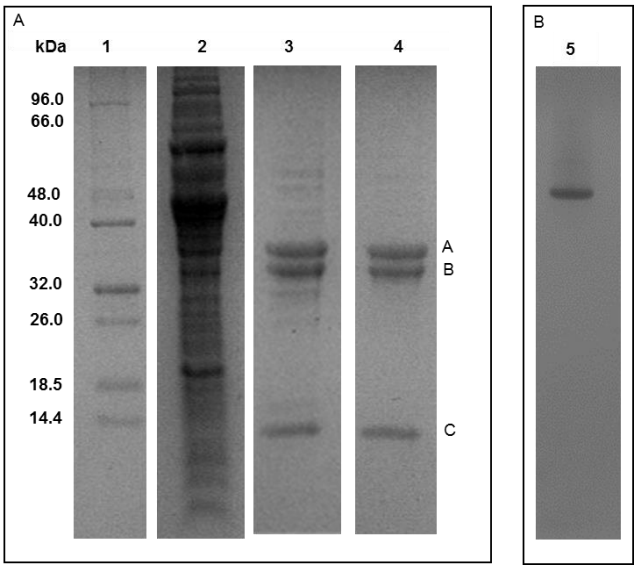

Figure 3.3 – A) Analysis of the fractions during DVU2103 purification. Lanes: 1. Low Molecular Mass Marker (LMW – NZYTech), 2. Soluble Fraction, 3. DVU2103 fraction after affinity chromatography, 4. DVU2103 fraction after ionic exchange chromatography. 12.5 % SDS-PAGE. B) PAGE of the purified DVU2103 after ionic exchange chromatography (10 % PAGE). Gels were stained with Coomassie Blue.

In fact, the Hi-Trap Q FF anionic exchange chromatography increased the purity of the sample, with a final fraction containing mainly three proteins bands that were postulated to be DVU2103, DVU2104 and DVU2108/ORP. These proteins form a complex as seen in the PAGE, but their separation may not be possible using this type of chromatography due to the similarity of their pI (pI of DVU2108 is approximately 5.7, pI of DVU2103 is 5.8 and pI of DVU2104 is 5.6).

The analysis of Figure 3.3–A shows the presence of more than one protein band in the fraction of DVU2103 after the last purification step (represented in lane 4). The molecular mass corresponding to these bands were compared with the molecular mass of proteins encoded by the *orp* operon. It is possible to identify three protein bands, two around 32 kDa and one of approximately 12 kDa. Since DVU2103 has an expected molecular mass of 31 kDa, we can conclude that one of the bands around 32 kDa in the SDS-PAGE might corresponds to DVU2103. The second band at 32 kDa could correspond to one of the two ATPases with [Fe-S] cluster inserted domain encoded by the *orp* operon, either DVU2103 or DVU2104, as both proteins have an expected molecular mass of 30 kDa (Table 1.2). The band at lower molecular mass is indicative of the presence of DVU2108 (expected molecular mass of 12 kDa), since it is the only protein of the *orp* operon that have this molecular mass.

These bands were also analysed by MALDI-TOF-MS, and this allowed the identification of the three protein bands observed in the final fraction, which form a single complex, as can be observed in the PAGE in Figure 3.3- B.

So, in order to identify the bands, present in the final fraction of SDS-PAGE (bands A, B and C), a Peptide Mass Fingerprint analysis by MALDI-TOF-MS was performed. For that we collaborated with Prof. Bart Devreese at L-ProBE (Laboratory for Protein Biochemistry and Biomolecular Engineering) in Ghent, Belgium, to whom we sent the samples (the protein bands were excised from the SDS-PAGE and send for analysis). The results are presented the table below (Table 3.1).

Table 3.1 - Identification of the three bands that form a complex through Peptide Mass Fingerprint analysis by MALDI-TOF-MS

Sample	Type of Protein	Database	Code	MM (kDa)
A	4Fe-4S binding protein	NCBI	499241840	30.46
B	4Fe-4S binding protein	NCBI	499241840	30.46
C	Hypothetical protein	NCBI	499241845	12.47

The peptide mass fingerprint identified that the two first bands, A and B, were of HisDVU2103 and that C corresponds to DVU2108. It could be that A and B are in fact DVU2103 and DVU2104 as some of the peptides might be identified as identical (Figure 3.4), specially the N-terminal of the two proteins has a high percentage identity (41 %) and a high homology (86 %). This fact needs to be confirmed in the future.

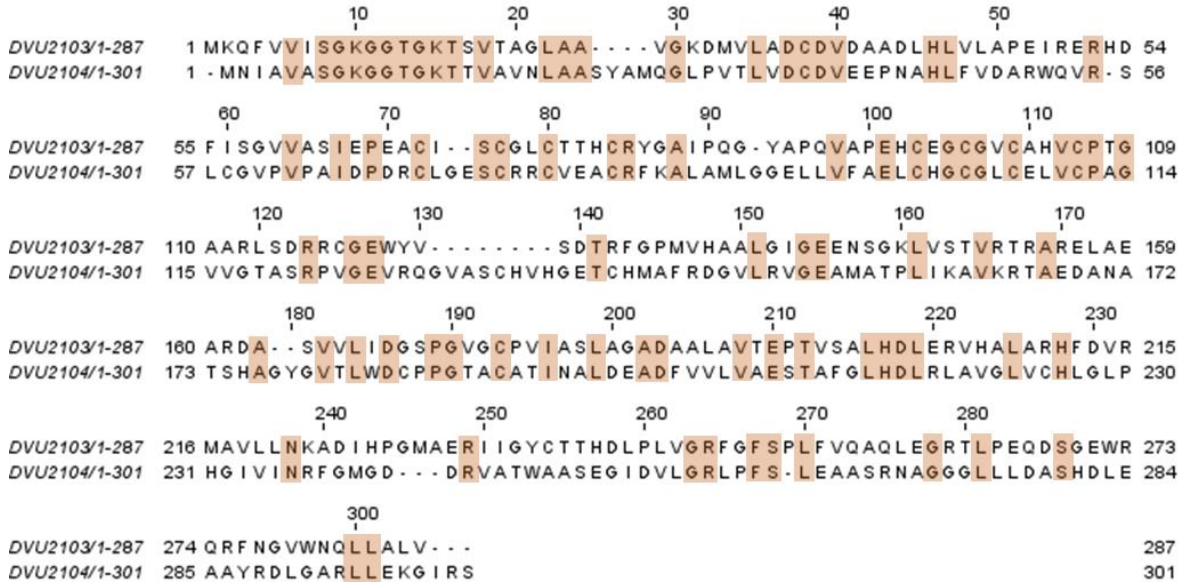

Figure 3.4 - Sequence alignment of DVU2103 and DVU2104 of *D. vulgaris* Hildenborough The sequences were obtained in the interface Blastp and bioinformatics CLUSTALX 2.1 and Jalview2.9 was used for multiple sequence alignment. Highlight the identical residues.

The fact that only DVU2103 was produced with a His-tag, which conferred it an extra 1 kDa of molecular mass have allowed the slightly separation between the two proteins in the SDS-PAGE. Nevertheless, the presence of the His-tag did not allow the separation of these two proteins, most probably due to the formation of the protein complex.

HisDVU2103 complex was purified with a yield of expression of approximately 58 µg/L of culture.

The fraction containing DVU2103 presented a brown colour throughout the entire purification process, which is an indication that the protein contained a metallic cluster. The UV-visible spectrum of the final fraction of DVU2103 complex is presented in Figure 3.5, and indicates the presence of a [Fe-S] cluster as it is possible to observe the broad absorption band characteristic of these type of centres, at around 400 nm. The purity ratio can be calculated by the values of absorbance at 400 nm and 280 nm. In this case the ratio Abs_{400nm}/Abs_{280nm} is around 0.52 (Table 3.2).

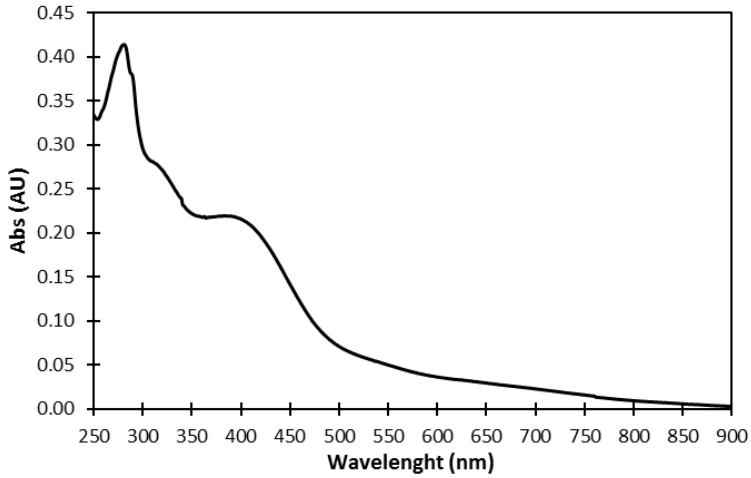

Figure 3.5 – UV-visible spectrum of as-isolated "DVU2103" complex of *D. vulgaris* Hildenborough in 20 mM Tris-HCl buffer pH 7.6 and 3 mM DTT**.**

The UV-visible spectrum of "DVU2103" complex, presented in Figure 3.5, has a broad absorption band at 400 nm indicating the presence of a [4Fe-4S] cluster in the sample. This absorption band is a characteristic charge transfer band of [Fe-S] and is commonly observed in proteins that contain this type of centre [18]. The extinction coefficient considered at 400 nm was 32600 M^{-1} cm^{-1} [67] obtained taking into account the putative number of iron atoms present in the cluster (2 centres of [4Fe-4S], 2 x [4Fe-4S]). Although, the number of Fe/protein is almost always lower than 8 (Table 3.2). In fact, if the complex of DVU2103 is also composed of DVU2104, which is also expected to have 2 x [4Fe-4S], this extinction coefficient is expected to be larger. Nevertheless, in any of the several purifications that were performed it was possible to obtained more than 7 Fe/protein. It is also important to mention that this ratio cannot be correctly determined, since DVU2103 complex is also composed of DVU2108 which has never been isolated with bound Fe, but contributes to the protein concentration.

Table 3.2 - Quantification of protein and Fe for the different purification performed during this work.

Purification	[Protein] (µM)	[Fe] (µM)	Fe/prot	A_{400nm}/A_{280nm}	Yield (µg/L)
#1 (20 L)	20 ± 0.01	86 ± 1.89	4.2 ± 0.1	0.49	49.4
#2 (20 L)	3.5 ± 0.003	16 ± 0.1	4.5 ± 0.3	0.50	6.5
#3 (30 L)	64 ± 0.006	216 ± 0.8	3.4 ± 0.2	0.50	116.5
#4 (40 L)*	102 ± 0.008	792.4 ± 2	7.77 ± 0.2	0.55	57.9
#5 (40 L)	66 ± 0.006	490 ± 1	7.4 ± 0.4	0.53	35.1
#6 (40 L)	125 ± 0.004	633 ± 0.2	5.1 ± 0.4	0.54	27.6

* Quantification of Mo atoms by ICP-AES was also performed for this purification. However, no Mo atoms were identified.

The Table 3.2 represents all DVU2103´s purifications performed during this work, as well as protein concentration, number of iron atoms per protein and ratio Abs_{400nm}/Abs_{280nm}. The amount of litres was increased at each purification in order to obtain higher concentration of protein possible. In each purification a broad absorption band at 400 nm was identified, sometimes more defined than others. The ratio Abs_{400nm}/Abs_{280nm} also increased at each purification confirming the presence of a [Fe-S] cluster in the purified fraction. Results of ICP-AES for iron atoms are more irregular ranging from 3 to 8 iron atoms per protein. These values are consistent with either a single or two [4Fe-4S] clusters. The fact that in some purifications the number of iron atoms per protein is not higher than 4 can reflect the loss of one of the clusters during the purification procedure, but also the presence of protein without [Fe-S] cluster, as DVU2108. In addition, although there are two Fe-S binding motifs in each DVU2103 and DVU2104, it could be that these proteins might only bind one of these centres under certain conditions.

Since it was observed that in the final fraction of DVU2103 there was not a single protein band, and that the pI of the identified proteins was similar, a size exclusion chromatography was performed under anoxic conditions to try to separate the three proteins or at least separate DVU2108 from this complex (Figure 3.6). A Superdex 75 10/300 GL column was used as described in Section 2.1.1.

The elution of proteins was monitored at 280 nm and 400 nm, which is represented in the following chromatogram (Figure 3.6).

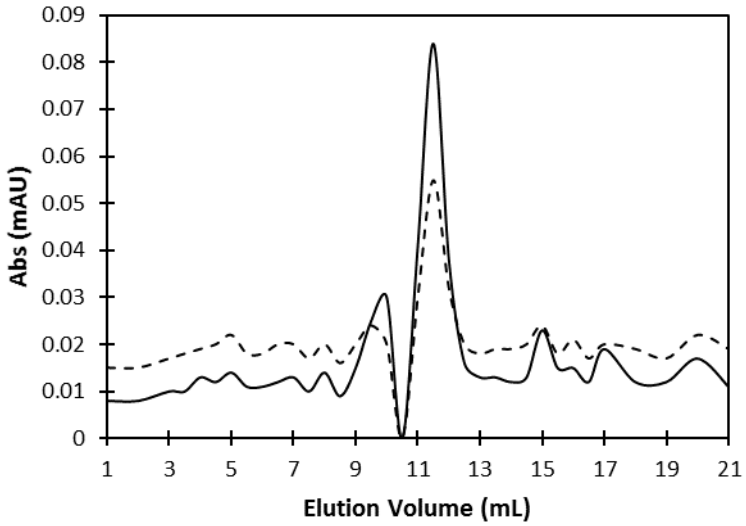

Figure 3.6 - Chromatographic profile of DVU2103 eluted in a Superdex75 10/300 GL column. The sample was eluted in a running buffer containing 20 mM Tris-HCl pH 7.6, 150 mM NaCl and 1mM DTT. Absorbance was monitored at 280 nm and 400nm. The chromatogram was obtained recurring to a Nanodrop. The chromatogram represents absorbance values at 280nm (full line) and at 400nm (dashed line).

As observed in Figure 3.6, a major peak that is eluted at around 11 mL, as well as some minor peaks around this volume. To identify the proteins eluted in each peak, a 12.5 % Tris-Tricine SDS-PAGE was performed (Figure 3.7). Analysis of SDS-PAGE allowed the identification of some bands of interest. The peak eluted at 11 ml presents protein bands at 30 kDa and also 12 kDa, which are the same as the ones found in the final fraction. A small protein of 12 kDa was also eluted at 14-15 ml, that might correspond to DVU2108.

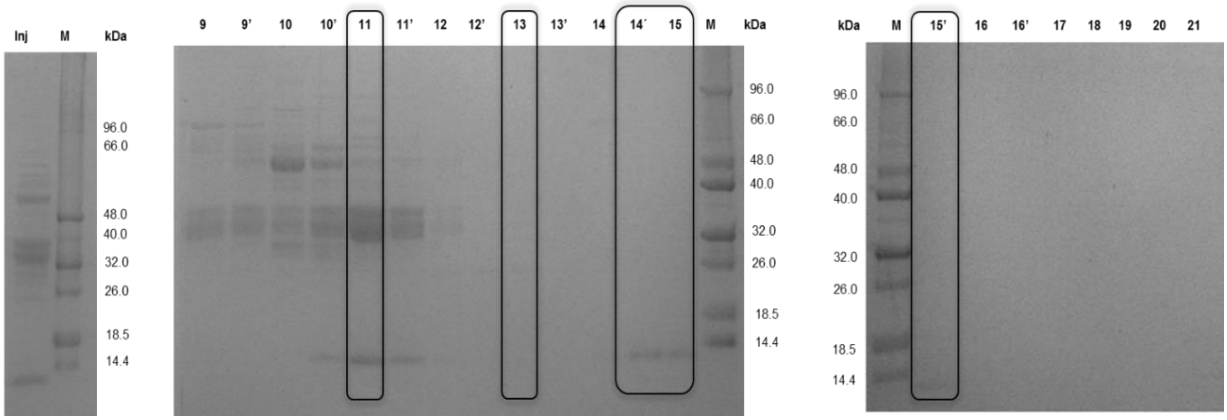

Figure 3.7 - SDS-PAGE acrylamide gel after size-exclusion chromatography purification. Proteins were eluted in 20 mM Tris-HCl pH 7.6, 150mM NaCl and 1mM DTT running buffer. M. Marker Low Molecular Mass (LMW – NZYTech) and numbers (9 to 21). Elution volume of collected fractions. Highlight the fractions of interest.

These fractions were also evaluated by UV-visible spectroscopy (Figure 3.8) for the presence or absence of a band at 400 nm in order to confirm the presence or absence of a [Fe-S] cluster. Figure 3.8–A shows the UV-visible spectrum of fraction 11, which presents the characteristic band at 400 nm indicating the presence of a [4Fe-4S] cluster. However, it is impossible to assure that the band appears due to the presence of DVU2103 protein, as the SDS-PAGE indicates the presence of a mixture of proteins (Figure 3.3). The UV-visible spectrum of fraction 14-15 is represented in Figure 3.8– B, which does not present an absorption band in the 350 nm - 400 nm region.

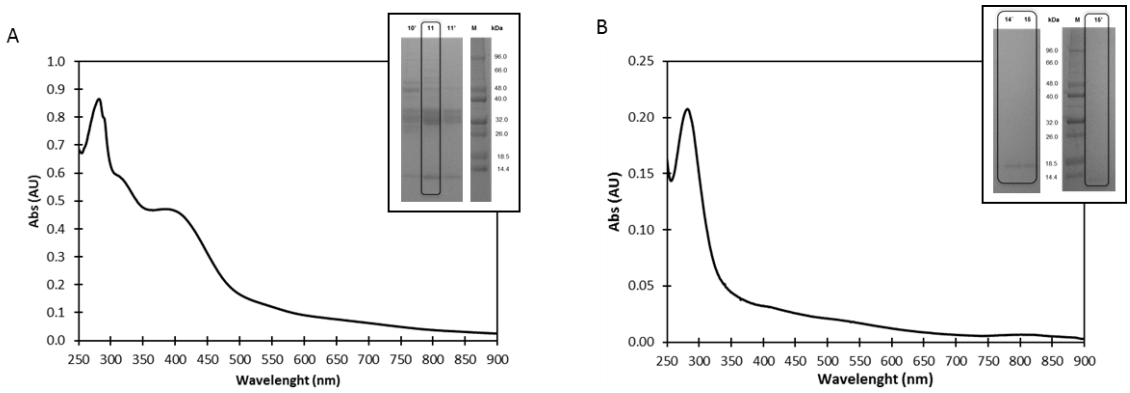

Figure 3.8 - UV–visible spectra of fractions of interest identified after size-exclusion chromatography in a Superdex75 10/300 GL in 20 mM Tris-HCl buffer pH 7.6 and 3 mM DTT. Panel A. Fraction 11, Panel B. Mix of fractions 14 to 15'.

Therefore, the complex cannot be separated using a size-exclusion chromatography. Moreover, there is a part of DVU2108 that is eluted separately, as a single peak. This protein does not show the presence of a metal cluster by the inspection of its visible spectrum. The reasons why there is the separation of this small fraction of DVU2108 from the complex are not known (see below).

As mentioned before, the purification performed only allowed the purification of a complex of proteins formed by DVU2103, DVU2104 and DVU2108 that cannot be separated, instead of a pure fraction, as expected. In the following sections, biochemical and spectroscopic characterization of this complex will be presented. Although, it is mentioned "DVU2103", we think that these data correspond to the complex formed by DVU2103/DVU2104/DVU2108 (or DVU2103/DVU2108, as the presence of DVU2104 has not yet been confirmed).

3.2 Biochemical Characterization

3.2.1 The Apparent molecular mass

3.2.1.1 Determination of the apparent molecular mass

The apparent molecular mass of "DVU2103" was determined by size-exclusion chromatography. For that a pre-packed column Superdex 200 10/300 GL (GE Healthcare) was used. This estimation was possible using a calibration curve, obtained with globular proteins of known molecular mass, which was presented in Figure 2.4, Section 2.3.5, Materials and Methods. The Figure 3.9 shows the chromatogram obtained upon elution of standard proteins and of "DVU2103" (in blue).

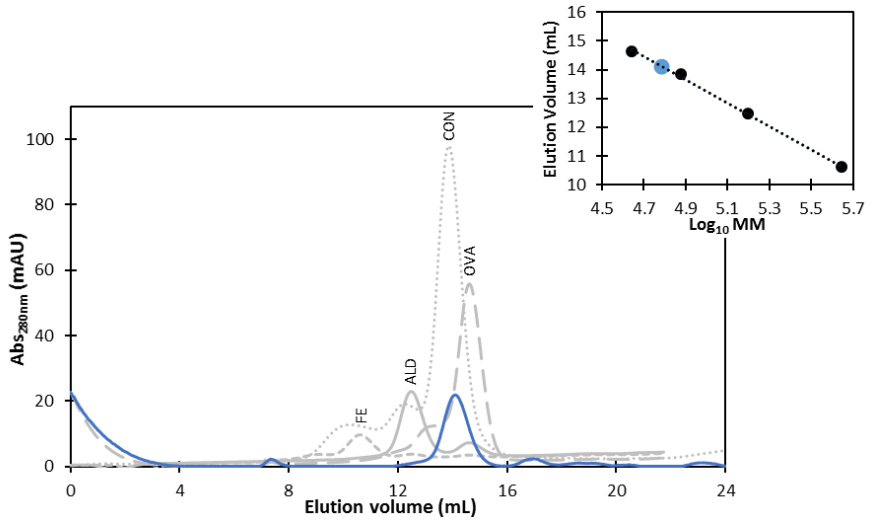

Figure 3.9 - Chromatogram obtained for the calibration curve of size-exclusion chromatography in a Superdex200 10/300 GL column. The figure represents the proteins of the calibration kit of size-exclusion chromatography (LMW GE Healthcare): FE – Ferritin, ALD – Aldolase, CON – Conalbumin and OVA - Ovalbumin (in grey) and "DVU2103" in the as-isolated form (blue). At the top right corner is represented the calibration curve for this column, the black circles are representative of the standard proteins and the blue circle is representative of "DVU2103" protein, Elution buffer: 50 mM Tris-HCl buffer pH 7.6, 150 mM NaCl and 1 mM DTT. Equation: Elution Volume = - 4.0559 x Log_{10}MM + 33.536, with a R = 0.9990.

The apparent molecular mass of "DVU2103" was estimated through elution volume of the protein complex and the equation of the calibration curve. "DVU2103" eluted at 14 mL, which corresponds to an apparent molecular mass of approximately 66 kDa.

Considering that the molecular mass of the polypeptide chain of DVU2103 is 31 kDa (Table 1.2), it could be considered that it was a dimer in solution. Nevertheless, taking into account the SDS-PAGE of this fraction, and that attempts to separate the complex are not possible, this corresponds to DUV2103/DVU2104/DVU2108, which has an expected molecular mass of 73 kDa. This value is lower than expected, but indicates that this protein complex is formed with a single polypeptide chain of each protein (heterotrimer of the type αβγ).

There is also a second peak that elutes with a higher elution volume (16.6 mL), which might correspond to DVU2108 with approximately 13 kDa, as expected (molecular mass of the polypeptide chain of 12.5 kDa, Table 1.2), that partially separates from the complex (as observed before). This value is not correctly determined since there is no standard protein below this protein.

3.2.1.2 Effect of ATP

It has been observed that ATP influences the apparent molecular mass of ATPases, by influencing the oligomeric state or the structure become more compact. For that a Superdex75 10/300 GL column was used, since the molecular mass of "DVU2103" was found to be 66 kDa, a value that falls within the interval separation of Superdex 75 (3 -70kDa). The elution volume of "DVU2103" was determined in the presence and absence of 0.5 mM ATP.

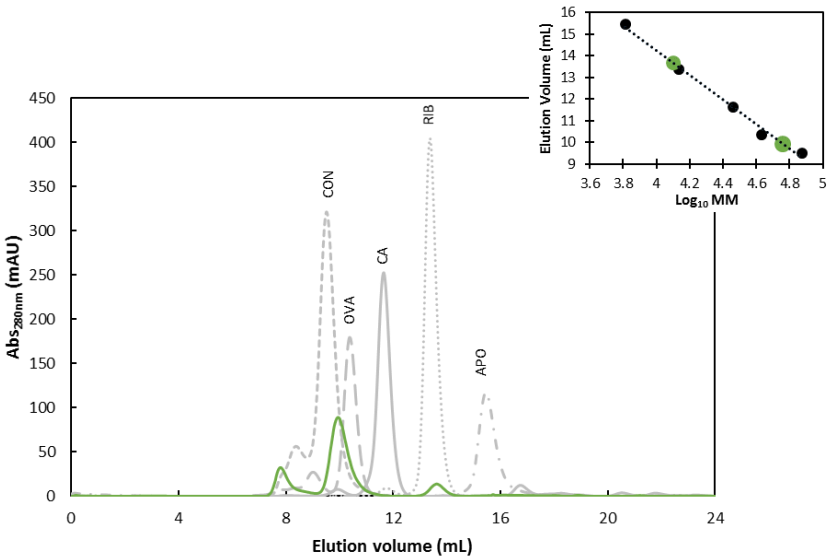

Figure 3.10 - Chromatogram obtained for the calibration curve of size-exclusion chromatography in a Superdex75 10/300 GL column. The figure represents the proteins of the calibration kit of size-exclusion chromatography (LMW GE Healthcare): CON – Conalbumin, OVA – Ovalbumin, CA – Carbonic Anhydrase, RIB – Ribonuclease, APO - Aprotinin (in grey) and "DVU2103" in the as-isolated form (green). At the top right corner is represented the calibration curve for the column, the black circles are representative of the standard proteins, the green circles are representative of "DVU2103" and DVU2108. Elution buffer: 50 mM Tris-HCl buffer pH 7.6, 150 mM NaCl and 1 mM DTT Equation: Elution Volume = -5.7026 x Log_{10}MW + 37.071, with a R = 0.9962.

The two chromatograms of the elution of “DVU2103” in the presence and in the absence of ATP are presented in Figure 3.11.

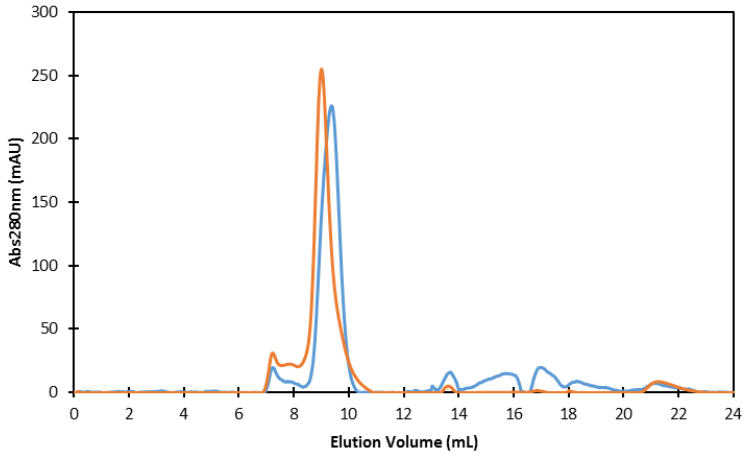

Figure 3.11 - Comparison of chromatograms obtained for size-exclusion chromatography in a Superdex75 10/300 GL column of "DVU2103" from *D. vulgaris* Hildenborough eluted with a buffer containing ATP (0.5 mM) (blue) and normal buffer (orange), with no ATP.

Using the equation of the calibration curve presented in Figure 3.10 the estimate value of "DVU2103"'s molecular mass was calculated, in order to compare the results of the two chromatograms. The results obtained are presented in Table 3.3.

Table 3.3 - Assignment of the molecular mass corresponding to the elution volume of the main peaks observed in the size-exclusion chromatography chromatogram (Figure 3.11) to determine the effect of the ATP.

	"DVU2103"	
	Elution Volume (mL)	**Molecular Mass (kDa)**
With ATP	9.75	62 ± 2
	13.68	13 ± 2
Without ATP	9.50	68 ± 2
	13.62	13 ± 2

In the presence of ATP, there is a main peak eluting with an elution volume around 9.75 mL, which corresponds to a molecular mass of 62 kDa (see Table 1.2). In addition, there is also a very

small peak at around 13.7 mL, that corresponds to a protein with an apparent molecular mass of 13 kDa. Comparing the molecular mass obtained for "DVU2103" protein in the presence and absence of ATP, it is possible to conclude that ATP affects the conformational structure of the protein, since in its presence the complex may be more compact, eluting as a smaller protein.

Some cases of ATP dependent molecular chaperones and changes in its conformational structure have already been described in literature. Biomolecular machines, as motor proteins and ATP dependent molecular chaperones undergoes a major conformational change upon ATP binding and hydrolysis [68]. Several proteins involved in membrane fusion events, cellular mechanisms (as protein turnover) and molecular mechanisms (as assembly and disassembly of protein complexes) have been described as couple ATP hydrolysis to protein-folding reactions [69]. The binding of ATP molecules in the ATPase domain of these proteins is responsible for the transmission of conformational changes along the binding site [68].

3.2.1.3 Effect of oxygen

The effect of oxidative conditions in the molecular mass of "DVU2103" was studied using chromatographic techniques. As in the case of ATP effect, a Superdex75 10/300 GL size-exclusion column was used. The elution volume of "DVU2103" was determined before and after exposure of "DVU2103" to oxic conditions during 96 h. The chromatogram representing the elutions of "DVU2103" are presented in Figure 3.12.

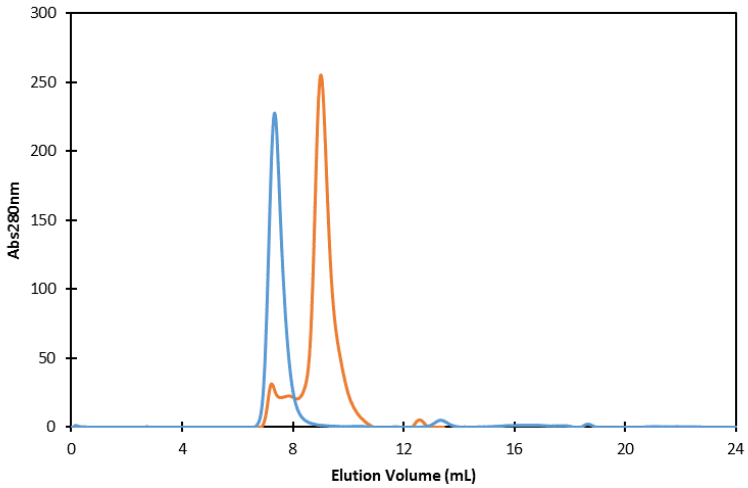

Figure 3.12 - Comparison of chromatograms obtained for size-exclusion chromatography in a Superdex75 10/300 GL column of "DVU2103" from *Desulfovibrio vulgaris* Hildenborough when exposed to oxic conditions (blue) and anoxic conditions (presence of reducing agent) (orange).

Table 3.4 - Assignment of the molecular mass (kDa) corresponding to elution volume (mL) of main peaks of the chromatogram of size-exclusion chromatography (Figure 3.12)

	"DVU2103"	
	Elution Volume (mL)	**Molecular Mass (kDa)**
Normal	9.50	68 ± 2
	12.67	13 ± 2
Oxygen exposed	7.33	> 70
	13.33	15 ± 2

In both chromatograms, it is observable a later peak at higher elution volume around 13 mL which corresponds to a molecular mass of 15 kDa (see Table 1.2). It is possible to assign this peak to DVU2108 protein (molecular mass of polypeptide chain of 12.5 kDa, Table 1.2. Under oxic conditions, a peak at higher elution volume was observed in the chromatogram around 7 mL. The corresponding molecular mass cannot be determined, since it is outside the range of separation of the column used. Since DVU2103 as an apparent molecular mass of 32 kDa (see Table 1.2), this peak can be assign to a protein complex of high molecular mass resulting of the oligomerization of protein present in the sample. As referred previously, "DVU2103" loses its [Fe-S] cluster when exposed to oxic conditions, resulting in oligomerization of the protein.

3.2.2 Malachite Green Phosphate Assay – Determination of ATP activity of "DVU2103"

With the aim of determining the ATPase activity of "DVU2103" complex, activity assays were performed as described in Section 2.3.6. The assay was performed at two concentrations of ATP (0.25 and 2.5 mM), and followed over time (min).

Highly sensitive methods for phosphate measurement are based on the change in the absorption spectra of basic dyes upon complex formation with phosphomolybdic heteropolyacid. Malachite Green is the most frequently used basic dye [70].

Malachite Green Phosphate Assay is based on the reaction of Malachite Green with phosphomolybdate which results in formation of a green complex, which is related with the evaluation of the free orthophosphate product from the ATPase reaction. The formation of the complex switch the colour of the reaction from orange to green, resulting in the appearance of an intense absorbance

band at 620 – 650 nm, allowing the measurement of the amount of phosphate produced during the reaction. The rate of free orthophosphate absorbance increase at 620 nm, which is proportional to the rate of steady-state ATP hydrolysis.

Activity of "DVU2103" as an ATPase was tested in two conditions in order to determine in which the protein is more active, and if the oxic conditions influence this activity. The results are presented in Figure 3.13.

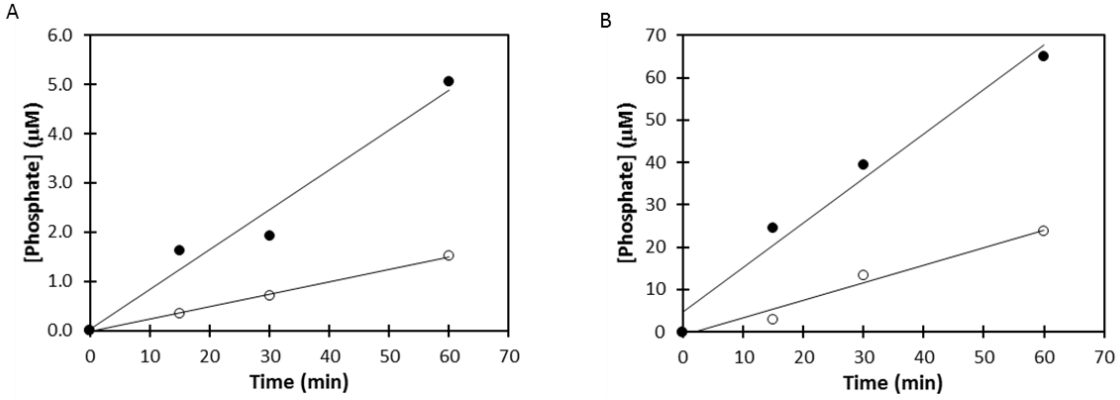

Figure 3.13 - Evaluation of phosphate concentration through time (min) for 10 µM "DVU2103" as ATPase. The assay was performed in 50 mM Tris-HCl buffer pH 8.1, 100 mM NaCl, 2 mM $MgCl_2$ and 2 mM DTT at room temperature. At various time intervals aliquots of the assay mixture were stopped by addition of a stop reagent, and inorganic phosphate was determined using the Malachite Green assay. Figure A and B represent two assays performed in two different conditions: in anoxic (full circles) and oxic conditions (open circles). A. Assay performed with 0.25 mM ATP, Equation (oxic condition): Phosphate concentration = 0.0253 x Time – 0.0215, R = 0.9999; Equation (anoxic condition): Phosphate concentration = 0.0811 x Time – 0.0201, with a R = 0.9831. B. Assay performed with 2.5 mM ATP, Equation (oxic condition): Phosphate concentration = 0.4145 x Time – 0.8781, R = 0.9858; Equation (anoxic condition): Phosphate concentration = 1.0482 x Time + 4.7324, with a R = 0.9870.

The results presented in Figure 3.13 show that "DVU2103" has a higher production of phosphate when the assay is performed under anoxic conditions at both ATP concentrations. As expected, phosphate production is higher when the protein has larger quantities of ATP available.

In the assay performed at 0.25 mM ATP, is observable that in anoxic conditions, "DVU2103" consume 3.2 times more phosphate when compared to oxic conditions, revealing that the protein is more active under anoxic environments.

Comparing the results obtained in both conditions, it is evident that "DVU2103" exhibits a higher ATPase activity under anoxic conditions. This can be attributed to the presence of the [Fe-S] cluster, which thus seems to be important for this activity, as under oxic conditions this cluster is destroyed.

3.3 Spectroscopic Characterization

3.3.1 UV-visible Spectroscopy

The UV-visible spectrum of "DVU2103" was acquired under different conditions, in order to determine the effect of reducing agents (sodium ascorbate and dithionite) in the absorption bands and also the effect of oxygen. This data will afterwards be compared with the EPR spectra acquired under similar conditions.

The UV-visible spectrum of "DVU2103", shown in Figure 3.14, shows the effect of ascorbate reduction. As mentioned above, the observed UV-visible spectrum of Fe-S proteins present a broad and intense absorption band in the visible region, at around 400 nm, due to [Fe-S] charge transfer bands. Proteins containing this type of cluster display a shoulder or a peak near 400 nm, which allows us to postulate the presence of [4Fe-4S] cluster [67]. Absorbance at this wavelength remains unchanged as the concentration of ascorbate in solution increases from 12 µM to 143 µM.

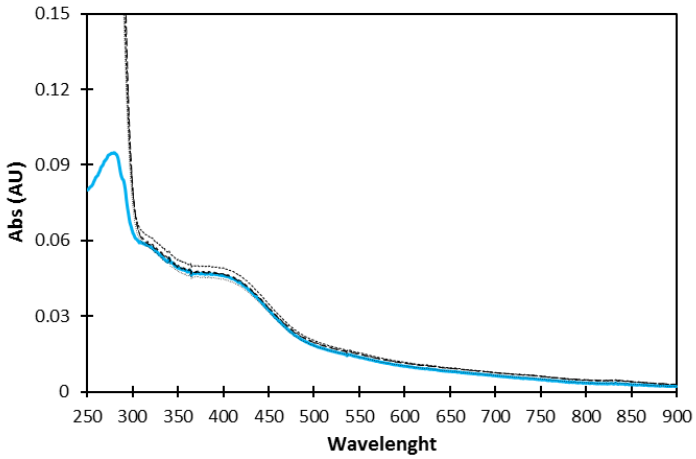

Figure 3.14 - Spectroscopic properties of *D. vulgaris* Hildenborough "DVU2103". UV–visible spectra of "DVU2103" in 20 mM Tris-HCl buffer pH 7.6 and 1 mM DTT. The as-isolated spectrum of "DVU2103" is shown as a continuous blue line and the reduced spectrum with increasing amount of ascorbate is shown as a dashed line.

The addition of increasing amounts of dithionite (Figure 3.15) to a buffered solution of "DVU2103" protein resulted in the progressive loss of the visible absorption spectrum characteristic of the native protein. The addition of a reducing agent as dithionite seems to progressively reduce the absorption at this wavelength. At higher dithionite concentration the peak simply disappears revealing that the cluster was fully reduced. The features of the [Fe-S] cluster can be recovered by oxidation under oxic conditions (Figure 3.16-A). So this process is reversible. However, after longer exposure to oxic conditions, the absorption band at around 400 nm is irreversibly lost, as the cluster is destroyed (Figure 3.16– B).

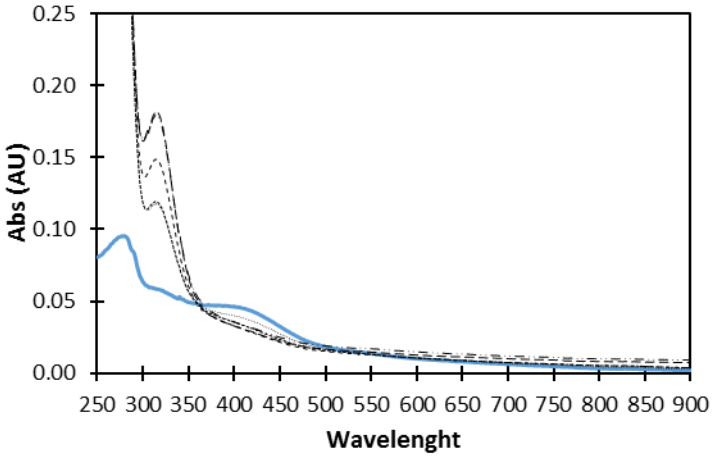

Figure 3.15 - Spectroscopic properties of *D. vulgaris* Hildenborough "DVU2103". UV–visible spectra of "DVU2103" in 20 mM Tris-HCl buffer pH 7.6 and 1 mM DTT. The as-isolated spectrum of "DVU2103" is shown as a continuous blue line and the reduced spectrum with increasing amount of dithionite is shown as a dashed line.

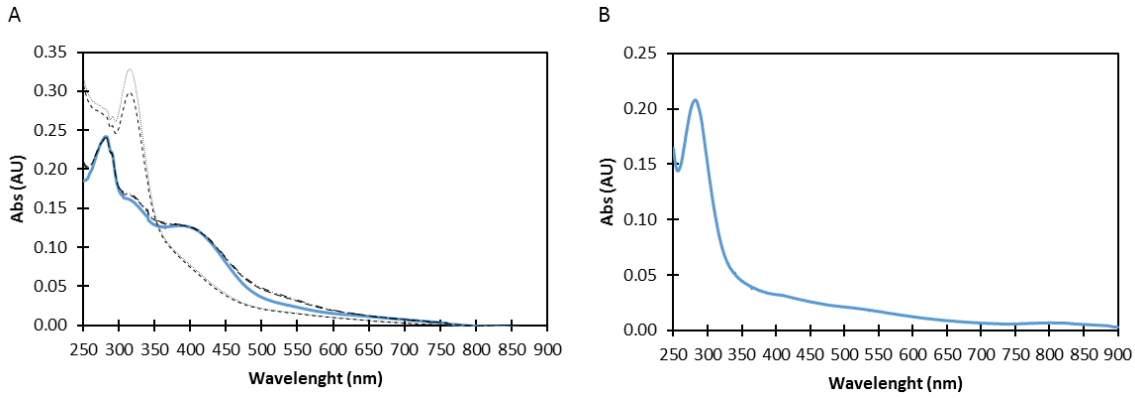

Figure 3.16 - Spectroscopic properties of *D. vulgaris* Hildenborough "DVU2103". UV–visible spectra of "DVU2103" in 20 mM Tris-HCl buffer pH 7.6 and 1 mM DTT. A) Recovery of the protein cluster reduced by dithionite after oxidation under oxic conditions. The as-isolated spectrum of "DVU2103" is shown as a continuous blue line and the oxidation spectrum with increasing incubation time under oxic condition is shown as a dashed line. B) UV-visible spectra of "DVU2103" 24 h after exposure to oxic conditions.

3.3.2 EPR Spectroscopy

As demonstrated in several cases in the literature, proteins containing [4Fe-4S] clusters have a large width of reduction potentials ranging from values between – 700 mV and – 150 mV for low-potential [Fe-S] proteins and + 100 mV and + 450 mV for high-potential [Fe-S] proteins (HiPIPs) with oxidation state from +1 to + 3 state [18]. In fact, two reduction couples can be found for these type of metal clusters in a functional way: $[4Fe\text{-}4S]^{3+/2+}$ or $[4Fe\text{-}4S]^{2+/1+}$ [67].

Magnetic spectroscopy as EPR are usually used to monitor [Fe-S] clusters as a function of their biological structure and mechanism of action [71]. Only two oxidation states of [4Fe-4S] clusters exhibit EPR signals (+ 1 and + 3), while + 2 state is EPR silent [8]. These signals can be detected at low temperatures, below 35 K [67]. The redox couple $[4Fe\text{-}4S]^{3+} \leftrightarrow [4Fe\text{-}4S]^{+}$ is characteristic of HiPIPs. Both redox states are paramagnetic and display characteristic EPR spectra [72]. The [4Fe-4S] clusters go from a $2Fe^{3+}$ - $2Fe^{2+}$ EPR silent state (S=0) to an Fe^{3+} - $3Fe^{2+}$ state (S=1/2) with an average EPR signal of around 1.96 [20]. The EPR spectrum of "DVU2103" as-isolated was acquired at two different temperatures: 10 K and 20 K (Figure 3.17).

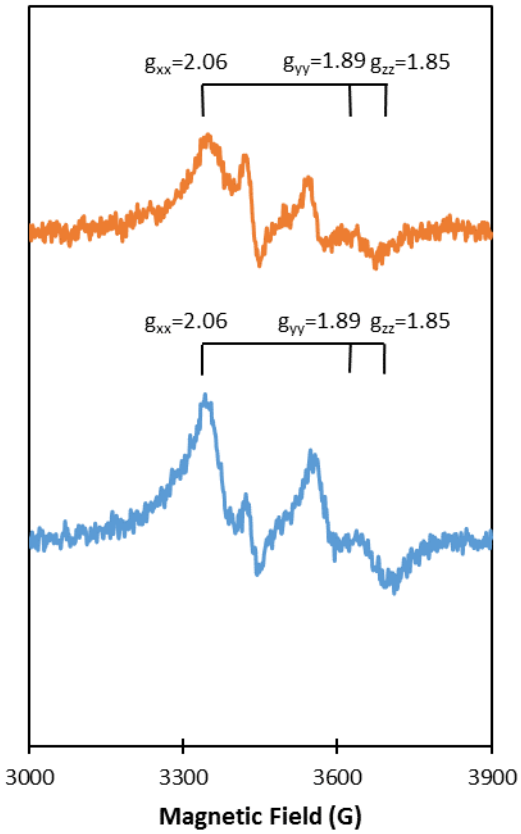

Figure 3.17 - X-band EPR spectrum of 126 µM "DVU2103" in 20 mM Tris-HCl buffer pH 7.6 and 3 mM DTT, at 9.65 GHz of frequency, 15 dB, 5 Gpp of modulation and 1×10^5 gain. The figure represents the as-isolated spectrum of "DVU2103" at 10 K (blue) and 20 K (orange).

The temperature dependence of the EPR spectra of the [Fe-S] clusters is strongly dependent on the population of multiple spin states of the spin-coupled systems [72]. At higher temperatures, excited states of the spin coupled systems become increasingly populated, so that signals from the S=1/2 ground states, particularly for the [4Fe–4S] clusters, disappear almost completely [72]. The analysis of the EPR spectra of "DVU2103" in the as-isolated form allowed us to state that when the temperature increases, the signals tends to lose intensity. In fact, comparing the signals of the two spectra we can notice that at 20 K, the signals appear to be less intense than the ones at 10 K, but this higher temperature is not enough to saturate the signals. From these results it is possible to conclude that the increase of temperature does not affect the position of the signals in the EPR spectrum of "DVU2103" protein.

In conclusion, the as-isolated EPR spectra of "DVU2103" presents a rhombic signal with g values at 2.06, 1.89 and 1.85, which is consistent with the presence of a paramagnetic species (Figure

3.17). There is also the presence of a signal at g = 4.7, which corresponds to free iron (signal located at approximately 1500 G is attributed to “free iron atoms” [73]) (Figure 3.18). This type of signals results from mononuclear high-spin Fe^{3+} ions in sites of low symmetry and are commonly found in a variety of solid state materials, chelates and metalloproteins [73].

As-isolated *D. vulgaris* Hildenborough “DVU2103” exhibits a rhombic signal. Comparing the EPR spectra obtained with characteristic spectra for [4Fe-4S] or [2Fe-2S] cluster proteins it is visible that they are similar in terms of g values, although the geometry of the centre might not be [18], the centre might be distorted. In order to see if these signals would disappear upon reduction two experiments were performed (Figure 3.18). In one, sodium ascorbate was added (which would reduce any metal centre with reduction potential above 0 mV *versus* SHE) (Figure 3.18). The analysis of this spectra indicates that there is reduction of the intensity of the EPR signals after 30 min of incubation, but the signal does not disappear completely. Further addition of sodium ascorbate or prolonged incubation would be needed to determine if the signal would disappear completely. Subsequent addition of sodium dithionite to this same sample originated a spectra presented in Figure 3.18. This is an intense axial EPR signal with g values at 2.06 and 1.94.

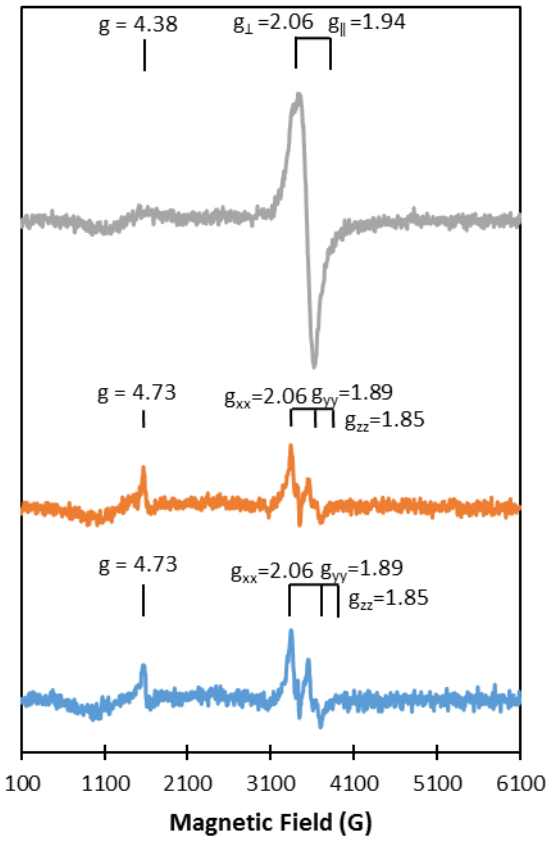

Figure 3.18 - X-band EPR spectrum of 126 µM "DVU2103" in 20 mM Tris-HCl buffer pH 7.6 and 3 mM DTT, at 10 K, 9.65 GHz of frequency15 dB, 5 Gpp of modulation and 1×10^5 gain. The figure represents the as-isolated (blue), ascorbate addition (orange) and dithionite addition (grey) spectra of "DVU2103".

The main signals were analysed in a small width that is represented in Figure 3.19.

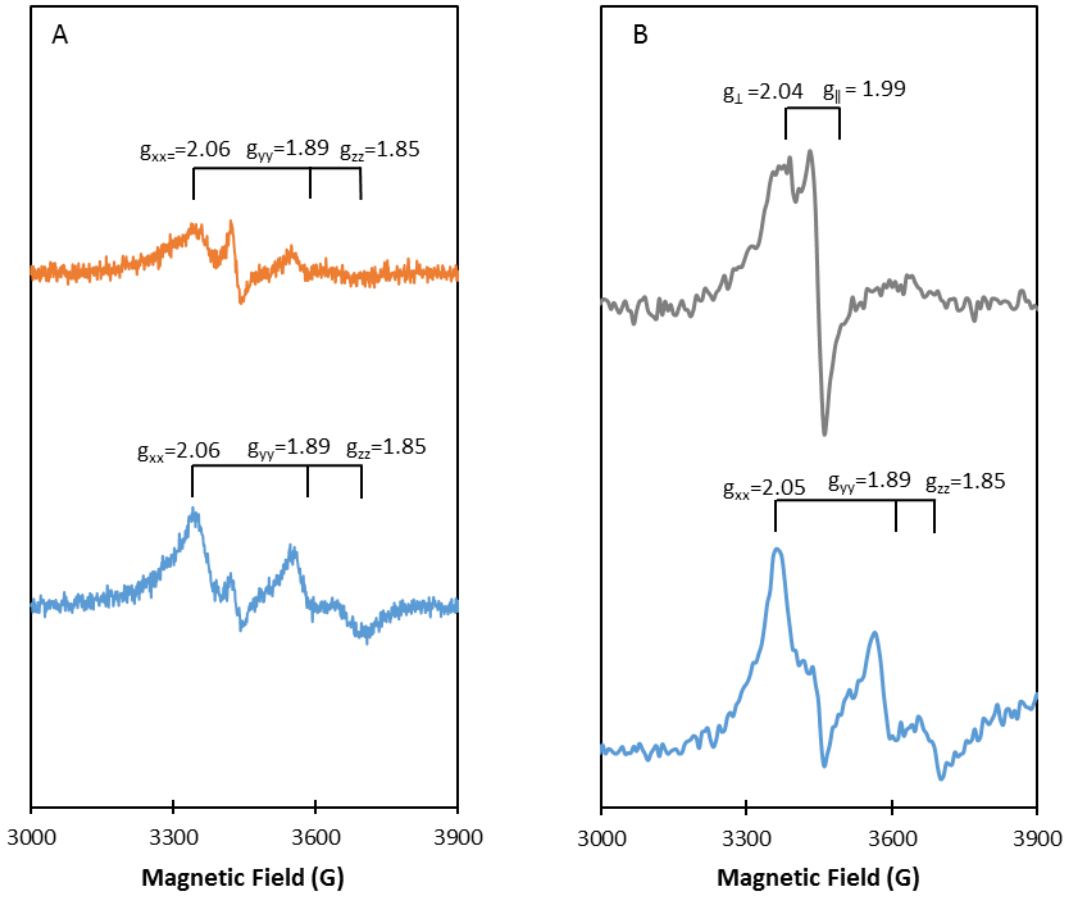

Figure 3.19 - X-band EPR spectrum of 126 µM "DVU2103" in 20 mM Tris-HCl buffer pH 7.6 and 3 mM DTT, at 10 K, 9.65 GHz of frequency 15 dB, 5 Gpp of modulation and 1×10^5 gain. A -Representative spectra of as-isolated (blue) and ascorbate reduction (orange) form. B – Representative spectra of as-isolated (blue) and dithionite reduction (grey) form.

Comparing the UV-visible spectrum with the EPR spectrum for "DVU2103" after reduction with an ascorbate solution (Figure 3.19–A), it is possible to relate the cluster conformation to the spin-spin interaction observed. The UV-visible spectrum points out that no significant change happens to the cluster when the ascorbate concentration is increased (as seen in Figure 3.14). This reflects no permanent alteration in the spin state of the [4Fe-4S] cluster, once intensities of EPR signals are recovered. These results allow us to conclude that "DVU2103"'s cluster cannot be completely reduced by sodium ascorbate. The feature that is observed in the EPR in the as-isolated form, decrease intensity with ascorbate, but this does not correlate with the any effect in its visible spectrum.

Another experiment was performed, in which sodium dithionite was added to another "DVU2103" sample after acquiring the as-isolated EPR spectra and incubated for 30 min (Figure 3.19-

B). This shows a different signal then before, an indication that after ascorbate addition or prolonged incubation with dithionite there is modification of the metal cluster. When this compound was added to the sample, the EPR signal changed from rhombic to axial, with the loss of signals above of 3500 G. EPR-detectable signals from “DVU2103” obtained after dithionite reduction is now more similar to the characteristic spectrum for [4Fe-4S] cluster in comparison with the spectra obtained after ascorbate reduction. This results leads us to conclude that dithionite addition lead to the reduction of the cluster, as previously confirmed by UV-visible spectroscopy (Figure 3.15). As previously mentioned, it is possible to infer, taking into account these results, that “DVU2103” protein possesses more elements than the [4Fe-4S] cluster with an EPR signal. In terms of redox state, this second reduction leads to the transformation of the cluster from a + 3 state to a + 1 state. Once both states possess EPR-detectable signals, the spectrum obtained is in line with the theory that dithionite reduction affect the paramagnetic state of the protein, creating a different paramagnetic specie.

The existence of two clusters and the fact that DVU2108 forms a stable complex with DVU2103 after purification can influence the EPR-detectable signals obtained. [8Fe-(7/8)S] or 2[4Fe-4S] clusters present different redox states comparing to [4Fe-4S] clusters [74]. In this case it can reach from diamagnetic (S=0) and therefore EPR silent, to both paramagnetic + 1 and + 2 oxidation states and EPR active [74].

Experiments conducted by Lanzilotta and Seefeldt in nitrogenase proteins proved that a sample in which the $[8Fe\text{-}(7/8)S]^{2+}$ state of a molybdenum-iron (MoFe) protein is mixed with a reduced Fe protein exhibits a particular EPR spectrum (Figure 6.1, Appendix 5) [74]. The signals assigned to the reduced state of the Fe protein ($[4Fe\text{-}4S]^{1+}$ cluster) disappeared, consistent with the oxidation of the [4Fe-4S] cluster to the + 2 oxidation state upon electron transfer to the MoFe protein [74]. When comparing the spectrum obtained by Lanzilotta and Seefeldt to that obtained for the as-isolated “DVU2103”, it is possible to see some similarities. One of the theories that can explain the results obtained is that EPR spectrum of as isolated form is a result of the combination of signals from the two [4Fe-4S] clusters present in “DVU2103” and the DVU2108. This may explain why as isolated EPR spectrum is not characteristic of a [4Fe-4S] cluster. When dithionite is added to the sample, it reduces only one of the [4Fe-4S] of "DVU2103". This consequently leads to the loss of the absorbance band at 400 nm in UV-visible spectrum. Once that only one [4Fe-4S] remains intact, the interaction between “DVU2103” clusters and DVU2108 gets lost, leading to the change of EPR-detectable signals. The final EPR spectrum obtained is now due to the [4Fe-4S] that remains intact and consequently characteristic of this type of centre.

3.4 Homologous expression of DVU2108 in *D. vulgaris* Hildenborough

The cells used to purify DVU2108 were collected, as in the case of DVU2103 protein, at the end of their exponential phase, approximately 24 h after inoculation (OD_{600nm} = 0.7) in Medium C (supplemented and not with $Na_2MoO_4.2H_2O$) without agitation under an anoxic condition. After harvesting the cells and cell lysis, the protein soluble extract was analysed in a 12.5 % Tris-Tricine SDS-PAGE. In Figure 3.20 is presented the profile of protein expression.

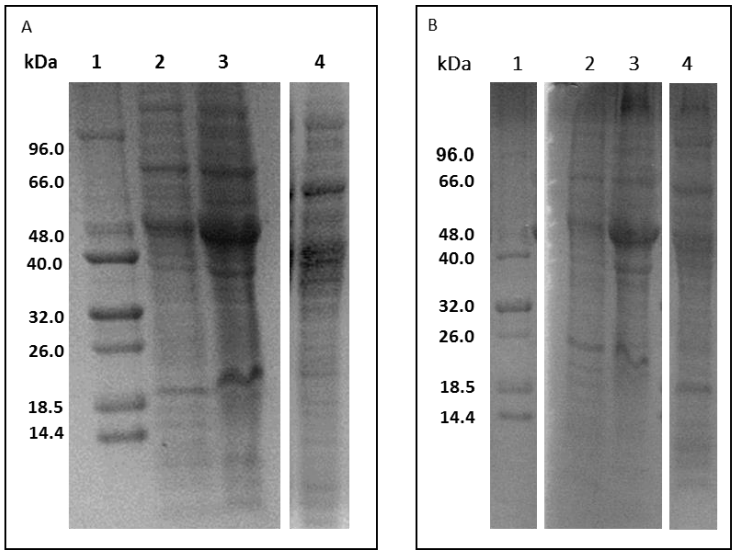

Figure 3.20 –Proteins profile in 12.5% Tris-Tricine SDS-PAGE. A) Normal Bacterial Growth. B) Supplemented Bacterial Growth. Lanes: 1. Low Molecular Mass Marker (LMW – NZYTech), 2. Cell debris, 3. Membrane fraction, 4. Soluble Fraction. Gels were stained with Coomassie Blue.

3.4.1 Purification of DVU2108

3.4.1.1 Normal Bacterial Growth

As in the case of DVU2103, DVU2108 was purified under anoxic conditions in order to preserve the [Fe-S] cluster that could be present. DVU2108 purification, as described in Section 2.2.1.1 Materials and Methods, was simplest when compared to the of DVU2103 and consisted in the use of a single affinity column, since the gene encoding this protein was cloned with a STREPII tag at its N-terminus.

A Strep-Trap HP column was used to separate the protein of interest from the remaining proteins. This chromatography consists in a high-performance matrix of StrepTaction Sepharose medium that allows an easy separation of contaminants by immobilized Strep-Tactin™ ligand, a specially-engineered streptavidin. Strep-Trap column is usually used to purify StrepII-tagged recombinant proteins. An elution buffer containing 2.5 mM desthiobiotin was used to elute DVU2108. This strategy was adopted in order to minimize the presence of contaminants in the sample that can interact non-specifically with the column matrix. Desthiobiotin present in the buffer acts as a competitor with the Strep-Tactin™ ligand that is attached to the matrix, allowing separation of the different proteins. The fact that the use of this kind of column allows the purification to be performed under physiological conditions and to preserve the activity of the target protein. DVU2108 was eluted in a total volume of 20 mL, collected in fractions of approximately 4 mL. The fraction obtained presented a brownish coloration, which could indicate the presence of a [Fe-S] cluster.

The fractions after chromatography column were monitored in a 12.5 % Tris-Tricine SDS-PAGE in order to identify the fractions containing the protein of interest. The SDS-PAGE with each of the main fractions during the purification is presented in Figure 3.21.

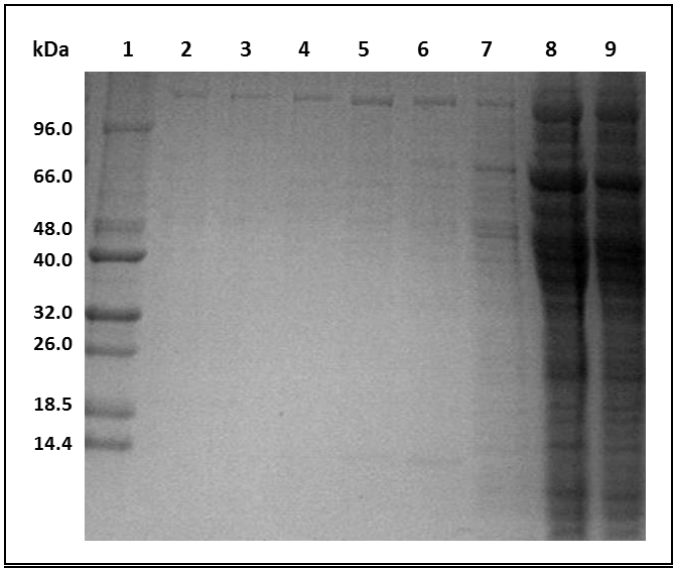

Figure 3.21 - SDS-PAGE acrylamide gel after DVU2108 purification recurring to an affinity column. Lanes: 1. Marker Low Molecular Mass (LMW – NZYTech), 2-7 Fractions corresponding to protein elution, 8. Washing step, 9. Soluble Protein Fraction. Gels were stained with Coomassie Blue.

From analysis of the SDS-PAGE (Figure 3.24) it is possible to realize that purification of DVU2108 was not very efficient, since some contaminants remain present in the protein fraction after the washing step. It was expected that after washing the column with a high ionic force buffer (500 mM NaCl) only DVU2108 protein appeared in protein fraction. The UV-visible spectrum of the fraction with more colour of DVU2108 is presented in Figure 3.22.

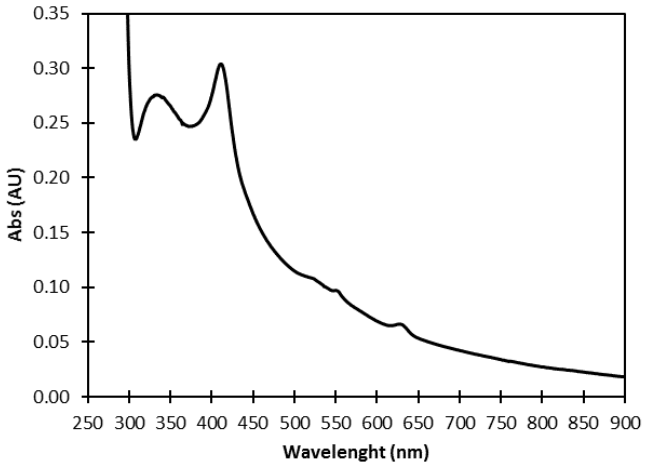

Figure 3.22 - UV–visible spectrum of as isolated hypothetical protein DVU2108 of *Desulfovibrio vulgaris* Hildenborough in 100 mM Tris-HCl buffer pH 7.6, 500 mM NaCl and 3 mM DTT.

In order to increase the purity of the sample eluted, a polishing step was performed using a size-exclusion column, Superdex75 10/300 GL. The size-exclusion chromatography was performed under anoxic conditions. The elution of proteins was monitored at 280 nm and 400 nm, which is represented in the following chromatogram (Figure 3.23).

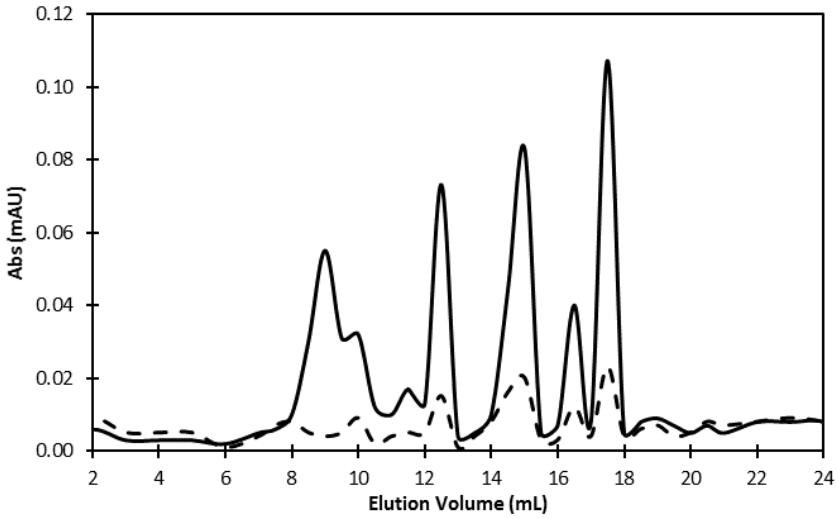

Figure 3.23 - Chromatographic profile of DVU2108 separation in a Superdex75 10/300 GL column. The sample was eluted in a running buffer containing 50 mM Tris-HCl pH 8.1, 150 mM NaCl and 1 mM DTT. Absorbance was monitored at 280 nm and 400 nm. The chromatogram was obtained recurring to a Nanodrop. The chromatogram represents absorbance values at 280 nm (full line) and at 400 nm (dashed line).

As observed in Figure 3.23, four peaks stand in the chromatogram obtained from the size-exclusion chromatography at 9, 12.5, 15 and 17.5 mL. To identify the proteins eluted in each peak, a 12.5 % Tris-Tricine SDS-PAGE was performed (Figure 3.24).

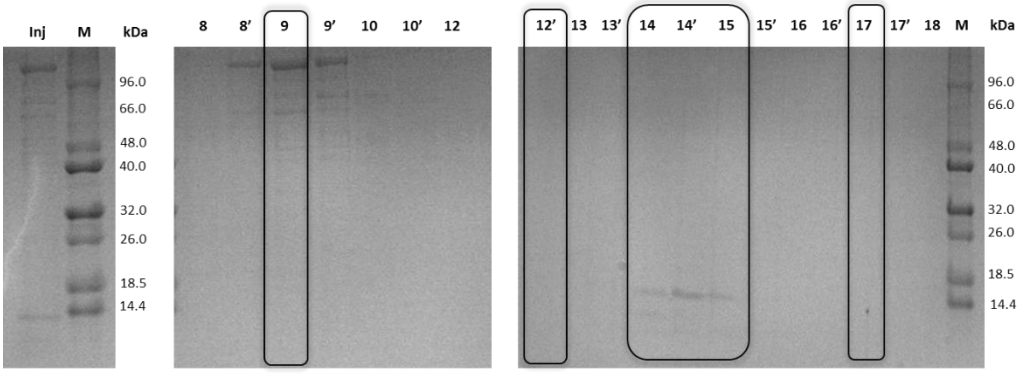

Figure 3.24 - SDS-PAGE of the fractions collected from the size-exclusion chromatography during DVU2108 purification. Proteins were eluted in 50 mM Tris-HCl pH 8.1, 150 mM NaCl and 1 mM DTT running buffer. Lanes: Inj. Injection, M. Marker Low Molecular Mass (LMW – NZYTech) and numbers (8 to 18). collected fractions during elution. Highlighted are the fractions of interest.

Analysis of SDS-PAGE allowed the identification of some bands of interest. The peak eluted at 15 mL presents protein band at 13 kDa, approximately, corresponding to StrepDVU2108, that is also present in fractions at 14 and 14.5 mL. Proteins of high molecular mass were eluted at 9 mL.

Fraction identified as containing StrepDVU2108 presented a slightly brownish coloration after the last step of purification. Fractions were concentrated using Vivaspin 500 (*cut off* 3kDa). The UV-visible spectrum of the concentrate final fraction of DVU2108 is presented in Figure 3.25. Its analysis indicate no significant absorption peak in the 400 nm region that are characteristic of major [Fe-S] charge transfer bands, although this band might be under the spectra of the cytochrome signature spectrum that was obtained

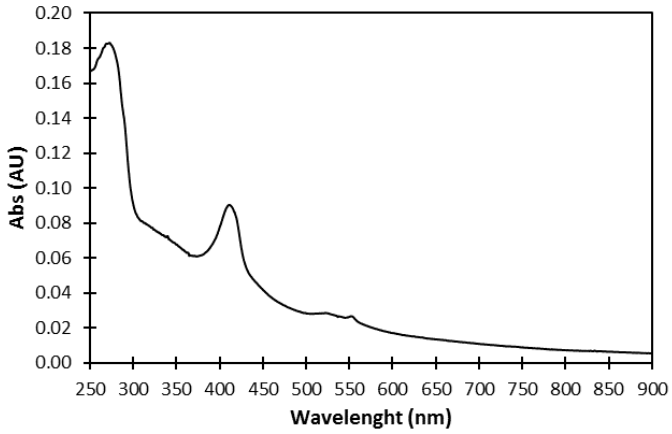

Figure 3.25 - UV–visible spectra of as-isolated hypothetical protein DVU2108 of *D. vulgaris* Hildenborough in 100 mM Tris-HCl buffer pH 7.6, 500 mM NaCl and 3 mM DTT after the size-exclusion chromatography.

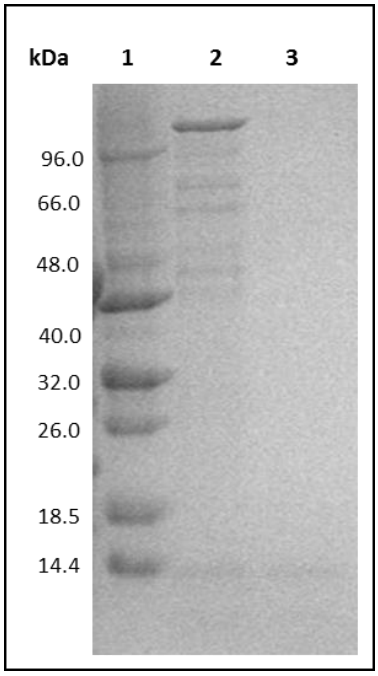

Figure 3.26 - Analysis of the fractions during DVU2108 purification. Lanes: 1. Low Molecular Mass Marker (LMW – NZYTech), 2. DVU2108 fraction before size-exclusion chromatography, 3. DVU2108 final fraction after size-exclusion chromatography. 12.5 % SDS-PAGE. Gels were stained with Coomassie Blue.

Analysis of SDS-PAGE of DVU2108 final fraction (Figure 3.26) indicates that a purer fraction (but still with some other proteins then DVU2108) was obtained after size-exclusion chromatography, making more efficient purification process since it allowed the separation of most of the contaminants present in the initial soluble fraction.

Previous studies have indicated the presence of either a Mo/Cu cluster (French team) or Fe-cluster (Portuguese team) in DVU2108 protein, metal quantification of Fe, Mo and Cu atoms was performed by ICP-AES. Samples of DVU2108 final fraction and DVU2108 fraction before polishing step were analysed and the results are presented in Table 3.5.

Table 3.5 - Data obtained from ICP-AES analysis for Fe, Mo and Cu atoms in DVU2108 protein. Quantification of performed by 660 nm Pierce Protein Quantification method.

Sample	[Protein] (µM)	[Fe] (µM)	Fe/prot	[Mo] (µM)	Mo/prot	[Cu] (µM)	Cu/prot	A_{400nm}/A_{280nm}
DVU2108 after Strep Trap chromatography	48 ± 0.02	1.28 ± 0.04	0	0	0	0	0	0.17
DVU2108 final fraction	5 ± 0.004	6.09 ± 0.51	1.2 ± 0.1	0	0	5.04 ± 5.34	1 ± 1	0.45

Results of ICP-AES show a ratio of around 1 iron atoms per protein, which suggest the presence of a metallic Fe-S cluster in StrepDVU2108. However, no metallic cluster Mo/Cu was observed in the protein after purification, since only 1 copper atom per protein and no Mo atom were identified, nor the visible spectrum is similar to the Mo/Cu Orange Protein [48]. Different growth and purification conditions were tested in order to obtain a native DVU2108 with an intact Mo/Cu cluster.

3.4.1.2 Supplemented Bacterial Growth

A bacterial growth of *D. vulgaris* Hildenborough in Medium C supplemented with molybdenum was performed, in order to obtain a protein with higher amounts of Mo in its centre. StrepDVU2108 was, as previously, purified under anoxic conditions in order to preserve the [Fe-S] cluster that could be present.

StrepDVU2108 was obtained after performing a series of pre-inoculums. As described in Section 2.2.2, $Na_2MoO_4.2H_2O$ final concentration in culture was increased step by step in order to let the bacterial culture adapt to the new growth conditions. Initially starting from in 2.81 µM to a final concentration of 45 µM $Na_2MoO_4.2H_2O$, the culture was successively transferred to higher Mo concentration, in order to adapt the cells to higher Mo concentrations (Table 3.6).

Table 3.6 - Growth of *D. vulgaris* Hildenborough in Medium C supplemented with Mo.

Day	Time (h)	[$Na_2MoO_4.2H_2O$] (mM)	Volume Inoculum (mL)	OD_{600nm}
0	0	0	5	0.6
1	24	2.81	5	0.79
2	48	5.625	5	0.79
3	72	11.25	5	0.65
4	96	19.8	5	0.66
5	120	24.75	5	0.75
6	144	29.7	5	0.82
7	168	37.75	5	0.59
12	288	40.5	5	0.63
13	312	40.5	5	0.64
14	336	40.5	5	0.73
15	360	45	5	0.82
18	432	45	5	0.69
21	504	45	5	0.78
22	528	45	5	0.71
23	552	45	10	0.73
24	576	45	10	0.77
25	600	45	10	0.63
26	624	45	10	0.71
27	648	45	10	0.78
28	672	45	100	0.72
29	696	45	100	0.69
30	720	45	100	0.83
31	744	45	100	0.76
32	768	45	100	0.75
33	792	45	100	0.78
34	816	45	100	0.68
35	840	45	1000	0.72

A Strep-Trap HP column was used to separate the protein of interest from the remaining proteins, as described in Section 2.2.2.1. An elution buffer containing 2.5 mM desthiobiotin was used to elute StrepDVU2108. Unlike what happened in purification of StrepDVU2108 growth in normal conditions (Section 3.4.1.1), in this case it was not possible to purify a pure fraction of protein. Instead of eluting from the column with the step of desthiobiotin, the protein was mostly eluted during the washing step. The fractions after chromatography column were monitored in a 12.5 % Tris-Tricine

SDS-PAGE. The SDS-PAGE with each of the main fractions during the purification is presented in Figure 3.27.

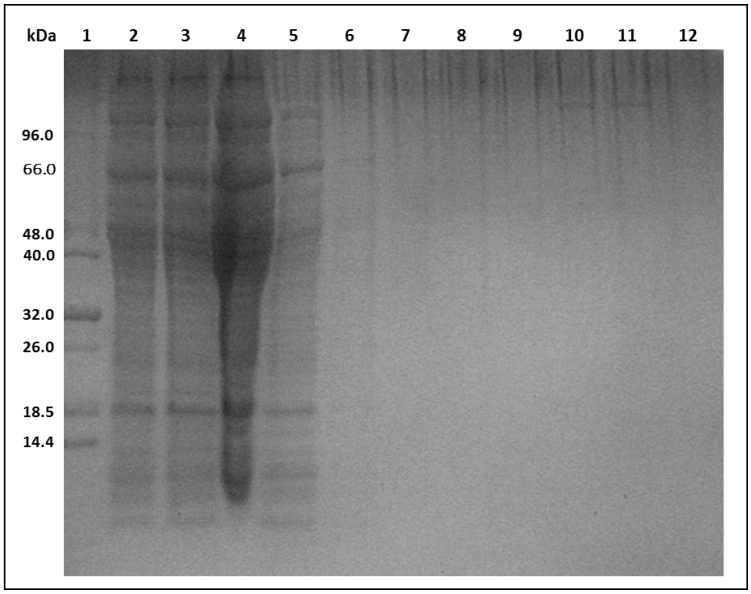

Figure 3.27 - SDS-PAGE acrylamide gel after DVU2108 purification recurring to an affinity column. Lanes: 1. Marker Low Molecular Mass (LMW – NZYTech), 2-3. Soluble Fraction 4-8. Fractions corresponding to wash steps. 9-12. Fractions corresponding to protein elution. Gels were stained with Coomassie Blue.

As observed in Figure 3.27, a slight band is present in the fractions 9 and 10 corresponding to protein elution. However, it is possible to see that most protein is present in fraction 4 and 5, which means that DVU2108 was mostly eluted somewhere in the washing steps. No brownish coloration was present in either fraction. Samples of DVU2108 eluted fractions were analysed and the results are presented in Table 3.7.

Table 3.7 - Quantification of performed by 660 nm Pierce Protein Quantification method for eluted fractions of StrepDVU2108 purification.

Fraction Eluted	[Protein] (µM)
4	1.64 ± 0.007
5	1.29 ± 0.006
6	4.51 ± 0.008
7	1.58 ± 0.008
8	2.00 ± 0.009
9*	1.28 ± 0.010
10*	3.43 ± 0.006
11	1.11 ± 0.008

*Fraction containing StrepDVU2108 fraction after purification.

Fraction identified as containing StrepDVU2108 were colourless and contained a total amount of protein of 4.71 µM ± 0.008. Since it was not possible to obtain sufficient amount of StrepDVU2108, no biochemical studies were performed. A repetition of this growth should be tried in the future, in order to obtain a higher amount and a purer fraction of StrepDVU2108 protein.

4

Conclusions and Future Perspectives

In this work, the homologous expression of HisDVU2103 in *D. vulgaris* Hildenborough was performed with a yield of approximately 58 ± 28 µg of purified protein per L of culture. Purification was performed under anoxic conditions in order to preserve the metallic cluster bound to the polypeptide chain. It was not possible to purify HisDVU2103 as a single protein, since it was purified with other two proteins of *orp* operon, DVU2104 and DVU2108. Separation of the proteins was tried using a size-exclusion chromatography, but it revealed unsuccessfully, since it was not possible to obtain a purer fraction. After the elution of the complex by ion-exchange chromatography, identification by MALDI-TOF-MS analysis of the several proteins co-eluted was performed. Results suggested the possibility of formation of a complex between the proteins with a physiologic meaning. This technique allowed the attribution of a specific molecular mass to each protein present in the protein complex facilitating its identification (DVU2103 and DVU2104 with 30.46 kDa and DVU2108 with 12.47 kDa).

The existence of two [4Fe-4S] clusters in DVU2103 was predicted by bioinformatic analysis, having been corroborated the presence of a [4Fe-4S] cluster by UV-visible characterization that present a broad absorption band at 400 nm, characteristic of this type of clusters. ICP-AES analysis for iron atoms range from 3 to 8 iron per protein, being consistent with either one or a two [4Fe-4S] clusters. EPR and UV-visible experiments were performed with two reducing agents (sodium dithionite and ascorbate) and data obtained was compared to better understand the structure of the centre. The purification process should be optimized, hereafter, in order to obtain a purer fraction and higher amount of HisDVU2103.

Biochemical characterization of the “DVU2103” complex, composed by DVU2103 DVU2104 and DVU2108 proteins was performed in order to better understand the complexity of its protein complex. Studies to determine the apparent molecular mass of “DVU2103” were performed using a size-exclusion chromatographic column confirming the purification of a protein complex of approximately 66 ± 2 kDa. This value is lower than expected (73 kDa) since DVU2103 has an estimate molecular mass of 31 kDa, as well as DVU2104, and DVU2108 a molecular mass of 12.5 kDa. Therefore, the sample forms a heterotrimer composed by a single polypeptide chain of each protein present in the complex, DVU2103, DVU2104 and DVU2108.

Different experiments were performed in order to understand the effect of ATP and oxic conditions in the apparent molecular mass of “DVU2103”. The experiment was performed in the presence and absence of 0.5 mM ATP and 1 mM DTT, observing that in the case in which ATP is present, the protein was eluted at an elution volume corresponding to 62 ± 2 kDa, 4 kDa less when compared with the protein eluted in a buffer without ATP (68 ± 2 kDa). A protein of 13 ± 2 kDa was also eluted in both cases, even if a protein with a similar size was detected in the SDS-PAGE of the main larger protein peak. The results obtained can be interpret as if the presence of ATP affects the conformational structure of the protein influencing its apparent molecular mass, making the complex more compact.

The effect of oxygen was also studied recurring this chromatographic techniques. The apparent molecular mass of “DVU2103” was compared before and after being exposed to oxic conditions during 96 h, and eluted in the presence of 1 mM DTT (to avoid formation of any disulphide bonds formed to the oxic conditions). In this last case, the protein complex eluted as having a higher molecular mass. The loss of the [Fe-S] cluster under oxic conditions can contribute to change the three-dimensional structure of the complex resulting in protein oligomerization.

ATP activity of "DVU2103" was determined and tested in two conditions (oxic and anoxic environment) in order to determine in which the protein was more active. The activity of "DVU2103" was calculated and the assay was performed with two ATP concentration (0.25 and 2.5 mM) through time (from 0 to 60 min). The results showed that “DVU2103” consumed a higher phosphate concentration under anoxic conditions. This can be attributed to the presence of the [Fe-S] cluster, which seems to be important for the ATPase activity of “DVU2103”, since under aerobic conditions the protein showed less activity, which may be associated to the destruction of the cluster when exposed to oxygen. Further work can focus in calculating the specific activity of “DVU2103” with different ATP concentration in order to estimate a K_M and $V_{máx}$. Effect of pH and others substrates, as GTP, should also be tested.

In order to determine the effect of two reducing agents (sodium dithionite and ascorbate), UV-visible spectra of “DVU2103” were acquired in different conditions. The spectrum obtained after addition of ascorbate presents a broad and intense absorption band in the visible region around 400 nm characteristic of the native protein. The absorbance remains unchanged at this wavelength as the concentrations of ascorbate is increased. In the case of sodium dithionite addition, the spectrum progressively reduces absorbance at 400 nm, and it is observed a progressively loss of the band. After complete reduction of the cluster with dithionite, it can be re-oxidized under oxic conditions in a reversible process. However, longer exposure to oxic conditions reflects in irreversibly loss of the absorption band at around 400 nm, which is explained by cluster destruction.

EPR spectroscopic characterization was performed in order to characterize the properties of the protein’s metallic cluster. The native form of “DVU2103” is EPR active, and thus it can be concluded that it is at least partially isolated in the Fe^{3+} - $3Fe^{+}$ form. Spectra were acquired at three different conditions: as-isolated and reduced with sodium dithionite and sodium ascorbate.

As-isolated spectrum of “DVU2103” presented a rhombic signal with g values at 2.06, 1.89 and 1.85 consistent with the presence of a paramagnetic species, and a signal at 4.7 corresponding to free iron. The spectrum obtained is similar when compared with the characteristic spectra for [4Fe-4S] or [2Fe-2S] cluster proteins, however is not identical what impel to think that EPR signal may not be exclusively to the cluster.

Ascorbate do not cause a significant change in the EPR signals, leading to the conclusion that the cluster cannot be completely reduced by ascorbate. Comparing the UV-visible spectrum with the EPR spectrum for “DVU2103” reduction it is possible to conclude that ascorbate do not change the structure of the [Fe-S] cluster, once that no permanent alteration in its state spin is noted.

Dithionite addition originated an intense axial EPR signal with g value at 2.06 and 1.94 indicating that prolonged incubation with this reducing agent leads to modification of the metal cluster of the protein.

Homologous expression of StrepDVU2108 in *D. vulgaris* Hildenborough was also performed. As in HisDVU2103 purification, all steps were performed under anoxic conditions to preserve the eventual presence of an [Fe-S] cluster. No significant absorption peak at 400 nm was detected, however ICP-AES results leads to believe that DVU2108 possess a [Fe-S] cluster in its structure. Previous studies mentioned DVU2108 containing a Mo/Cu cluster, however the protein purified in this work does not suggest that. Despite having been tested in this work, purification of StrepDVU2108 from a growth in a medium containing Mo should be repeated in

the future as an attempt to conserve Mo/Cu cluster in its native form, which was not possible in this work. Biochemical characterization of DVU2108 will allow hereafter to characterize the properties of the metallic cluster.

ITC and NMR studies should also be accomplished to define and characterize the interaction of ATPase DVU2103 with DVU2108, when pure samples of both proteins are obtained.

5

References

[1] G. Muyzer and A. J. M. Stams, “The ecology and biotechnology of sulphate-reducing bacteria,” *Nat. Rev. Microbiol.*, vol. 6, no. June, pp. 441–454, 2008.

[2] I. Encyclipaedia Britannica, *Enciclopaedia Britannica*. 2008.

[3] L. L. Barton and F. a Tomei, “Characteristics and Activities of Sulfate-Reducing Bacteria.,” in *Sulfate-Reducing Bacteria*, 1995, pp. 1–32.

[4] L. L. Barton and G. D. Fauque, *Chapter 2 Biochemistry, Physiology and Biotechnology of Sulfate-Reducing Bacteria*, 1st ed., vol. 68, no. 9. Elsevier Inc., 2009.

[5] S. M. Bertolino, I. C. Rodrigues, R. Guerra-Sa, S. F. Aquino, and V. A. Leao, “Implications of volatile fatty acid profile on the metabolic pathway during continuous sulfate reduction,” *J. Environ. Manag.*, vol. 103, pp. 15–23, 2012.

[6] R. Singleton, “The Sulfate-Reducing Bacteria : An Overview,” in *The Sulfate-Reducing Bacteria: Contemporary Perspectives*, 1993, pp. 1–20.

[7] T. a. Hansen, “Metabolism of sulfate-reducing prokaryotes,” *Antonie van Leeuwenhoek, Int. J. Gen. Mol. Microbiol.*, vol. 66, no. 1–3, pp. 165–185, 1994.

[8] H. Fossing, V. A. Gallardo, B. B. Jørgensen, M. Hüttel, L. P. Nielsen, H. Schulz, D. E. Canfield, S. Forster, R. N. Glud, J. K. Gundersen, J. Küver, N. B. Ramsing, A. Teske, B. Thamdrup, and O. Ulloa, “Concentration and transport of nitrate by the mat-forming sulphur bacterium Thioploca,” *Nature*, vol. 374, no. 6524, pp. 713–715, 1995.

[9] J. F. Heidelberg, R. Seshadri, S. a Haveman, C. L. Hemme, I. T. Paulsen, J. F. Kolonay, J. a Eisen, N. Ward, B. Methe, L. M. Brinkac, S. C. Daugherty, R. T. Deboy, R. J.

Dodson, a S. Durkin, R. Madupu, W. C. Nelson, S. a Sullivan, D. Fouts, D. H. Haft, J. Selengut, J. D. Peterson, T. M. Davidsen, N. Zafar, L. Zhou, D. Radune, G. Dimitrov, M. Hance, K. Tran, H. Khouri, J. Gill, T. R. Utterback, T. V Feldblyum, J. D. Wall, G. Voordouw, and C. M. Fraser, "The genome sequence of the anaerobic, sulfate-reducing bacterium Desulfovibrio vulgaris Hildenborough," *Nat. Biotechnol.*, vol. 22, no. 5, pp. 554–559, 2004.

[10] G. Voordouw, "Minireview The Genus Desulfovibrio : The Centennial †," *Appl. Environ. Microbiol.*, vol. 61, no. 8, pp. 2813–2819, 1995.

[11] S. a Haveman, E. A. Greene, C. P. Stilwell, J. K. Voordouw, and G. Voordouw, "Physiological and Gene Expression Analysis of Inhibition of Desulfovibrio vulgaris Hildenborough by Nitrite Physiological and Gene Expression Analysis of Inhibition of Desulfovibrio vulgaris Hildenborough by Nitrite †," *J. Bacteriol.*, vol. 186, no. 23, pp. 7944–7950, 2004.

[12] B. Roche, L. Aussel, B. Ezraty, P. Mandin, B. Py, and F. Barras, "Iron/sulfur proteins biogenesis in prokaryotes: Formation, regulation and diversity," *Biochim. Biophys. Acta - Bioenerg.*, vol. 1827, no. 8–9, pp. 923–937, 2013.

[13] F. Ramel, G. Brasseur, L. Pieulle, O. Valette, A. Hirschler-Réa, M. L. Fardeau, and A. Dolla, "Growth of the Obligate Anaerobe Desulfovibrio vulgaris Hildenborough under Continuous Low Oxygen Concentration Sparging: Impact of the Membrane-Bound Oxygen Reductases," *PLoS One*, vol. 10, no. 4, p. e0123455, 2015.

[14] S. Johnston, S. Lin, P. Lee, S. M. Caffrey, J. Wildschut, J. K. Voordouw, S. M. Silva, I. A. C. Pereira, and G. Voordouw, "A genomic island of the sulfate-reducing bacterium Desulfovibrio vulgaris Hildenborough promotes survival under stress conditions while decreasing the efficiency of anaerobic growth," *Environ. Microbiol.*, vol. 11, pp. 981–991, 2009.

[15] R. Lill, "Function and biogenesis of iron–sulphur proteins," *Nature*, vol. 460, no. 7257, pp. 831–838, 2009.

[16] R. Grazina, S. R. Pauleta, J. J. G. Moura, and I. Moura, *Iron–Sulfur Centers: New Roles for Ancient Metal Sites*, vol. 3. Elsevier Ltd., 2013.

[17] B. Py and F. Barras, "Building Fe–S proteins: bacterial strategies," *Nat. Rev. Microbiol.*, vol. 8, no. 6, pp. 436–446, 2010.

[18] J. Liu, S. Chakraborty, P. Hosseinzadeh, Y. Yu, S. Tian, I. Petrik, A. Bhagi, and Y. Lu,

"Metalloproteins containing cytochrome, iron-sulfur, or copper redox centers," *Chem. Rev.*, vol. 114, no. 8, pp. 4366–4369, 2014.

[19] K. Brzóska, S. Męczyńska, and M. Kruszewski, "Iron-sulfur cluster proteins : electron transfer and beyond *," *Acta Biochim. Pol.*, vol. 53, no. 4, pp. 685–691, 2006.

[20] E. I. Stiefel and G. N. George, "Ferredoxins, Hydrogenases, and Nitrogenases: Metal-Sulfide Proteins," in *Bioinorganic Chemistry*, 1994, pp. 365–453.

[21] W. V Sweeney and J. C. Rabinowitz, "Proteins Containing 4Fe-4S Clusters: An Overview," *Annu. Rev. Biochem.*, vol. 49, pp. 139–161, 1980.

[22] D. C. Johnson, D. R. Dean, A. D. Smith, and M. K. Johnson, "Structure, Function, and Formation of Biological Iron-Sulfur Clusters," *Annu. Rev. Biochem.*, vol. 74, no. 1, pp. 247–281, 2005.

[23] L. Liu, T. Nogi, M. Kobayashi, and K. Miki, "Ultrahigh-resolution structure of high-potential iron - sulfur protein from Thermochromatium tepidum," *Acta Crystallogr. Sect. D Biol. Crystallogr.*, vol. D58, pp. 1085–1091, 2002.

[24] Z. H. Zhou and M. W. W. Adams, "Site-Directed Mutations of the 4Fe-Ferredoxin from the Hyperthermophilic Archaeon Pyrococcus furiosus : Role of the Cluster-Coordinating Aspartate in Physiological Electron Transfer Reactions †," *Biochemistry*, vol. 36, no. 36, pp. 10892–10900, 1997.

[25] A. Mukhopadhyay, A. V. Kladova, S. A. Bursakov, O. Y. Gavel, J. J. Calvete, V. L. Shnyrov, I. Moura, J. J. G. Moura, M. J. Romão, and J. Trincão, "Crystal structure of the zinc-, cobalt-, and iron-containing adenylate kinase from Desulfovibrio gigas: a novel metal-containing adenylate kinase from Gram-negative bacteria," *J. Biol. Inorg. Chem.*, vol. 16, no. 1, pp. 51–61, 2011.

[26] D. R. Breiters, T. E. Meyere, I. Raymentll, and H. M. Holdensii, "The Molecular Structure of the High Potential Iron-Sulfur Protein Isolated from Ectothiorhodospira halophila Determined at 2 . 5-A Resolution *," *J. Biol. Chem.*, vol. 266, no. 28, pp. 18660–18667, 1991.

[27] Z. Dauter, K. S. Wilson, L. C. Sieker, J. Meyer, and J. Moulis, "Atomic Resolution (0 . 94 Å) Structure of Clostridium acidurici Ferredoxin . Detailed Geometry of [4Fe-4S] Clusters in a Protein," *Biochemistry*, vol. 2960, no. 27, pp. 16065–16073, 1997.

[28] J. W. Peters, "Structure and mechanism of iron-only hydrogenases," *Curr. Opin. Struct. Biol.*, vol. 9, pp. 670–676, 1999.

[29] P. Knörzer, A. Silakov, C. E. Foster, F. A. Armstrong, W. Lubitz, and T. Happe, "Importance of the Protein Framework for Catalytic Activity of [FeFe]-Hydrogenases," *J. Biol. Chem.*, vol. 287, no. 2, pp. 1489–1499, 2012.

[30] M. K. J. S. Bandyopadhyay, K. Chandramouli, "Iron-Sulphur Cluster Biosynthesis," *Biochem. Soc. Trans.*, vol. 36, no. Pt 6, pp. 1112–1119, 2008.

[31] E. M. Shepard, E. S. Boyd, J. B. Broderick, and J. W. Peters, "Biosynthesis of complex iron – sulfur enzymes," *Curr. Opin. Chem. Biol.*, vol. 15, pp. 319–327, 2011.

[32] R. L. Tatusov, S. F. Altschul, and E. V Koonin, "Detection of conserved segments in proteins: Iterative scanning of sequence databases with the alignment blocks," *Proc. Natl. Acad. Sci.*, vol. 91, pp. 12091–12095, 1994.

[33] E. V Koonin, "A common set of conserved motifs in a vast variety of putative nucleic acid-dependent ATPases including MCM proteins involved in the initiation of eukaryotic DNA replication," *Nucleic Acids Res.*, vol. 21, no. 11, pp. 2541–2547, 1993.

[34] T. Rad, M. Bierlein, D. Rosa, and S. W. Nelson, "An Interaction between the Walker A and D-loop Motifs Is Critical to ATP Hydrolysis and Cooperativity in Bacteriophage T4 Rad50," *J. Biol. Chem.*, vol. 286, no. 29, pp. 26258–26266, 2011.

[35] E. Pathak, N. Atri, and R. Mishra, "Role of highly central residues of P-loop and it ' s flanking region in preserving the archetypal conformation of Walker A motif of diverse P-loop NTPases Abstract : Background :," *Bioinformation*, vol. 9, no. 1, 2013.

[36] C. Wiese, J. M. Hinz, R. S. Tebbs, P. B. Nham, S. S. Urbin, D. W. Collins, L. H. Thompson, D. Schild, L. S. Division, and L. Berkeley, "Disparate requirements for the Walker A and B ATPase motifs of human RAD51D in homologous recombination," *Nucleic Acids Res.*, vol. 34, no. 9, pp. 2833–2843, 2006.

[37] C. Ramakrishnan, V. S. Dani, and T. Ramasarma, "A conformational analysis of Walker motif A [GXXXXGKT (S)] in nucleotide-binding and other proteins The sequence GXXXXGKT / S , popularly known as Walker motif A , is widely believed to be the site for binding nucleotides in many proteins . Examination," *Protein Eng.*, vol. 15, no. 10, pp. 783–798, 2002.

[38] M. S. Mitchell and V. B. Rao, "Novel and deviant Walker A ATP-binding motifs in bacteriophage large terminase – DNA packaging proteins," *Virology*, vol. 321, pp. 217–221, 2004.

[39] K. Karata, T. Inagawa, A. J. Wilkinson, T. Tatsuta, and T. Ogura, "Dissecting the Role

of a Conserved Motif (the Second Region of Homology) in the AAA Family of ATPases," *J. Biol. Chem.*, vol. 274, no. 37, pp. 26225–26232, 1999.

[40] J. E. Walker, M. Saraste, M. J. Runswick, and N. J. Gay, "Distantly related sequences in the α- and - subunits of ATP synthase, myosin, kinases and other ATP-rquiring enzymes and a common nucleotide binding fold," *EMBO J.*, vol. I, no. 8, pp. 945–951, 1982.

[41] F. L. L. Stratford, M. Ramjeesingh, J. C. Cheung, L. Huan, and C. E. Bear, "The Walker B motif of the second nucleotide-binding domain (NBD2) of CFTR plays a key role in ATPase activity by the NBD1 – NBD2 heterodimer," *Biochem. J.*, vol. 586, pp. 581–586, 2007.

[42] G. N. George, I. J. Pickering, E. Y. Yu, R. C. Prince, S. A. Bursakov, O. Y. Gavel, and I. Moura, "A Novel Protein-Bound Copper - Molybdenum Cluster," *J. Am. Chem. Soc.*, vol. 122, no. 34, pp. 8321–8322, 2000.

[43] S. a. Bursakov, O. Y. Gavel, G. Di Rocco, J. Lampreia, J. Calvete, a. S. Pereira, J. J. G. Moura, and I. Moura, "Antagonists Mo and Cu in a heterometallic cluster present on a novel protein (orange protein) isolated from Desulfovibrio gigas," *J. Inorg. Biochem.*, vol. 98, no. 5, pp. 833–840, 2004.

[44] C. F. Mills, I. Bremner, and R. Summers, "Thiomolybdates in Rumen Contents and Rumen Cultures," *J. Inorg. Biochem.*, vol. 18, pp. 323–334, 1983.

[45] S. H. Laurie, "Thiomolybdates - Simple but very versatile reagents," *Eur. J. Inorg. Chem.*, no. 12, pp. 2443–2450, 2000.

[46] J. G. Zeevaart, L. Wang, V. V Thakur, C. S. Leung, J. Tirado-, C. M. Bailey, R. a Domaoal, K. S. Anderson, and L. William, "Tetrathiomolybdate Inhibits Copper Trafficking Proteins Through Metal Cluster Formation," *Science (80-.).*, vol. 130, no. 29, pp. 9492–9499, 2009.

[47] S. R. Pauleta, A. G. Duarte, M. S. Carepo, A. S. Pereira, P. Tavares, I. Moura, and J. J. G. Moura, "NMR assignment of the apo-form of a Desulfovibrio gigas protein containing a novel Mo–Cu cluster," *Biomol. NMR Assign.*, vol. 1, no. 1, pp. 81–83, 2007.

[48] M. S. P. Carepo, S. R. Pauleta, A. G. Wedd, J. J. G. Moura, and I. Moura, "Mo–Cu metal cluster formation and binding in an orange protein isolated from Desulfovibrio gigas," *J. Biol. Inorg. Chem.*, vol. 19, no. 4–5, pp. 605–614, 2014.

[49] a. Fievet, L. My, E. Cascales, M. Ansaldi, S. R. Pauleta, I. Moura, Z. Dermoun, C. S.

Bernard, a. Dolla, and C. Aubert, “The Anaerobe-Specific Orange Protein Complex of Desulfovibrio vulgaris Hildenborough Is Encoded by Two Divergent Operons Coregulated by 54 and a Cognate Transcriptional Regulator,” *J. Bacteriol.*, vol. 193, no. 13, pp. 3207–3219, 2011.

[50] R. L. Tatusov, E. V Koonin, and D. J. Lipman, “A genomic perspective on protein families.,” *Science (80-.).*, vol. 278, no. 5338, pp. 631–637, 1997.

[51] Z. Dermoun, A. Foulon, M. D. Miller, D. J. Harrington, A. M. Deacon, C. Sebban-Kreuzer, P. Roche, D. Lafitte, O. Bornet, I. a. Wilson, and A. Dolla, “TM0486 from the Hyperthermophilic Anaerobe Thermotoga maritima is a Thiamin-binding Protein Involved in Response of the Cell to Oxidative Conditions,” *J. Mol. Biol.*, vol. 400, no. 3, pp. 463–476, 2010.

[52] D. Bose, T. Pape, P. C. Burrows, M. Rappas, S. R. Wigneshweraraj, M. Buck, and X. Zhang, “Organization of an Activator-Bound RNA Polymerase Holoenzyme,” *Mol. Cell*, vol. 32, no. 3, pp. 337–346, 2008.

[53] E. Moretfl and L. Segoviat, “The sigma54 Bacterial Enhancer-Binding Protein Family : Mechanism of Action and Phylogenetic Relationship of Their Functional Domains,” *J. Bacteriol.*, vol. 175, no. 19, pp. 6067–6074, 1993.

[54] B. K. Maiti, I. Moura, J. J. G. Moura, and R. Pauleta, “The small iron-sulfur protein from the ORP operon binds a [2Fe-2S] cluster,” *Biochim. Biophys. Acta*, vol. 1857, pp. 1422–1429, 2016.

[55] M. S. P. Carepo, C. Carreira, R. Grazina, M. E. Zakrzewska, A. Dolla, C. Aubert, S. R. Pauleta, J. J. G. Moura, and I. Moura, “Orange protein from Desulfovibrio alaskensis G20 : insights into the Mo – Cu cluster protein - assisted synthesis,” *J. Biol. Inorg. Chem.*, vol. 21, pp. 53–62, 2016.

[56] P. S. Dehal, M. P. Joachimiak, M. N. Price, J. T. Bates, J. K. Baumohl, D. Chivian, G. D. Friedland, K. H. Huang, K. Keller, P. S. Novichkov, I. L. Dubchak, E. J. Alm, and A. P. Arkin, “MicrobesOnline: An integrated portal for comparative and functional genomics,” *Nucleic Acids Res.*, vol. 38, no. SUPPL.1, pp. 1–5, 2009.

[57] I. Letunic, T. Doerks, and P. Bork, “SMART: Recent updates, new developments and status in 2015,” *Nucleic Acids Res.*, vol. 43, no. D1, pp. D257–D260, 2015.

[58] B. A. Gasteiger E., Hoogland C., Gattiker A., Duvaud S., Wilkins M.R., Appel R.D., “Protein Identification and Analysis Tools on the ExPASy Server,” *Proteomics Protoc.*

Handb., pp. 571–607, 2005.

[59] J. R. Postgate, *The sulphate reducing bacteria*. 1984.

[60] C. Carreira, "O operão da proteína laranja : novas proteínas envolvidas na divisão celular em bactérias redutoras de sulfato," 2012.

[61] M. A. Larkin, G. Blackshields, N. P. Brown, R. Chenna, P. A. Mcgettigan, H. Mcwilliam, F. Valentin, I. M. Wallace, A. Wilm, R. Lopez, J. D. Thompson, T. J. Gibson, and D. G. Higgins, "Clustal W and Clustal X version 2 . 0," *Bioinforma. Appl. Note*, vol. 23, no. 21, pp. 2947–2948, 2007.

[62] J. Lutkenhaus and M. Sundaramoorthy, "MinD and role of the deviant Walker A motif , dimerization and membrane binding in oscillation," *Mol. Microbiol.*, vol. 48, pp. 295–303, 2003.

[63] J. M. Boyd, J. L. Sondelski, and D. M. Downs, "Bacterial ApbC protein has two biochemical activities that are required for in vivo function," *J. Biol. Chem.*, vol. 284, no. 1, pp. 110–118, 2009.

[64] Y. Hu, M. C. Corbett, A. W. Fay, J. A. Webber, K. O. Hodgson, B. Hedman, and M. W. Ribbe, "FeMo cofactor maturation on NifEN," *Proc. Natl. Acad. Sci.*, vol. 103, no. 46, pp. 17119–17124, 2006.

[65] J. M. Boyd, A. J. Pierik, D. J. A. Netz, R. Lill, and D. M. Downs, "Bacterial ApbC can bind and effectively transfer iron-sulfur clusters," *Biochemistry*, vol. 47, no. 31, pp. 8195–8202, 2008.

[66] D. D. Leipe, Y. I. Wolf, E. V Koonin, and L. Aravind, "Classification and evolution of P-loop GTPases and related ATPases.," *J. Mol. Biol. Biol.*, vol. 317, no. 1, pp. 41–72, 2002.

[67] W. V Sweeney and J. C. Rabinowitz, "Protein Contaning 4Fe-4S Clusters: An Overview," *Annu. Rev. Biochem.*, vol. 49, pp. 139–161, 1980.

[68] P. Delarue, P. Senet, and A. Nicolaı, "Decipher the Mechanisms of Protein Conformational Changes Induced by Nucleotide Binding through Free- Energy Landscape Analysis : ATP Binding to Hsp70," *PLOS Comput. Biol.*, vol. 9, no. 12, pp. 1–20, 2013.

[69] I. Rouiller, V. M. Butel, M. Latterich, R. A. Milligan, and E. M. Wilson-kubalek, "A Major Conformational Change in p97 AAA ATPase upon ATP Binding," *Mol. Cell*, vol.

6, pp. 1485–1490, 2000.

[70] A. A. Baykov, O. A. Evtushenko, and S. M. Avaeva, “A Malachite Green Procedure for Orthophosphate Determination and Its Use in Alkaline Phosphatase-Based Enzyme Immunoassay,” *Anal. Biochem.*, vol. 171, pp. 266–270, 1988.

[71] A. H. Priem, Æ. A. A. K. Klaassen, E. J. Reijerse, Æ. T. E. Meyer, W. R. Dunham, and Æ. W. R. Hagen, “EPR analysis of multiple forms of [4Fe – 4S] 3+ clusters in HiPIPs,” *J. Biochem. Chem.*, vol. 10, pp. 417–424, 2005.

[72] R. Cammack and F. MacMillan, “Electron Magnetic Resonance of Iron-Sulfur Proteins in Electron-Transfer Chains: Resolving Complexity,” in *Metals in Biology: Applications of High-Resolution EPR to Metalloenzymes*, 2010, pp. 11–45.

[73] F. B. Æ. N. D. Chasteen, “Spin concentration measurements of high-spin (g 0 = 4 . 3) rhombic iron (III) ions in biological samples : theory and application,” *J. Biol. Inorg. Chem.*, vol. 13, pp. 15–24, 2008.

[74] W. N. Lanzilotta and L. C. Seefeldt, “Electron Transfer from the Nitrogenase Iron Protein to the [8Fe- (7 / 8) S] Clusters of the Molybdenum - Iron Protein †,” *Biochemsitry*, vol. 2960, no. 96, pp. 16770–16776, 1996.

6

Appendixes

Appendix 1 – *D. vulgaris Hildenborough* Growth

Table 6.1 - Growth of *D. vulgaris* Hildenborough in Medium C.

Inoculum Volume	Timeframe	OD_{600nm}
5 mL	24 h	0.68
10 mL	24 h	0.75
100 mL	24 h	0.73
1 L	24 h	0.68
	30 h	0.71
2 L	24 h	0.63
	30 h	0.69

Appendix 2 – Medium C

Table 6.2 - Composition of Medium C for *Desulfovibrio vulgaris* Hildenborough growth. The medium was sterilized in autoclave at 120° C for 20 min at 1 bar. The recipe presented is for a total volume of 1 L.

Chemical Formula	Compound	Concentration (g/L)
KH_2PO_4	Potassium phosphate monobasic	0.5
NH_4Cl	Ammonium chloride	1
Na_2SO_4	Sodium sulphate	4.5
$MgSO_4.7H_2O$	Magnesium Sulphate Heptahydrate	0.06
$CaCl_2.2H_2O$	Calcium Chloride Dihydrate	0.04
$C_3H_6O_3.Na$	Na-Lactate 60 %	3.18
	Yeast Extract	1
$FeSO_4.7H_2O$	Iron (II) Sulphate heptahydrate	0.004
$Na_3C_6H_5O_7$	Sodium Citrate	0.3
$C_6H_8O_6$	Ascorbic Acid	0.1
$C_2H_4O_2S$	Thioglycolic Acid	0.1

Appendix 3 - Quantitative composition of gels and solutions for electrophoretic SDS-PAGE and PAGE

Table 6.3 - Quantitative composition of polyacrylamide gels 12.5 % (m/v) and 10 % (m/v) in buffer solution Tris-Tricine. Independently of the percentage of the running gel, the stacking gel's concentration is always the same. APS (Ammonium Persulphate) and TEMED (Tetramethylethylenediamine, $(CH_3)_2NCH_2CH_2N(CH_3)_2$) are only added at the end of gel preparation. All solutions are stored at 4° C, except APS that is stored at -20° C. Stock of Acrylamide/Bis-acrylamide and gel buffer solutions is 41.5 % /1.5 % (m/v) and 3 M Tris-HCl pH 8.3 and 0.3 % SDS (m/v), respectively. For PAGE gels, gel buffer composition is different (without denaturant agent, SDS) in the same volume.

Reagent	Running Gel 12.5 %	Running Gel 10 %	Stacking Gel 12.5 %
Acrylamide/Bis-acrylamide	1.1 mL	0.9 mL	0.2 mL
Gel Buffer	1.4 mL	1.4 mL	0.6 mL
Glycerol 100 %	0.7 mL	0.7 mL	---
Milli-Q Water	1 mL	1.25 mL	1.6 mL
APS 10 %	35 µL	35 µL	16 µL
TEMED	3.5 µL	3.5 µL	2.4 µL

Table 6.4 - Quantitative composition of staining solution for SDS-PAGE and PAGE gels.

Reagent	Volume
Distilled Water	95 mL
Methanol	90 mL
Acetic Acid Glacial	15 mL
Coomassie Brilliant Blue R250	1 g

Table 6.5 - Quantitative composition of distaining solution for SDS-PAGE and PAGE gels.

Reagent	Volume
Distilled Water	475 mL
Methanol	450 mL
Acetic Acid Glacial	75 mL

Appendix 4 – Size-exclusion Chromatography

Table 6.6 - Proteins of the calibration kit of size-exclusion chromatography (LMW GE Healthcare) used to construct the calibration curve for MM determination for Superdex 200 10/300 GL.

Protein	Elution volume (mL)	Molecular Mass (kDa)	Concentration (mg/mL)
Ovalbumin	10.6	43	3
Conalbumin	12.5	75	3
Aldolase	13.9	158	3
Ferritin	14.6	440	0.3

Table 6.7 - Proteins of the calibration kit of size-exclusion chromatography (LMW GE Healthcare) used to determine the molecular mass for Superdex 75 10/300 GL.

Protein	Elution Volume (mL)	Molecular Mass (kDa)	Concentration (mg/mL)
Aprotinin	15.5	6.5	2
Ribonuclease A	13.4	13.7	5
Carbonic Anhydrase	11.6	29	2
Ovalbumin	13.4	43	3
Conalbumin	9.5	75	3

Appendix 5 – EPR spectra

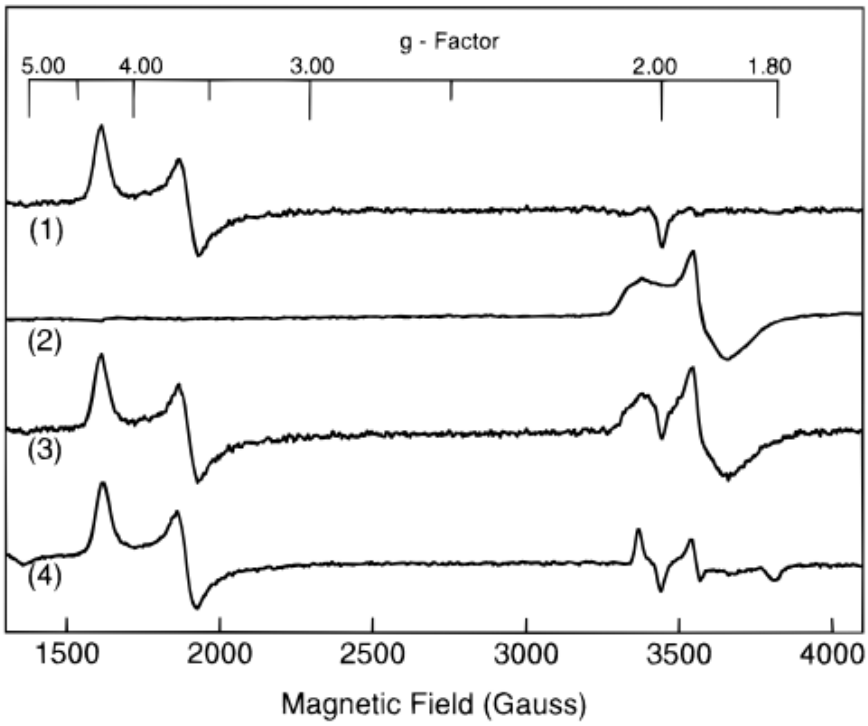

Figure 6.1 – Electron transfer from the L127ΔFe protein to the P-clusters of the MoFe protein monitored by perpendicular mode EPR spectroscopy. MoFe protein, with each P-cluster oxidized by two electrons (P^{2+} state), and the reduced but dithionite-free L127Δ Fe protein were prepared as described in Experimental Procedures. All samples were incubated for 2 min prior to freezing in liquid nitrogen, and the buffer was 50 mM MOPS (pH 7.0). Perpendicular mode EPR spectra are shown for the oxidized (P^{2+}) state of the MoFe protein (54 μM) (trace 1), the reduced state of the L127Δ Fe protein (91 μM) (trace 2), the mathematical additive spectrum for traces 1 and 2 (trace 3), and the mixture of L127ΔFe protein (91íM) and the P2+ state of the MoFe protein (54 μM) (trace 4). All spectra were recorded at 12 K with a microwave frequency of 9.64 GHz, a modulation frequency of 100 kHz, a modulation amplitude of 5.028 G, a time constant of 20.48 ms, and a microwave power of 10.1 mW. Image from [74]

Appendix 6 – EPR spectra DVU2103

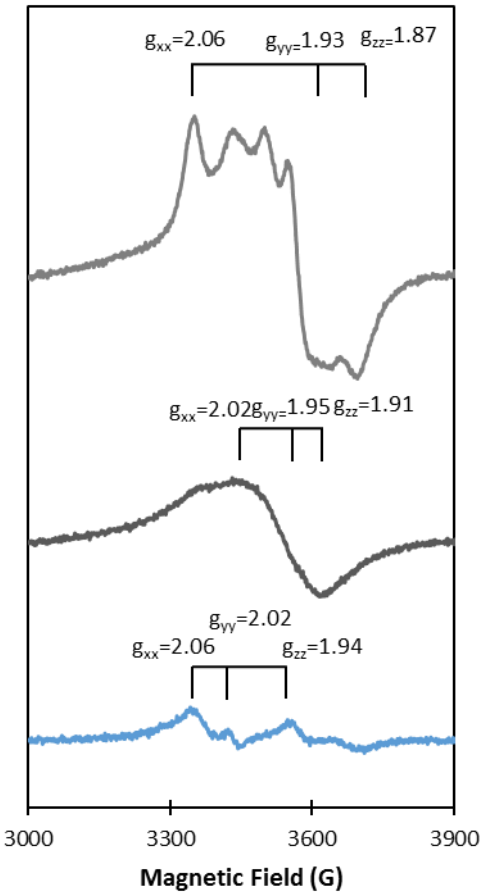

Figure 6.2 - X-band EPR spectrum of 126 µM "DVU2103" in 20 mM Tris-HCl buffer, pH 7.6 and 3 mM DTT, at 10 K, 9.65 GHz of frequency, 15 dB, 5 Gpp of modulation and 1×10^5gain. The figure represents the as-isolated spectrum of "DVU2103" (blue) and dithionite addition: after 30 min (grey) and 1h (dark grey).